

Copyright

By

Wei-luen Allen Yu

2007

**The Dissertation Committee for Wei-luen Allen Yu certifies that this is the approved
version of the following dissertation:**

**Studies of the Biosynthesis of the Nitro Sugar D-Kijanose and
the Function of the Glycosyltransferase Helper Proteins in
Glycosylation of Macrolide Antibiotics**

Committee:

Hung-wen Liu, Supervisor

David Hoffman

Christian Whitman

Walter Fast

Marvin Hackert

**Studies of the Biosynthesis of the Nitro Sugar D-Kijanose and
the Function of the Glycosyltransferase Helper Proteins in
Glycosylation of Macrolide Antibiotics**

by

Wei-luen Allen Yu, B.S.; M.S.

Dissertation

Presented to the Faculty of the Graduate School of
the University of Texas at Austin
in Partial Fulfillment
of the Requirements
for the Degree of

Doctor of Philosophy

The University of Texas at Austin

December 2007

**Studies of the Biosynthesis of the Nitro Sugar D-Kijanose and
the Function of the Glycosyltransferase Helper Proteins in
Glycosylation of Macrolide Antibiotics**

Publication No. _____

Wei-luen Allen Yu, Ph.D.

The University of Texas at Austin, 2007

Supervisor: Hung-wen Liu

The appended sugar residues of many natural products from Actinomyces are important for their biological activities. Many of these unusual sugar biosynthetic gene clusters have been isolated and many glycosyltransferases from various antibiotic-producing organisms have been identified. The increasing knowledge about these sugar biosynthetic pathways opens up the possibility of generating novel bioactive glycosylated compounds through combinatorial biosynthesis. The work described in this dissertation focuses on the investigation of the biosynthetic pathway of a rare nitro-containing sugar, D-kijanose, from an antibiotic, kijanimicin, and the glycosyltransferase helper proteins involved in the glycosylation of macrolide antibiotics.

D-Kijanose, especially its nitro group, plays an important role in conferring the biological activities of the parent antibiotics. Cloning and sequencing of the kijanimicin biosynthetic gene cluster have allowed the proposal of the biosynthetic pathway of D-kijanose. The functions of the enzymes encoded by each open-reading frame in the cluster were also assigned based on sequence comparison with known enzymes found in other biosynthetic reactions. In this thesis, the functions of KijB1, a TDP-4-keto-6-deoxy-hexose 2,3-dehydratase, and KijD2, a TDP-hexose C-3 aminotransferase, were verified. The TDP-3-amino-4-keto-2,3,6-trideoxyhexose produced as an intermediate in the early stage of D-kijanose biosynthesis was also identified. In the second part of this dissertation, the *in vivo* protein-protein interaction between D-desosaminyl glycosyltransferase, DesVII, and its auxiliary protein, DesVIII, was established by yeast two-hybrid assay. The complex formation between these two proteins was also demonstrated by *in vitro* binding assay. Several strategies were tried to overexpress the D-mycaminosyl glycosyltransferase and its auxiliary protein, TylM2 and TylM3, although none of them were successful. A two-plasmid *in vivo* glycosylation system was also developed to test the competence of various DesVIII homologues to serve as the helper protein for glycosyltransferase DesVII, MycB and NbmD. In summary, the work in this dissertation has provided important information on the biosynthesis of D-kijanose and also significant insight into the function of the helper proteins of macrolide glycosyltransferases. These results could be useful for future studies of natural product biosynthesis and exploitation of glycodiversification.

Table of Content

Chapter 1. Background and Significance	1
1. INTRODUCTION.....	1
2. UNUSUAL SUGAR BIOSYNTHESIS AND RELATED ENZYME MECHANISMS.....	5
2-1 Nucleotidyl Activation of Sugar.....	5
2-2 Biosynthesis of 6-deoxyhexose (6DOH)	7
2-3 C-2 Deoxygenation in the Biosynthesis of 2,6-dideoxyhexoses	8
2-4 C-3 Deoxygenation by E ₁ - and E ₃ - in the Biosynthesis of 3,6-dideoxyhexose.....	10
2-5 C-4 Deoxygenation by DesI and DesII in the Biosynthesis of D-Desosamine.....	15
2-6 Biosynthesis of aminosugars	19
3. GLYCOSYLTRANSFERASES AND THEIR CATALYTIC MECHANISMS.....	21
3-1 The Variety of Glycosyltransferases	22
3-2 Classification of Glycosyltransferases	23
3-3 General Enzyme Mechanism of Glycosyltransferases	24
3-4 Folding Types and Structures of Glycosyltransferases	26
3-5 Natural Product Glycosyltransferases	30
4. NATURAL PRODUCT BIOSYNTHETIC ENGINEERING AND GLYCODIVERSIFICATION	33
5. THESIS STATEMENT.....	38
Chapter 2. Biosynthetic Studies of D-Kijanose in Antibiotic Kijanomicin from <i>Actinomadura kijaniata</i>	39
1. INTRODUCTION.....	39
2. EXPERIMENTAL PROCEDURES	48
3. RESULTS AND DISCUSSION	66
4. CONCLUSION	84
Chapter 3. Macrolide Glycosyltransferases and Their Auxiliary Proteins	85

1. INTRODUCTION.....	85
2. EXPERIMENTAL PROCEDURES.....	90
3. RESULTS AND DISCUSSION.....	117
4. CONCLUSION	139
REFERENCES.....	140
Vita	155

List of Tables

Table 2-1	Proposed kijanimicin biosynthetic gene functions	46
Table 2-2	Primer pairs for cloning the putative D-kijanose biosynthetic genes	52
Table 2-3	Plasmid constructs containing the putative D-kijanose biosynthetic genes	54
Table 3-1	Primer pairs for constructing yeast two-hybrid plasmids	97
Table 3-2	Primer pairs for constructing pCM37	98
Table 3-3	Primer pairs for cloning glycosyltransferases and helper proteins	99
Table 3-4	Primer pairs for protein overexpression plasmids	100
Table 3-5	Primer pairs for cloning <i>TyIM2cx</i> and <i>TyIM3cx</i>	101
Table 3-6	Buffer compositions for <i>TyIM2cx</i> and <i>TyIM3cx</i> renaturation	106
Table 3-7	Yeast two-hybrid assay results	121
Table 3-8	Glycosylation ratio of the two-plasmid <i>in vivo</i> glycosylation assay	136

List of Figures

Figure 1-1	Catalytic mechanism of D-Glucose-1-phosphate thymidyltransferase	6
Figure 1-2	Catalytic mechanism of TDP-D-glucose 4,6-dehydratase	8
Figure 1-3	Catalytic mechanism of TDP-4-keto-6-deoxy-D-glucose 2,3-dehydratase, TyIX3, and the biosynthetic pathway of TDP-L-mycarose	10
Figure 1-4	Biosynthetic pathway of CDP-L-ascarylose	11
Figure 1-5	Catalytic mechanism of E ₁ /E ₃ for C-3 deoxygenation of CDP-L-ascarylose biosynthesis	13
Figure 1-6	Catalytic mechanism of C-3 dehydrase, ColD, in the GDP-L-colitose biosynthetic pathway	15
Figure 1-7	Proposed mechanism of DesII-catalyzed C-4 deamination	18
Figure 1-8	Catalytic mechanism of DesI	20
Figure 1-9	Catalytic mechanism of glucosamine-6-phosphate synthase	21
Figure 1-10	Catalytic mechanisms of glycosyltransferases	26
Figure 1-11	Folding types of Glycosyltransferases	29
Figure 1-12	Substrate flexibility of natural product glycosyltransferase DesVII	31
Figure 1-13	Reversible glycosyltransferases	32
Figure 1-14	Natural product biosynthetic engineering	36
Figure 1-15	Metabolic engineering of TDP-D-desosamine biosynthetic pathway	37
Figure 2-1	Map of kijanimicin biosynthetic gene cluster	45
Figure 2-2	Maps of the expression plasmids containing the putative D-kijanose biosynthetic genes	55
Figure 2-3	Reaction scheme of KijD5 and KijD4 and partial sequence alignment of KijD4	67
Figure 2-4	Reaction scheme for KijB1 and KijD2	68
Figure 2-5	Phylogenic tree of deoxysugar aminotransferases	69
Figure 2-6	The tri-gene sub-clusters of three C-3-nitro-sugar biosynthetic gene clusters	72
Figure 2-7	Expression and purification of KijB1	74
Figure 2-8	SDS-PAGE of FPLC-MonoQ purified KijD2	75
Figure 2-9	Pyridoxal-5'-phosphate reconstitution of KijD2	76

Figure 2-10	Transamination reaction of PLP-dependent aminotransferase	76
Figure 2-11	Spectrophotometry of KijD2 transamination	77
Figure 2-12	HPLC traces of KijB1 and KijD2 reactions	79
Figure 2-13	HPLC traces of large-scale KijB1/KijD2 coupled reaction	79
Figure 2-14	High-resolution ESI-MS/MS of maltol, TDP, and KijD2 product	80
Figure 2-15	SDS-PAGE of purified KijD1, KijD3, KijD6, and KijD7	82
Figure 2-16	Spectrophotometry of KijD7 transamination	83
Figure 3-1	Glycosylation reactions catalyzed by glycosyltransferases and the specific auxiliary proteins	87
Figure 3-2	PCR procedures to make TylM3cx construct	103
Figure 3-3	Maps of the overexpression plasmids of the glycosyltransferases and helper proteins	104
Figure 3-4	Plasmid maps of the yeast two-hybrid expression system	108
Figure 3-5	Plasmid maps of pCM37 and GT/Helper protein-pAX702	109
Figure 3-6	Yeast two-hybrid system	118
Figure 3-7	Yeast two-hybrid assay results for sample #1-6	122
Figure 3-8	S•tag protein pull-down assay	123
Figure 3-9	Overexpression and purification of N'-His-TylM2	125
Figure 3-10	Overexpression and purification of N'-His-TylM3	126
Figure 3-11	Overexpression and Purification of TylM2cx and TylM3cx	127
Figure 3-12	Purification of denatured TylM2cx and TylM3cx	129
Figure 3-13	Purification of coexpressed TylM2cx and TylM3cx	129
Figure 3-14	Two-plasmid system for <i>in vivo</i> biosynthesis of glycosylated products and its adaption to test the GT tolerance to different helper proteins	131
Figure 3-15	Final steps of the biosynthesis of macrolide antibiotics in <i>Streptomyces venezuelae</i>	133
Figure 3-16	The glycosylated natural products and their biosynthetic GTs and helper proteins	134
Figure 3-17	TLC analysis of the two-plasmid <i>in vivo</i> glycosylation assay	135
Figure 3-18	The alignment of glycosylation ratio with amino acid sequence identities of helper proteins	138

Chapter 1. Background and Significance

1. INTRODUCTION

Carbohydrates are the most abundant and versatile biomolecules on Earth. In addition to be the major bio-energy source, carbohydrates play essential roles in various structural and physiological functions. For example, the rigid component of bacterial cell walls is composed of cross-linked peptidoglycan, whereas the cell walls of plants are formed of mere polysaccharides, cellulose. The extracellular matrix of multicellular animals is filled with interlocking meshwork of polysaccharides and fibrous proteoglycans such as collagen, elastin, fibronectin, and laminin. The glycosylation of proteins leads to the alternation of the folding properties and biological activities of the protein molecules. Such modification could also determine the interactions between proteins and other biomolecules. Lipopolysaccharides (LPS), the dominant surface component of the outer membrane of gram-negative bacteria, are responsible for the toxicity and immuno-properties of the possessors. In addition, numerous natural products are also glycosylated compounds in which the sugar residues provide not only the solubility to aqueous environment but also the biological activity.

Eukaryotic organisms use only ten monosaccharide units to construct the complex glycosylated system.¹ On the contrary, more than one hundred monosaccharides have been found in the glycosylated biomolecules produced by prokaryotic organisms.^{2,3} In addition to those monosaccharides used as the building blocks for cell surface and in the

modifications of macromolecules, studies of the unusual sugar monomers that appear in antibiotics, alkaloids and drug-related natural compounds have become an important subject in modern glycochemistry/glycobiology research because of their potential in diagnostic and therapeutic applications. Decades of research on those non-primary metabolite sugar monomers focused on their pharmacological activities and biosynthesis. With the accumulating knowledge of unusual sugar molecules, we could devise methods to synthesize more glycosylated compounds as drug candidates and test them for clinical applications.^{4, 5}

Recent studies on the formation of sugar-containing natural products have been devoted mainly to two areas. One is the elucidation of the biosynthetic pathways and characterization of enzymes involved in the pathways. The other is to manipulate known biosynthetic machineries to generate novel unnatural glycosides. To study the biosynthesis of glycosylated compounds, the secondary metabolites produced by Gram-positive bacteria Actinomycetes have attracted more attention because they account for approximately two-thirds of known microorganism-generating natural products. As for most secondary metabolism in prokaryotes, the biosynthetic genes responsible for glycosylated nature products are usually clustered together in the genome and even transcribed into a poly-cistronic messenger. With advances in modern molecular biological techniques, more and more biosynthetic gene clusters of natural glycosides have been identified and the function of each responsible gene in the biosynthetic pathways are assigned by *in vitro* or *in vivo* activity assays. Those accumulating experimental results have substantially extended our knowledge about nature's strategies

for sugar biosynthesis and have also uncovered several conserved mechanisms among sugar biosynthetic enzymes. A general review of unusual sugars biosynthesis and a summary of selected modifying enzymes will be presented in Section **2** of this chapter.

Glycosyltransferases (GTs) are enzymes that catalyze glycosylation reactions to a diverse set of acceptor molecules, commonly referred as the aglycones. Glycosylation reactions usually happen at the later stage of the glycoside biosynthesis, namely, after the assembly of the aglycone and unusual sugar residues. Some tailoring modifications occur after the glycosylation step. Because of the important roles played by the sugar moieties in determining the activities of the glycosylated natural products, GT catalyzed reactions are critical in the biosynthesis of these compounds. Disruption of GT-encoding genes usually results in losing biological activity of un-glycosylated compounds. Recent studies have shown that many natural product GTs are substrate-promiscuous, allowing them to be used in both *in vivo* and *in vitro* glycodiversification work to alter the sugar structures attached to different aglycones.⁶ Accordingly, studying factors controlling GT activity and specificity has become a hot topic which may lead to the construction of new glycosylated compounds with interesting biological properties. Summaries of the general characteristics and the catalytic mechanisms of GTs will be presented in Section **3** of this chapter.

The biosynthesis of natural products typically involves the repeated use of the same types of reaction because the same genetic blueprints have been passed on during evolution. The structural diversity in natural products is achieved by the actions of a few different types of enzymes which are capable of modifying the same common

precursors. Further modification is carried out on the assembled scaffold by additional, more product-specific enzymes. The co-linear relationship between the proteins involved in the biosynthesis and the chemical structures of the end product makes it possible to accomplish combinatorial biosynthesis of natural products through alteration of the genetic blueprints by combining the biosynthetic machineries that are responsible for assembling portions of different natural products.⁷⁻¹⁰ Recently, combinatorial strategies for sugar structure alteration through pathway engineering or analogue feeding were performed *in vitro* or *in vivo*. All of these strategies have proven effective in generating new glycosylated products, which may have potential biological activities against microorganisms and tumor cells. Those successful strategies and the new compounds will be discussed in Section 4 of this chapter.

Overall, this introductory chapter presents general background information of unusual sugar biosynthesis, glycosyltransferase activity, and the strategies for structural alteration of natural product sugar moieties. Knowledge and practical experience in the identification of sugar biosynthetic pathways and related glycosyltransfers, and manipulation of these pathways to generate novel natural glycosides have grown tremendously in recent years. By learning Nature's strategies for synthesizing and transferring unusual sugars to various aglycone scaffolds and by demonstrating the feasibility of making structural alterations to the sugar components of natural products, we have forayed into new era of biochemical research which has great potential for the betterment of mankind. This background information not only summarizes the knowledge which has been discovered in the sugar biosynthesis field, but also highlights

the many gaps remaining to be filled to achieve glycodiversification of nature product.

2. UNUSUAL SUGAR BIOSYNTHESIS AND RELATED ENZYME MECHANISMS

2-1 Nucleotidyl Activation of Sugar

Sugar-containing natural products are synthesized by coupling the aglycone and the sugar residues through the action of glycosyltransferases. The free energy of glycosidic bond formation is acquired through the conversion of monosaccharide units to nucleotidyl sugars as in the case of biosynthesis of disaccharides, oligosaccharides, and polysaccharides. A nucleotide at the anomeric carbon of a sugar molecule usually serves as a good leaving group and thereby facilitates the glycosidic bond formation catalyzed by glycosyltransferases. The nucleotides that participate in natural glycoside biosynthesis include ADP, CDP, GDP, TDP, UDP and CMP. Most nucleotidyl sugar biosynthesis involves the coupling of a sugar-1-phosphate to a nucleotidyl monophosphate moiety from the corresponding nucleoside triphosphate (NTP) by a nucleotidyltransferase (E_p). The sugar-1-phosphate is typically a primary metabolic intermediate, such as the product of an anomeric kinase reaction or a mutase reaction from the corresponding sugar-6-phosphate. The reaction of E_p is believed to proceed via a single displacement mechanism which is consistent with the structure of an enzyme-substrate complex determined by protein crystallography.¹¹ In this reaction, the formation of a phosphodiester bond on one side of the α -phosphorus atom occurs concurrently with the breaking of a phosphodiester bond on the opposing face (to give

PP_i as the leaving group) (Figure 1-1). Some nucleotidyltransferases display unusual promiscuity toward either its nucleotide triphosphate (NTP) or the sugar phosphate substrates.¹² This substrate promiscuity makes those E_p enzymes excellent tools to connect diverse sugar phosphates to the respective nucleotide sugars. Only a few sugars are activated by directly coupling of the anomeric hydroxyl group to the α-phosphate atom of CTP and releasing PP_i. One well-known example is sialic acid activation by CMP-sialic acid synthetase. The CMP-sialic acid product is used by sialyltransferases that incorporate this keto acid into glycoproteins and glycolipids.¹³

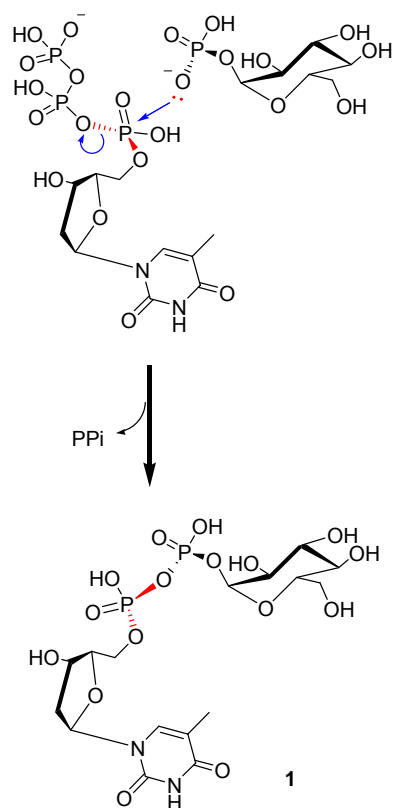


Figure 1-1 Catalytic mechanism of D-Glucose-1-phosphate thymidyltransferase. The proposed enzymatic mechanism based on the structures of substrate- and product-bound E_p.

2-2 Biosynthesis of 6-deoxyhexose (6DOH)

Natural unusual sugars are derived from common sugars, such as glucose and mannose, through enzyme-catalyzed modifications at C-2 to C-6 of the sugar backbone after nucleotidyl activation. A vast majority of these sugars are 6-deoxyhexoses (6DOH), and share the C-6 deoxygenation step catalyzed by an NAD^+ dependent 4,6-dehydratase, also known as an oxidoreductase (E_{od}).¹⁴⁻¹⁶ The dehydration product, NDP-4-keto-6-deoxy-D-hexose, is a common intermediate for further modifications, including deoxygenation, transamination, ketoreduction, methylation, epimerization, etc.

The catalytic mechanism of E_{od} proceeds through a three-step oxidation-dehydration-reduction process (Figure 1-2). The first step in the process involves C-4 oxidation of the hydroxyl group to a ketone, activating the C-5 proton for abstraction. The C-6 hydroxyl group is then protonated and leaves in a stepwise elimination to form a glucoseen intermediate. The glucoseen intermediate is subsequently reduced by addition of hydride at C-6 and protonation at C-5. From the structures of TDP-D-glucose 4,6-dehydratase RmlB from *Salmonella typhimurium*, the conserved tyrosine 167 residue is the base responsible for the initial deprotonation of the C-4 hydroxyl group. The conserved aspartate 134 and glutamate 135 serve as the general acid and base for the subsequent dehydration reaction (Figure 1-2).¹⁷ For transferring the hydride from C-4 through NAD^+ to C-6, the 4-keto-glucosene intermediate may re-orientate to accept the hydride from NADH at the C-6 position. The formation of a keto group at C-4 provides the necessary sugar ring activation for subsequent modifications in sugar biosynthesis.

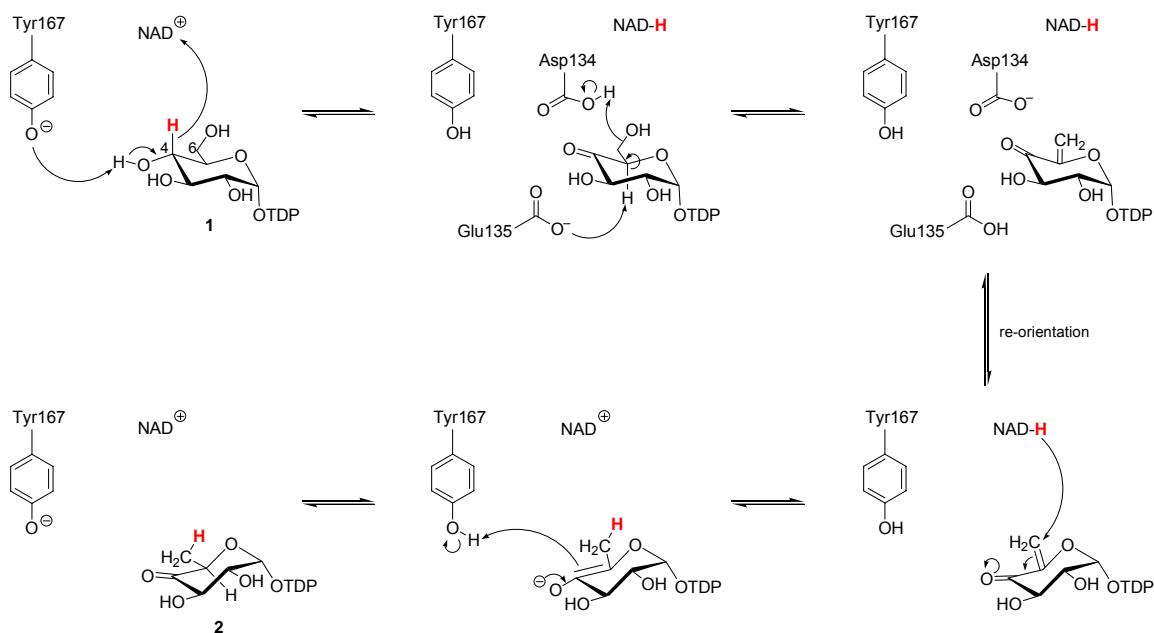


Figure 1-2 The proposed enzymatic mechanism of TDP-D-glucose 4,6-dehydratase (RmlB).¹⁸

2-3 C-2 Deoxygenation in the Biosynthesis of 2,6-dideoxyhexoses

Like C-6 deoxygenation, a similar reaction sequence occurs in the C-2 deoxygenation reaction catalyzed by TylX3 in the TDP-L-mycarose (**8**, Fig. 1-3) biosynthetic pathway of *Streptomyces fradiae*.¹⁹ Here, the 4-keto group of 6DOH substrate (**2**) helps the deprotonation at C-3 and the elimination of the C-2 hydroxyl group to make 2,6-dideoxyhexose. In the analysis of TylX3 protein composition, a divalent zinc ion (Zn^{2+}) was found in the enzyme, and its existence is required for the activity of TylX3. Interestingly, the formation of maltol (**7**) and TDP was found when TDP-4-keto-6-deoxy-D-glucose (**2**) was incubated with TylX3 or other 2,3-dehydratase

homologues, for example, OleV and EvaA.¹⁹⁻²¹ However, when **2** was incubated with TylX3 and TylC1 in the presence of NADPH, a new product TDP-2,6-dideoxy-D-*glycero*-4-hexulose (**6**) was synthesized. TylC1 is a C-3 ketoreductase acting on the unstable TylX3 product, a 2,6-dideoxy-3,4-diketo-hexose intermediate (**5**), using NADPH as the reducing cofactor which is bound to an extended Rossman fold in TylC1. From the results of deuterium-labeled TylX3/TylC1 reaction assay, the catalytic mechanism of C-2 deoxygenation was proposed as shown in Figure 1-3. First, the Zn²⁺ ion in TylX3 may have a role in C-3 deprotonation by activating an active-site-bound water molecule as a base. Alternatively, it may stabilize the enediolate intermediate (**3**) or act as a general acid in the elimination of the C-2 hydroxyl group (**3** → **4**). Tautomerization of **4** yields the unstable 3,4-diketone (**5**), which is reduced by TylC1, to give the 2,6-dideoxyhexose product **6**. There exist dozens of different 2,6-dideoxyhexoses in nature, and the conserved genes of 2,3-dehydratases can be found in their biosynthetic gene clusters. Due to the instability of the dehydration product, enzymes catalyze C-3 reduction or C-3 transamination reactions may work together with 2,3-dehydratase to produce the more stable 3-hydroxyl- or 3-amino-4-keto-2,6-dideoxysugar, like TylX3 and TylC1.

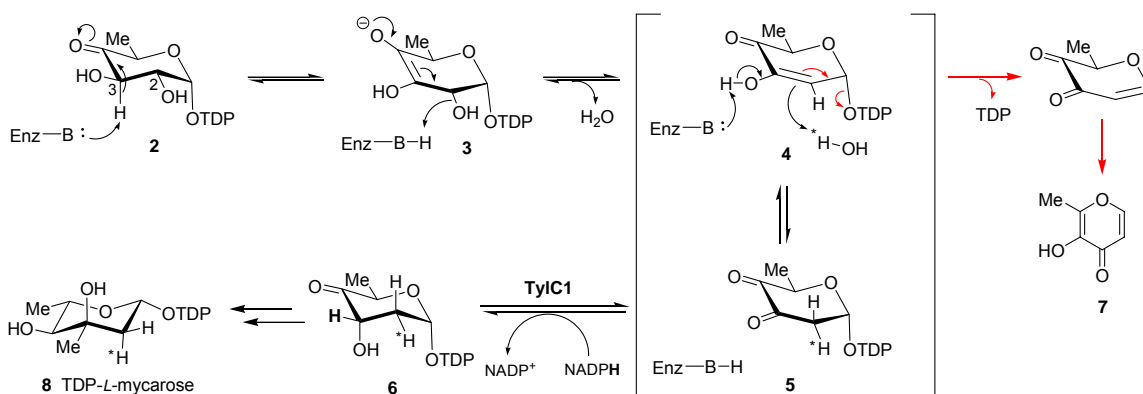


Figure 1-3 The proposed enzymatic mechanism of TDP-4-keto-6-deoxy-D-glucose 2,3-dehydratase, TylX3, and the biosynthetic pathway of TDP-L-mycarose.¹⁹

2-4 C-3 Deoxygenation by E₁- and E₃- in the Biosynthesis of 3,6-dideoxyhexose

The 3,6-dideoxyhexoses are found in the lipopolysaccharides of gram-negative bacteria, where they have been shown to be the dominant antigenic determinants.²² The biosynthetic gene cluster of L-ascarylose was cloned and sequenced from *Yersinia pseudotuberculosis* V.^{23, 24} The CDP-L-ascarylose (**14**) biosynthetic pathway has been proposed (Figure 1-4) and verified *in vitro* and *in vivo*. The C-3 deoxygenation step proceeds through a radical mechanism and requires a unique pair of enzymes, E₁ (*ascC*) and E₃ (*ascD*).^{25, 26} E₁ contains a [2Fe-2S] center and is also pyridoxamine 5'-phosphate (PMP) dependent.²⁷ E₃ is an iron-sulfur flavoprotein containing a flavin and a [2Fe-2S] center, and uses NADH as the reductant.^{28, 29}

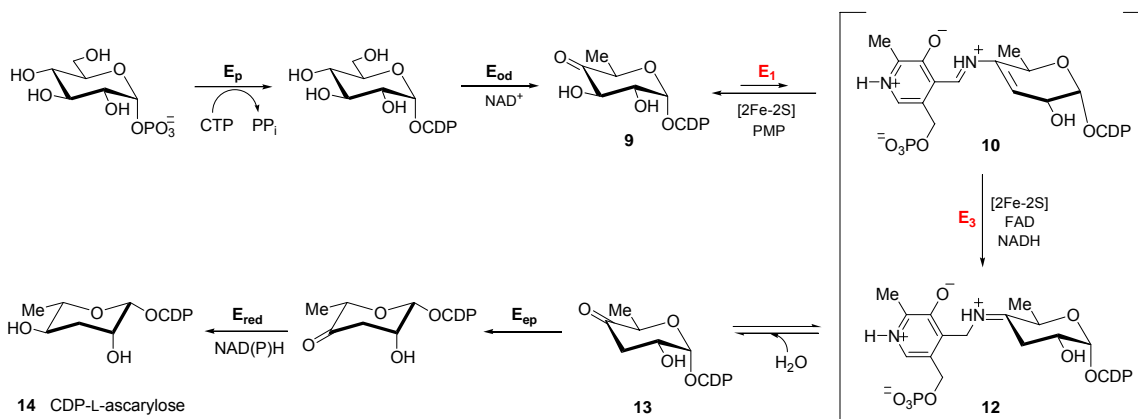


Figure 1-4 The biosynthetic pathway of CDP-L-ascarylose. E_p (α -D-glucose cytidylyltransferase, ascA), E_{od} (CDP-D-glucose 4,6-dehydratase, ascB), E_1 (CDP-6-deoxy-L-threo-D-glycero-4-hexulose-3-dehydrase, ascC), E_3 (CDP-6-deoxy- $\Delta^{3,4}$ -glucoseen reductase, ascD), E_{ep} (CDP-3,6-dideoxy-D-glycero-D-glycero-4-hexulose-5-epimerase, ascE), and E_{red} (CDP-3,6-dideoxy-L-glycero-D-glycero-4-hexulose-4-reductase, ascF).

The mechanism of C-3 deoxygenation in the biosynthesis of 3,6-dideoxysugars is more complex than C-2 and C-6 deoxygenation because the scissile C–O bond is adjacent to the 4-keto group (**9**, Figure 1-5). Thus, C–O bond cleavage cannot be triggered by an initial α -proton abstraction event as in the cases of C-2 and C-6 deoxygenation. The C-3 deoxygenation reaction requires the pyridoxamine 5'-phosphate (PMP) cofactor of E_1 to form a Schiff base between the 4-keto group of **9**, followed by the abstraction at 4' hydrogen of PMP. This act triggers the expulsion of the C-3 hydroxyl group, giving **10** as the intermediate which then undergoes reduction catalyzed by E_3 .³⁰⁻³² E_3 reductase transfers two electrons from NADH to **10**, which resides in the active site of E_1 , through a relay system consisting of the FAD and [2Fe–2S] center in E_3 and the [2Fe–2S] center in

E_1 .^{25, 33} A radical intermediate **11**, more likely a sugar-PMP quinonoid species, could be detected by EPR spectroscopy.³⁴ This radical-stabilization role of PMP cofactor in the E_1/E_3 reaction is unprecedented, since most PMP/PLP-dependent enzymes employ anionic chemistry in their catalysis.^{35, 36} In the last step of E_1/E_3 catalysis, hydrolysis of the reduced species **12** gives the 3,6-dideoxyhexose product **13** and regenerates PMP. Because of the electron transfer property of E_1/E_3 , complex formation between the two proteins is anticipated and has been substantiated by *in vitro* and *in vivo* experiments.³⁷ Recently, another E_1/E_3 -like C-3 deoxygenation has been identified in the biosynthetic pathway of forosamine, a 4-dimethylamino-2,3,4,6-tetradeoxy-D-hexose found in insecticide spinosyns.³⁸ The C-3-dehydrase, SpnQ, shows good sequence homology to AscC (E_1), containing a PMP cofactor and [2Fe–2S] redox center. However, the lack of E_3 homologue in the spinosyn biosynthetic gene cluster and the successful demonstration of SpnQ activity using a common cellular reductase system (flavodoxin/flavodoxin reductase) strongly suggest that a specific reductase, like E_3 , is not necessary for SpnQ-catalyzed C-3 deoxygenation.

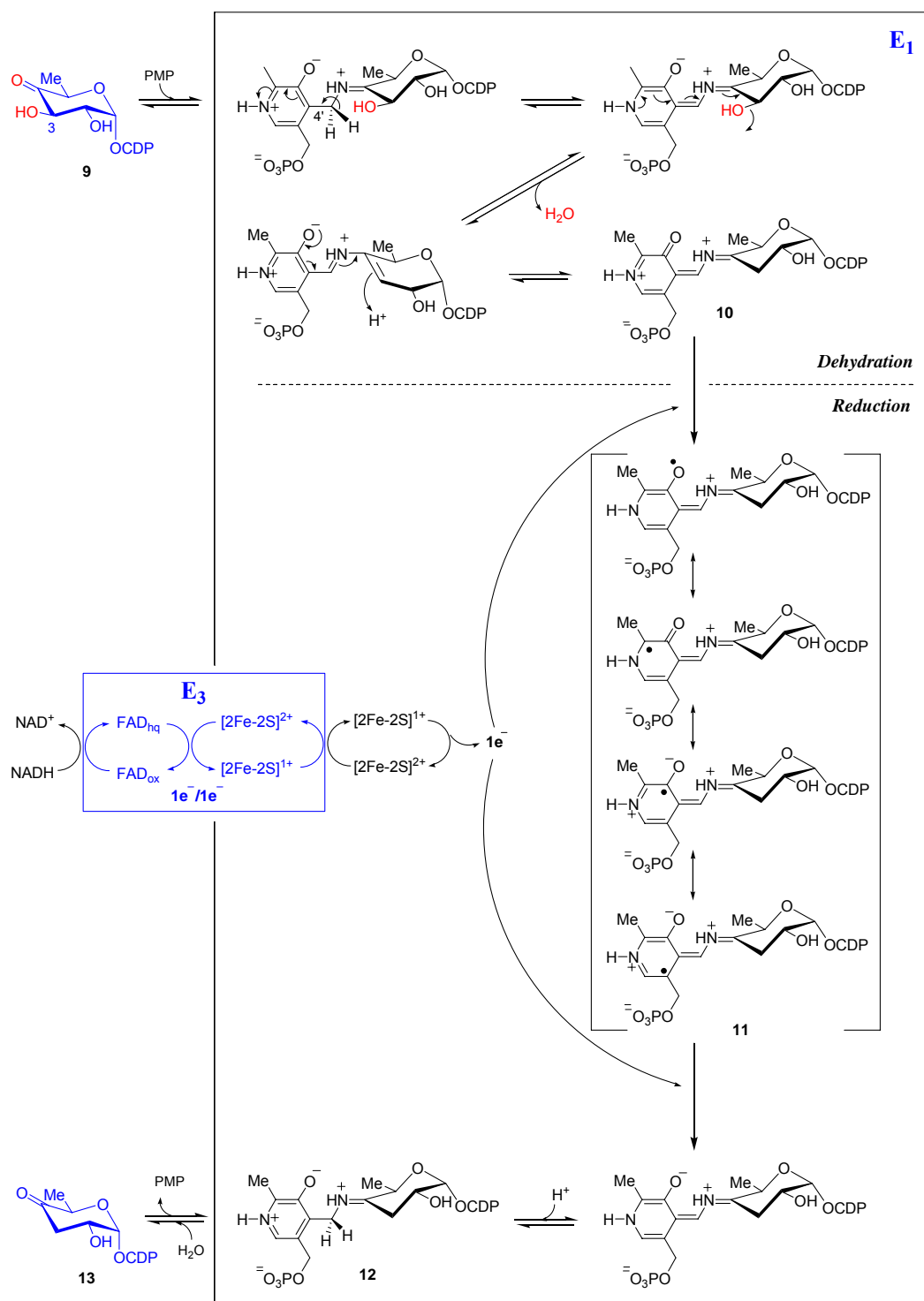


Figure 1-5 The proposed enzymatic mechanism of E₁/E₃ for C-3 deoxygenation of CDP-L-ascarylose biosynthesis.

L-Colitose (**15**) is a 3,6-dideoxyhexose found in the *O*-antigen of gram-negative lipopolysaccharides. The biosynthetic gene cluster of L-colitose has been cloned from *Yersinia pseudotuberculosis* VI and sequenced. The biosynthetic pathway was proposed to have four steps starting from GDP-D-mannose (**16**, Figure 1-6A).³⁹ In this pathway to **15**, the C-3 deoxygenation is catalyzed by ColD, an E₁-like PMP-dependent dehydrase. Interestingly, ColD shows some different characteristics as compared to E₁, in particular, the lack of a [2Fe–2S] center. It has transaminase activity capable of converting PLP and L-glutamate to PMP and α -ketoglutarate. From the study of ColD catalytic mechanism (Figure 1-6B), ColD was found to catalyze the same PMP-dependent E₁-like C-3 dehydration reaction, but using its aminotransferase activity to regenerate PMP cofactor instead of relying on a reductase partner as in the cases of E₁ and SpnQ.^{39, 40} These findings are a strong testament to the phenomena that enzymes catalyzing the same type of reaction may proceed via distinct mechanisms, highlighting the evolutionary diversity in biological deoxygenation events.

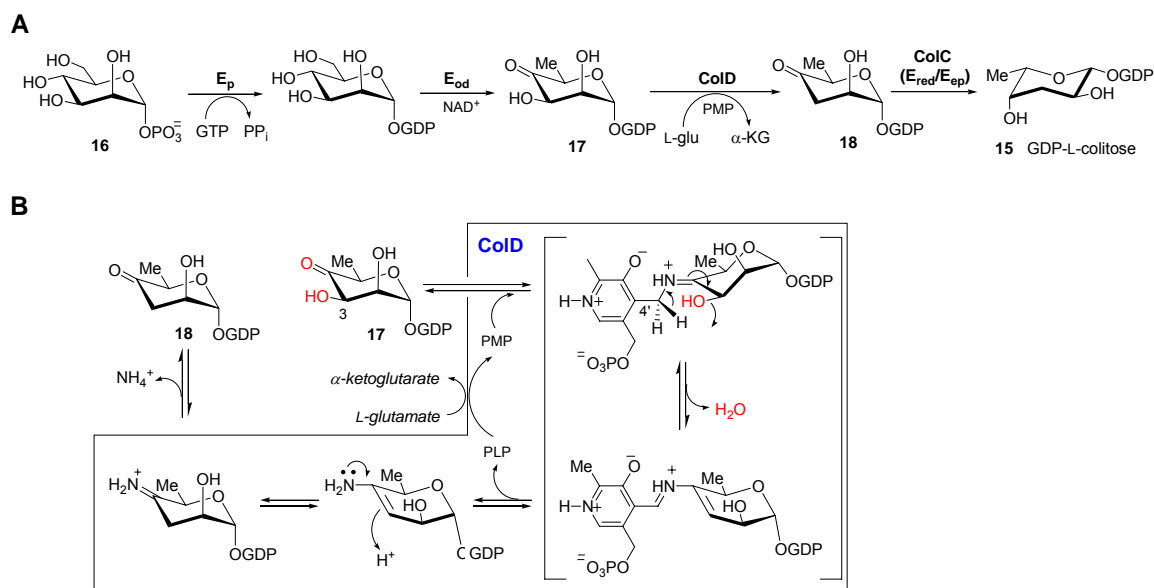


Figure 1-6 (A) The biosynthetic pathway of GDP-L-colitose. (B) Catalytic mechanism of C-3 dehydrase, ColD, in the GDP-L-colitose biosynthetic pathway.

2-5 C-4 Deoxygenation by DesI and DesII in the Biosynthesis of D-Desosamine

The conversion of TDP-6-deoxy-4-keto-D-glucose (**2**) into TDP-4,6-dideoxy-3-keto-D-glucose (**20**) is a key step in the biosynthesis of D-desosamine (**21**), a 3-dimethylamino-3,4,6-trideoxyhexose found in erythromycin (**22**), methymycin (**23**), pikromycin (**24**), and several other macrolide antibiotics (Figure 1-7A).^{41, 42} Studying the biosynthesis of D-desosamine in *Streptomyces venezuelae* has resulted in the identification of *desI* and *desII*, whose protein products are required for the C-4 deoxygenation step, in the methymycin/pikromycin gene cluster.^{43, 44} From the sequence alignment, *DesI* shows sequence homology to pyridoxal 5'-phosphate- (PLP) and L-glutamate-dependent C-4 aminotransferase. The function of DesI was later

confirmed by gene knock-out experiment and by *in vitro* activity assay with purified protein.⁴⁴ DesII, which contains a [4Fe-4S] consensus motif (CXXXCXXC), belongs to the recently identified radical *S*-adenosylmethionine (SAM) superfamily enzymes.⁴⁵ When DesI-product, TDP-4,6-dideoxy-4-amino-D-glucose (**19**), was incubated with DesII and SAM, **20** was identified as the sole TDP-sugar product.⁴⁶ These findings strongly suggest that the C-4 deoxygenation in D-desosamine biosynthesis proceeds in two independent steps, in which DesI catalyzes the C-4 transamination of **2** to **19**, and DesII carries out the subsequent oxidative deamination of **19** to give **20**.

The key mechanistic features of this reaction are reminiscent of those used in the reaction catalyzed by lysine 2,3-aminomutase (LAM), which is a [4Fe-4S]-containing enzyme that requires PLP, SAM and a reductase system (flavodoxin/flavodoxin reductase) for activity.⁴⁷⁻⁴⁹ Based on the mechanistic model of LAM and the results of DesI/DesII activity assays, two possible mechanisms of DesII-catalyzed reaction were proposed (Figure 1-7B).⁴⁶ As shown in the Figure, generation of the 5'-deoxyadenosyl radical (**25**) is expected to be the first step of the reaction catalyzed by the reduced [4Fe-4S]⁺ center as found in other radical-SAM-dependent enzymes.⁵⁰ Then, the radical **25** may trigger the abstraction of a hydrogen atom at C-3 of **19** to give **26**. The mechanism for the subsequent transformation is less obvious, but may parallel the reaction catalyzed by the coenzyme B₁₂ dependent ethanolamine ammonia lyase, which converts ethanolamine into ammonia and acetaldehyde.⁵¹ As shown in Figure 1-7B (path **a**), the key step may be a radical-induced deamination followed by the re-addition of ammonia to the resulting cation radical intermediate (**27**). Reclaiming a hydrogen atom from 5'-deoxyadenosine

results in the formation of **28** and the regeneration of **25**, or more likely the reduced [4Fe-4S]⁺-SAM complex. Elimination of an ammonium ion from **28** would afford the desired product **20**. On the other hand, the reaction may also involve deprotonation of the 3-hydroxy group of **26** to yield a ketyl radical anion (**29**), whose resonance form facilitates the β-elimination of the 4-amino group, probably in the ammonium ion form (Figure 1-7B, path **b**). The mechanism of path **b** is based on the reaction catalyzed by (*R*)-2-hydroxyacyl-CoA dehydratase, which involves a similar ketyl radical anion to expel a hydroxyl group.⁵²

2-6 Biosynthesis of aminosugars

Aminosugars are common structural components of a wide variety of glycoproteins, glycolipids and natural products. The amino groups on the sugar backbone can be further modified to the methylated, acetylated, or oxidized form. The replacement of a hydroxyl group with an amino group can significantly change the chemical nature of the parent sugar, such as the hydrogen bonding properties, the charge-bearing capability, and the overall hydrophobicity of the molecules. Therefore, aminosugars play important roles in the biochemical functions of many glycoconjugates.

One common transamination mechanism in aminosugar biosynthesis is the PLP-dependent aminotransfer between an amine donor and a ketosugar acceptor (Figure 1-8). Transfer occurs through two half-reactions, where in the first half-reaction the amino group is transferred from the donor, usually L-glutamate, to the PLP cofactor generating the α -keto acid (e.g., α -ketoglutarate) and the aminated cofactor, PMP (**30**). In the second half-reaction, the amino group is transferred from the PMP cofactor to the nucleotidyl keto sugar substrate forming the aminosugar and regenerating PLP cofactor. DesI is a typical example of an aminotransferase catalyzing the C-4 transamination to TDP-4-keto-6-deoxyhexose in the D-desosamine biosynthetic pathway. Dozens of such sugar transaminases have been identified from many natural product biosynthetic gene clusters of natural products. All these transaminases show high sequence-homology (>50% homology among 30 sequences), and can be divided into subclasses based on their sugar substrate structures (explained in details in Chapter 2).

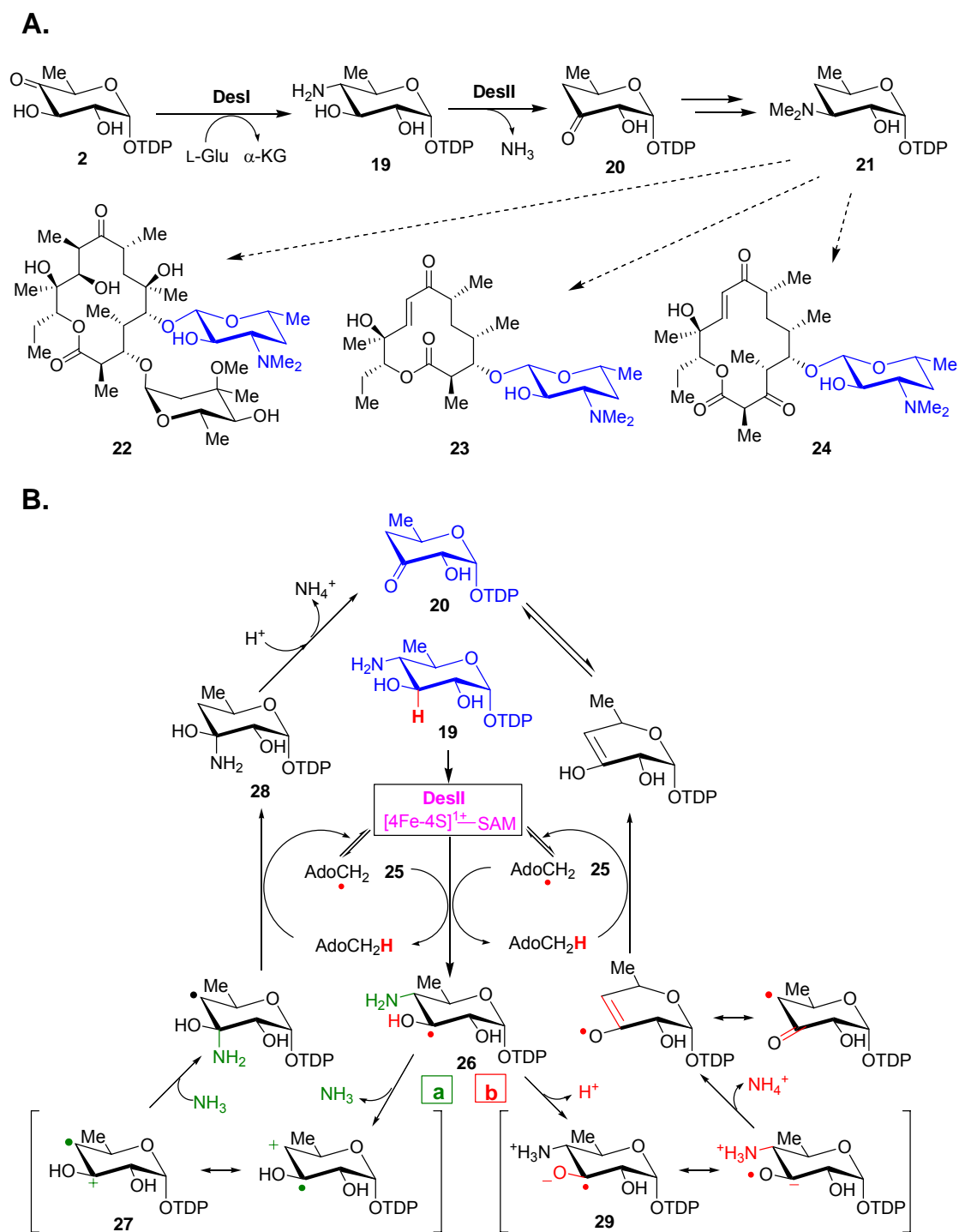


Figure 1-7 (A) The C-4 deoxygenation in the biosynthetic pathway of TDP-D-desosamine and macrolide antibiotics containing D-desosamine; (B) Possible mechanisms of DesII-catalyzed C-4 deamination reaction.

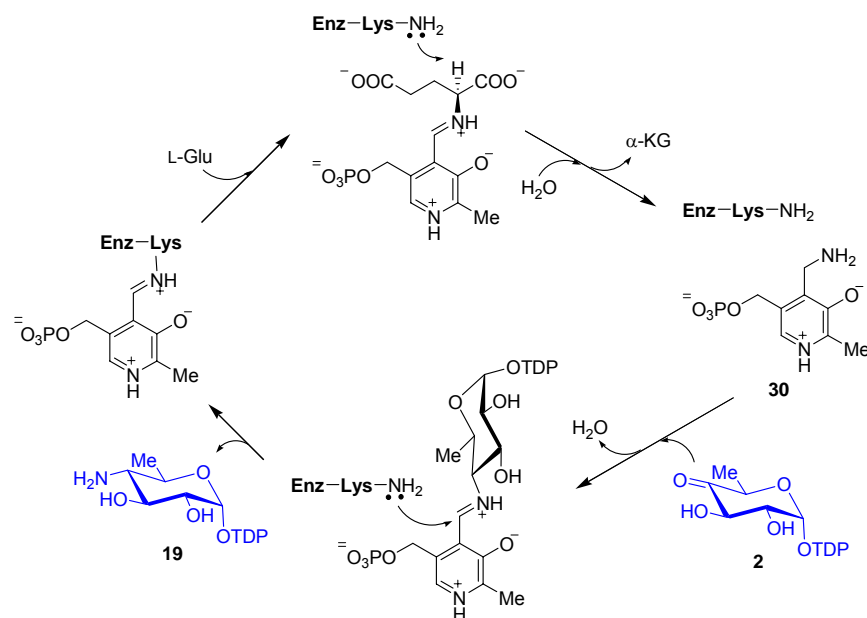


Figure 1-8 The catalytic mechanism of DesI, a C-4 aminotransferase of TDP-4-keto-6-deoxy-D-glucose (2)

Another type of C-N bond-formation mechanism is exemplified by the reaction catalyzed by glucosamine-6-phosphate synthase in the biosynthesis of glucosamine, a common aminosugar found in eukaryotic systems. Glucosamine-6-phosphate synthase, encoded by *glmS* in *E. coli*, catalyzes the conversion of D-fructose-6-phosphate (31) into D-glucosamine-6-phosphate (32). This enzyme (GlmS) exhibits high sequence homology to the amidotransferases that utilize the amide functional group of glutamine as the nitrogen source. The overall catalytic mechanism of this enzyme consists of two transformations: the hydrolysis of L-glutamine (33) to generate L-glutamate (34) and ammonia and the amination of D-fructose-6-phosphate which needs to be isomerized

from the ketose to an aldose form at the end of reaction (Figure 1-9). The ammonia which transfers from the glutaminase domain to the synthase domain cannot be substituted by exogenous NH_3 .⁵³ This result indicated that the glutamine hydrolysis and sugar aminating activities must be tightly coupled. It has been proposed that the glucosamine-6-phosphate synthase undergoes a conformational change upon binding of substrates to initiate the hydrolysis of **33**, and the nascent NH_3 is then channeled to the highly shielded acceptor site, where the amination reaction takes place. This hypothesis gained support recently by the elucidation of GlmS 3D-structure, which reveals the presence of an internal 18 Å channel connecting the two active sites.^{54, 55} An ordered binding of substrates, with the sugar binding occurs prior to the amino acid substrate, causes the closure of active sites in the same order. The closure of the L-glutamine (**33**) binding site also lifts the Trp74 residue blocking the ammonia channel.

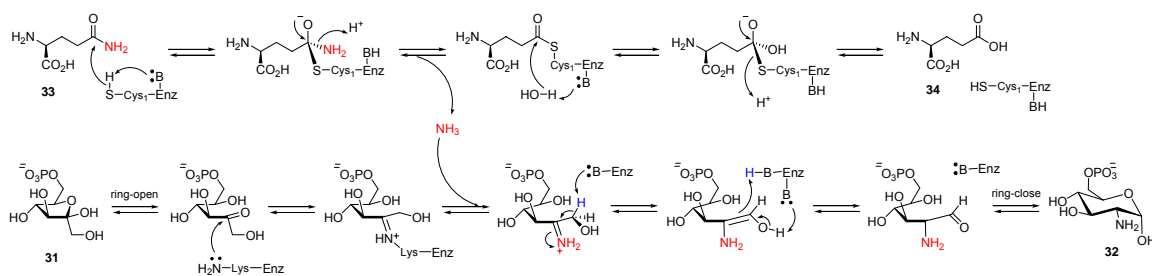


Figure 1-9 The catalytic mechanism of glucosamine-6-phosphate synthase

3. GLYCOSYLTRANSFERASES AND THEIR CATALYTIC MECHANISMS

To understand the functional basis of the incredibly diverse set of glycan

structures observed in nature is one of the central questions in glycol-biochemistry. What we know is that there are a myriad of glycosyltransferases, each with its own donor, acceptor and linkage specificity, which are responsible for the biosynthesis of these remarkably complex structures. Study of these glycosyltransferases has begun to shed new light on the biosynthesis of bacterial secondary metabolites and mammalian glycosylated macromolecules.^{6, 56} Moreover, the roles played by glycosyltransferases in the etiology of diseases, as well as their potential as therapeutic targets, are also now becoming more appreciated.⁵⁷⁻⁵⁹

3-1 The Variety of Glycosyltransferases

Carbohydrates are by far the most variable and complex of all biological polymers found in nature. The complexity and diversity of glycosylation arise from first, a vast variety of sugar donor substrates are used as building blocks by different glycosyltransferases. Second, the donor sugars can be attached to the acceptor molecules through *O*-, *N*-, or *C*-linkage. Third, the acceptor substrate of a glycosyltransferase may be a sugar molecule, a nucleic acid, a lipid, a topological protein epitope, or a natural product aglycone. Fourth, the glycosyltransferase-catalyzed reaction is regio- as well as stereospecific. For example, when the acceptor molecule is another sugar, different glycosyltransferases are required for transferring the same donor sugar to different hydroxyl groups on the same acceptor sugar. Finally, glycosyltransferases can exist as soluble globular proteins, integral membrane bound proteins, or as lipid-anchored enzymes in the intracellular environment. In the

eukaryotic cell, glycosyltransferases can reside in almost all cellular compartments including the inter-membrane space of mitochondria and chloroplasts.

Glycosyltransferases comprise a dominant fraction (approximately 1%) of expressed eukaryotic open reading frames. Their glycosylated products are required for many different biological functions, including development, signal transduction, and cell adhesion. They also provide both effectiveness and resistance to antibiotics, as well as afford molecular refuge from heat, dryness, and degradation. Due to the versatile characteristics of glycosyltransferases, they have been divided into many categories. Their classifications based on structure and function provide some fundamental information of each enzyme.

3-2 Classification of Glycosyltransferases

A vast number of glycosyltransferase sequences have been identified during the genome sequencing efforts in recent years. Thus, a large number of putative glycosyltransferase sequences are now available in the databanks. To correlate these sequences to protein structure, mechanism and specificity has attracted more attentions. Traditionally, glycosyltransferases, as with other enzymes, have been classified on the basis of their donor, acceptor and product specificity, according to the recommendations by the International Union of Biochemistry and Molecular Biology (IUBMB).⁶⁰ There are, however, several limitations to use this system for classification of glycosyltransferases (EC 2.4.x.y), such as substrate-promiscuity, and the lack of mechanistic and structural information. The major obstacle is because the functions of

most putative glycosyltransferases have not been verified.⁶¹

In 1997, Henrissat and colleagues proposed a new classification of glycosyltransferases by grouping them into families on the basis of similarities in amino acid sequence.⁶² Based on this classification, the Carbohydrate Active enZyme databank (CAZy) was established and has expanded to 90 families to date.⁶³ The resultant grouping of enzymes with different donor, acceptor or product specificity into polyspecific families provides useful insight into the divergent evolution of glycosyltransferase families. Most importantly, the molecular mechanism is conserved within a given family, which inspires strategies for the utilization of genomic information.

3-3 General Enzyme Mechanism of Glycosyltransferases

Functionally, glycosyltransferases can be divided into “retaining” or “inverting” enzymes, according to whether the stereochemistry of the donor’s anomeric bond is retained ($\alpha \rightarrow \alpha$) or inverted ($\alpha \rightarrow \beta$) during the transfer reaction (Figure 1-10A).⁶⁴ In the CAZy classification, every glycosyltransferase in each family has the same type of function.⁶¹ The retaining and inverting enzymes proceed via different mechanisms to account for the product stereochemistry (Figure 1-10B). However, no matter what type of reaction they catalyzed, both the retaining and inverting enzymes are thought to proceed through an oxocarbenium-ion-like transition state, similar to that proposed for glycosidase reactions.⁶⁵ The inverting reaction is mechanistically straightforward. It involves the nucleophilic attack on the non-hydroxylated face of the donor anomeric

carbon by the enzymatically deprotonated acceptor, releasing the diphosphonucleotide (a favorable leaving group) and resulting in inversion of the anomeric center (Figure 1-10B, path a).

There is more debate about the mechanism of the retaining reaction, which is still under debate. The favored model for the retention mechanism is the “double-displacement” model that involves two sequential S_N2 substitutions yielding a net retention of stereochemistry of the anomeric configuration of the donor sugar. This mechanism is initiated by a nucleophilic attack, probably by the enzyme, to form a covalent intermediate, which is subsequently attacked by the acceptor (Figure 1-10B, path b). However, doubts concerning the double displacement mechanism have arisen because of the inability to identify the inverted enzyme-sugar covalent intermediate. Another doubt concerning the double displacement mechanism is the lack of a strong nucleophile in the active site of the enzyme crystal structure of several retention enzymes.^{64, 66} Explanation for the latter concern is that glycosyltransferases often exhibit a high level of molecular motion and disorder in portions of their active sites, and thus it is possible that these disordered regions contain appropriate nucleophiles.

The other possible model is that the retaining enzymes may utilize an unusual S_N2 -like mechanism called S_Ni (Figure 1-10B, path c).⁶⁷ Mechanistically, it forms a similar oxocarbenium-ion transition state as the inverting enzymes, though the nucleophilic attack by the acceptor comes from the same side of the anomeric carbon as the leaving group resides. Such a mechanism is not without merit, although it is extremely rare and still lacks supporting evidence.

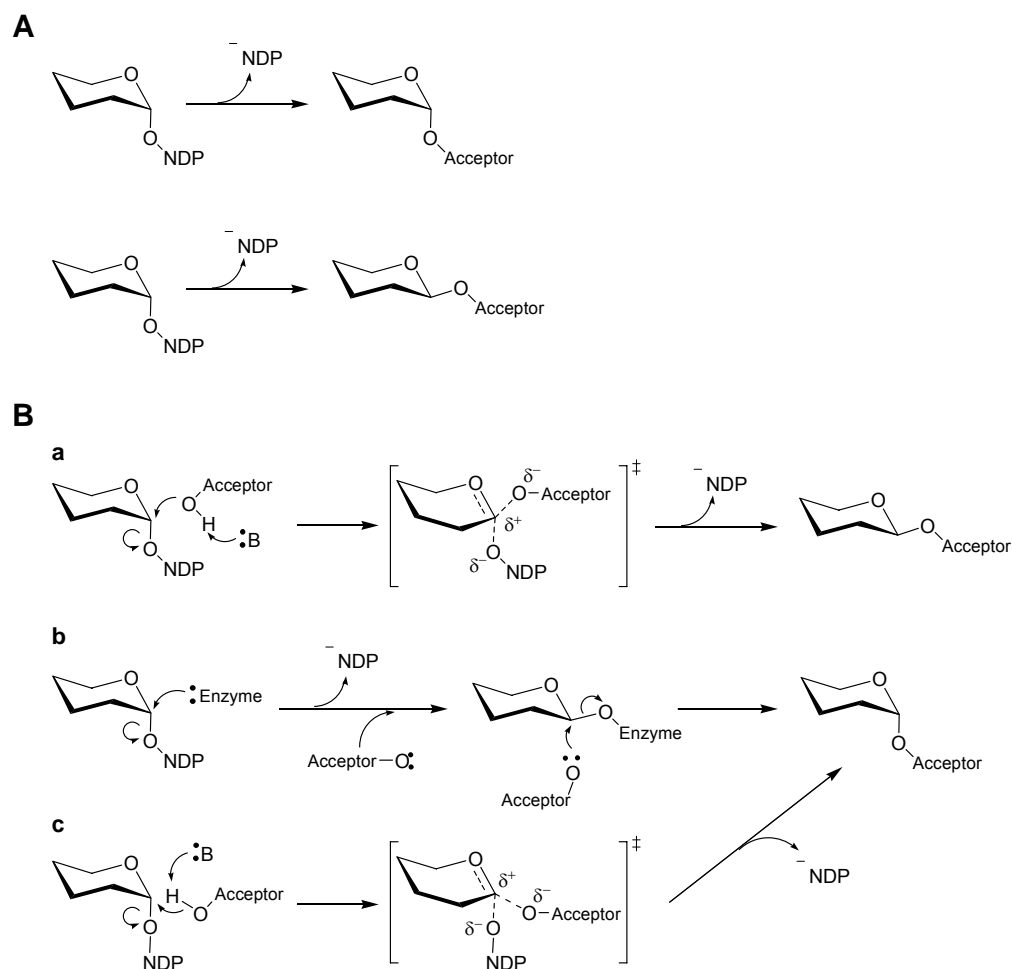


Figure 1-10 Glycosyltransferases are separated into two functional classes (A), and the proposed mechanisms for inverting (a) and retaining (b, c) glycosyltransferases (B).

3-4 Folding Types and Structures of Glycosyltransferases

As mentioned before, approximately 1% of the genes in all sequenced genomes are found to be glycosyltransferases, which are categorized into 90 families. Before mid-1999, only one glycosyltransferase structure was solved, and today, 27

glycosyltransferase families have members whose structures have been determined.^{64, 66} Clearly, significant advances have been made in the last few years. However, the structures of the representative glycosyltransferases of many other families remain to be elucidated. The slow progress of this effort can be attributed to their membrane-associated character, low expression levels, and dynamic conformation in solution. But even with the limited number of available glycosyltransferase structures, it is already possible to deduce a few general principles to categorize enzyme structures and to correlate structures to enzyme functions.

In eukaryotes, most glycosyltransferases are resident membrane proteins of the endoplasmic reticulum and the Golgi apparatus where they participate in the synthesis of complex glycans.⁵⁶ These membrane-bound glycosyltransferases are type II transmembrane proteins consisting of a short amino-terminal cytoplasmic domain followed by a transmembrane stem region, and a large globular catalytic domain facing the luminal side. Soluble or membrane-associated GT forms are also present in the eukaryotic cellular compartments. They are synthesized in the same manner as the membrane-bound proteins and released by proteolytic cleavage in the stem region. Prokaryotic glycosyltransferases are not strictly regulated by their cellular localization, although some show similar membrane-associated properties as eukaryotic GTs.^{68, 69}

Except the membrane-associated regions, the catalytic domains of most glycosyltransferases display one of the two major folding types designated GT-A or GT-B (Figure 1-11).^{61, 66} Examples of retaining and inverting enzymes having either the GT-A and GT-B type fold are known, thus this structural characteristic does not directly

correlate to the stereospecificity of the reaction. The GT-A fold (Figure 1-11A) may be considered as two tightly associated and adjoining $\beta/\alpha/\beta$ domains that tend to form a continuous central sheet consisting of at least eight β -strands (hence, some people called this as a single domain fold). The GT-A enzymes share a common metal-binding DxD (Asp-X-Asp) motif, which coordinates the diphosphate moiety of the diphosphonucleotidyl (NDP) sugar donor through a divalent metal ion, usually Mn^{2+} .⁷⁰ Also shared among the inverting GT-A members is a structurally equivalent carboxylate, Asp or Glu, which acts as a catalytic base to deprotonate the hydroxyl group of the receptor. The GT-B fold (Figure 1-11B) displays two Rossmann-like $\beta/\alpha/\beta$ domains. But unlike the tightly associated GT-A fold, the two domains are usually separated by a wide deep crevice when the enzyme is not bound with substrates. This is referred to as the unliganded “open” conformation.⁷¹ Enzymes with the GT-B type fold have been suggested to proceed with a step-wise reaction mechanism, where substrate binding in the “open” form is expected to induce a conformational change through main chain rotations to generate the “closed” form to correctly align the sugar donor and the acceptor in the active site for catalysis. Based on the limited structural data, the nucleotide moiety of sugar donor appears to bind to the N-terminal domain of the GT-A enzymes and to the C-terminal domain of the GT-B enzymes, with the corresponding acceptor binds to the other domain.^{64, 72}

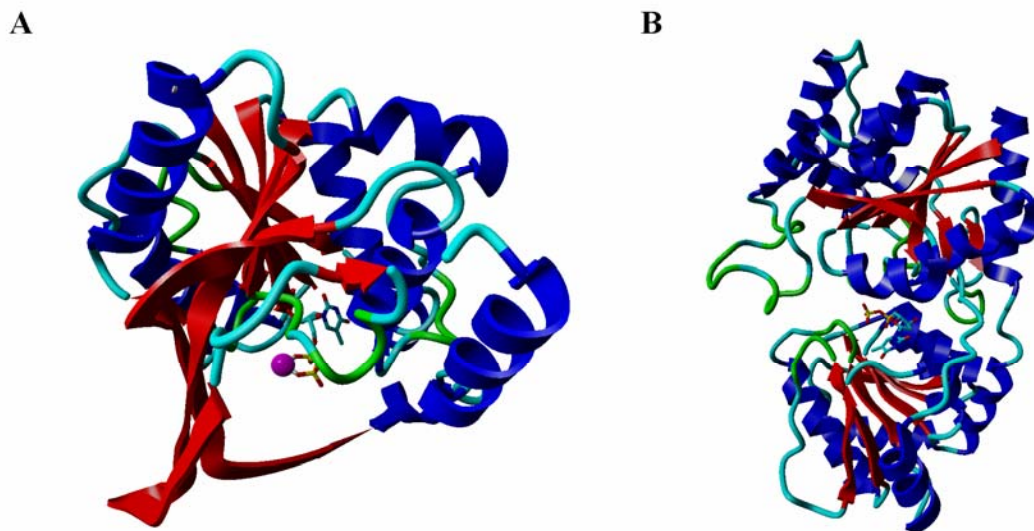


Figure 1-11 The two typical glycosyltransferase folds. (A) GT-A fold, from *Bacillus subtilis* SpsA;⁷³ (B) GT-B fold, from *Amycolatopsis orientalis* A82846 GtfA.⁷²

In addition to the two typical folds of glycosyltransferases, there are two minor groups of folding, GT-C and GT-D folds, that have been described in the literature.^{74, 75} Because the catalytic centers of GT-C and GT-D proteins reside within the transmembrane loops, these proteins are intrinsically difficult to crystallize. Currently, there is no structurally characterized example of either the GT-C or GT-D fold types. Recently, the crystal structures of the peptidoglycan glycosyltransferase (PGT) domains from different organisms have been resolved. Interestingly, their crystal structures exhibit a different fold from all other glycosyltransferase structures known so far.^{76, 77} It shows some structural resemblance to λ -lysozyme, an enzyme that degrades the carbohydrate chains of peptidoglycan, and implicates a processive elongation model for

glycan chain polymerization.

3-5 Natural Product Glycosyltransferases

Natural product glycosyltransferases belong to the GT-2 family, whose members retain a GT-B fold and carry out glycosylation via an inverting mechanism.⁶ Recent studies have shown that many natural product GTs are substrate-flexible, allowing them to be used both *in vivo* and *in vitro* to catalyze the attachment of alternate sugars to natural product aglycones.⁷⁸ The substrate flexibility of natural product GT is not only observed for the donor substrate (NDP-sugar) but also for the acceptor substrate (aglycone or glycosylated acceptor). For example, the glycosyltransferase DesVII of the methymycin/pikromycin biosynthetic pathway transfers the D-desosamine group from TDP-D-desosamine (**21**) to the aglycone acceptor, 10-deoxymethynolide (**35**) or narbonolide (**36**), in the presence of DesVIII. In the *in vitro* DesVII/DesVIII glycosylation studies, seven different sugar donors and five aglycones, including **35** and **36**, were recognized and processed by DesVII to generate various new glycosylated products (Figure 1-12).⁷⁹ The high substrate-promiscuity of these natural product glycosyltransferases makes them good catalysts to vary the glycosylation patterns of known glycosides.

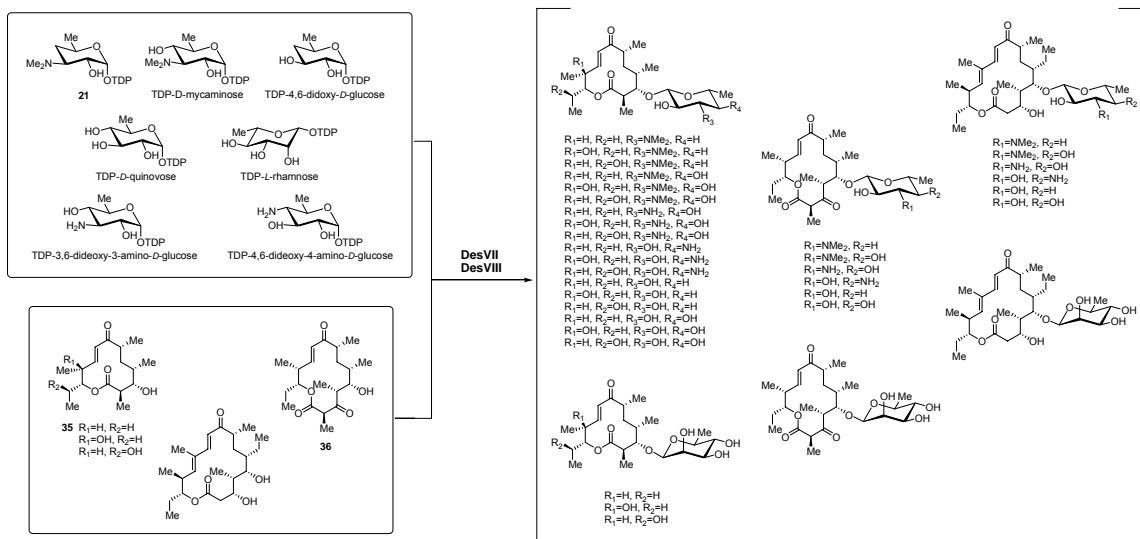


Figure 1-12 *In vitro* substrate specificity study of glycosyltransferase DesVII

Recently, the Eguchi and Thorson research groups demonstrated that several natural product glycosyltransferases are capable of catalyzing the reverse reactions *in vitro*.^{80, 81} In the presence of a glycosylated natural product and NDP, these glycosyltransferases can generate the corresponding NDP-sugar and aglycone. VinC is a glycosyltransferase catalyzing the transfer of TDP-vicenisamine (37) to vicenilactam (38) in the last step of vicenistatin (39) biosynthesis (Figure 1-13A). In the reaction containing 39, TDP, and VinC, the products of this reverse reaction, 37 and 38, were isolated from the mixture although the percentage of conversion was low.⁸¹ Interestingly, UDP could also be used as the nucleotidyl diphosphate substrate to generate the non-natural nucleotidyl sugar, UDP-vicenisamine. When other aglycones were added into the above reverse reaction mixture, different β -linked vicenisaminides were generated in the one-pot aglycone-switch reaction. Similar behaviors were also

observed for the glycosyltransferases, CalG1 (Figure 1-13B) and CalG4, from the calicheamicin biosynthetic pathway and GtfD and GtfE from the vancomycin biosynthetic pathway.⁸⁰ Thus, the reversibility of the glycosyltransferase-catalyzed reaction could provide easy access to various NDP-sugars for *in vitro* studies. Moreover, this reversibility can be exploited to perform one-pot sugar and aglycone exchange reactions to produce various unnatural glycosylated derivatives for glycobiology and glycochemistry research.^{82, 83}

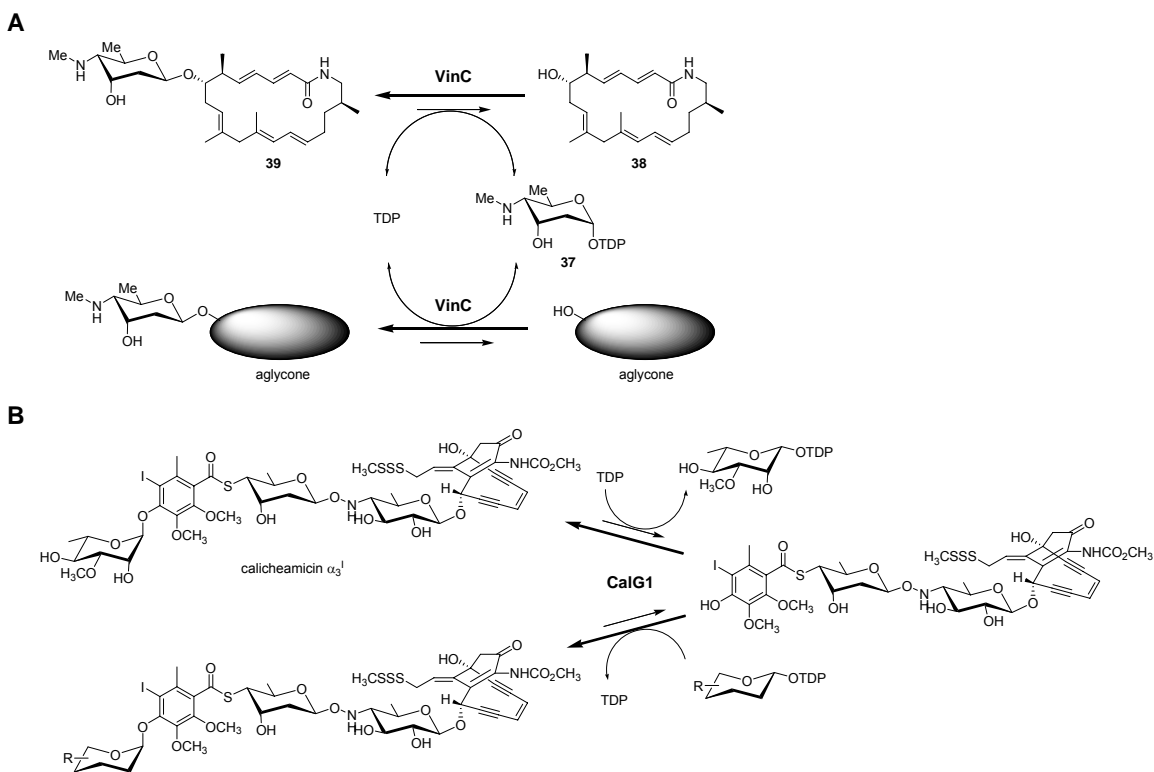


Figure 1-13 Aglycone-swap (**A**) and sugar-swap (**B**) catalyzed by reversible GTs

4. NATURAL PRODUCT BIOSYNTHETIC ENGINEERING AND GLYCODIVERSIFICATION

The importance of sugar residues in the biological activities of natural products and the increasing resistances against existing therapeutic glycosides have urged the development of technologies and strategies for the glycosylation of secondary metabolites. Decades of research have led to the identification of more than 100 natural product biosynthetic gene clusters, and the characteristics of many sugar biosynthetic enzymes and glycosyltransferases. Several *in vitro* and *in vivo* strategies have also been developed to manipulate these biosynthetic machineries to generate new glycosides, which may possess therapeutic potential (Figure 1-14).

For *in vitro* synthesis of glycosylated compounds, the availability of various NDP-sugar and aglycone substrates is crucial to the success of this approach. Several different strategies were developed in the past few years to generate diverse pools of NDP-activated deoxysugars, varying from complete enzymatic synthesis to full organic synthesis, which includes the hydrolysis of available natural products followed by chemical activation of the resulting sugar moieties.⁸⁴ Recently, small libraries of NDP-sugars have also been made by *in vitro* glycorandomization that uses engineered substrate-flexible anomeric sugar kinases and nucleotidyltransferases (E_p) for the conversion of diverse sugars to their NDP-activated forms (Figure 1-14A).⁸⁵ The size of the NDP-sugar library could be expanded when the starting sugar bears functional groups that can be later modified by chemical methods (e.g. click chemistry). In addition, the discovery of the reversible properties of glycosyltransferases provides an alternative

strategy to synthesize NDP-sugars, and also allows directly glycodiversification through aglycone-swap or sugar-swap (Figure 1-14B).

Microorganisms producing glycosylated compounds can be used as cellular factories to generate new glycosylated compounds. Generally, *in vivo* natural product biosynthetic engineering can be divided into three categories: precursor-directed biosynthesis, mutational biosynthesis, and combinatorial biosynthesis. Precursor directed biosynthesis involves feeding analogues of a building block known to be used in the biosynthesis of a natural product to the producing organism to effect structural changes in the final product.⁸⁶ Several variations have been documented, including feeding chemically modified aglycones, structurally related natural aglycones, or the starter unit analogues for building aglycones to a glycoside-producing strain to alter the glycosylation patterns (Figure 1-14C). Mutational biosynthesis involves the biosynthetic gene disruptions leading to the accumulation of biosynthetic intermediates which may be used as the building blocks to couple with the feeding analogue to make new products in the mutant organisms (Figure 1-14D). The advantage of this method over precursor-directed biosynthesis is that the feeding analogue, which is often not a very competent substrate, does not need to compete with the natural building block. The manipulation of the TDP-D-desosamine biosynthetic machinery in the methymycin/pikromycin biosynthetic pathway of *S. venezuelae* is a good example of mutational biosynthesis to make new glycosylated macrolides. As shown in Figure 1-15A, individual disruption of four TDP-D-desosamine biosynthetic genes, *desI*, *desII*, *desV* and *desVI*, led to the formation of new macrolide analogues **38-41** carrying sugars

corresponding to the accumulated TDP-D-desosamine pathway intermediates **2**, **19**, **20** and **37**.^{43, 44, 87, 88}

Combinatorial biosynthesis, or metabolic engineering, involves alterations of the original sugar biosynthetic genes of the producing hosts or introduction of sugar biosynthetic genes of different pathways from other glycoside producers to generate new glycosylated compounds.⁸⁹ For example, the expression of gene cassettes encoding TDP-D-dihydrostreptose biosynthetic genes (*strM* and *strL*) from *Streptomyces griseus*, or TDP-D-mycaminose (**43**) biosynthetic genes (*tyllA*) from *S. fradiae* in a mutant of the TDP-D-desosamine producing *S. venezuelae* lacking a functional *desI* gene (*KdesI*) led to new methymycin/pikromycin derivatives bearing L-rhamnose (**42**) or D-mycaminose (**44**), respectively (Figure 1-15B).^{90, 91} A non-producer host could also be endowed with the capability to synthesize new glycosylated products by introducing complete cassettes of biosynthetic genes of nucleotidyl sugars and aglycones.^{92, 93}

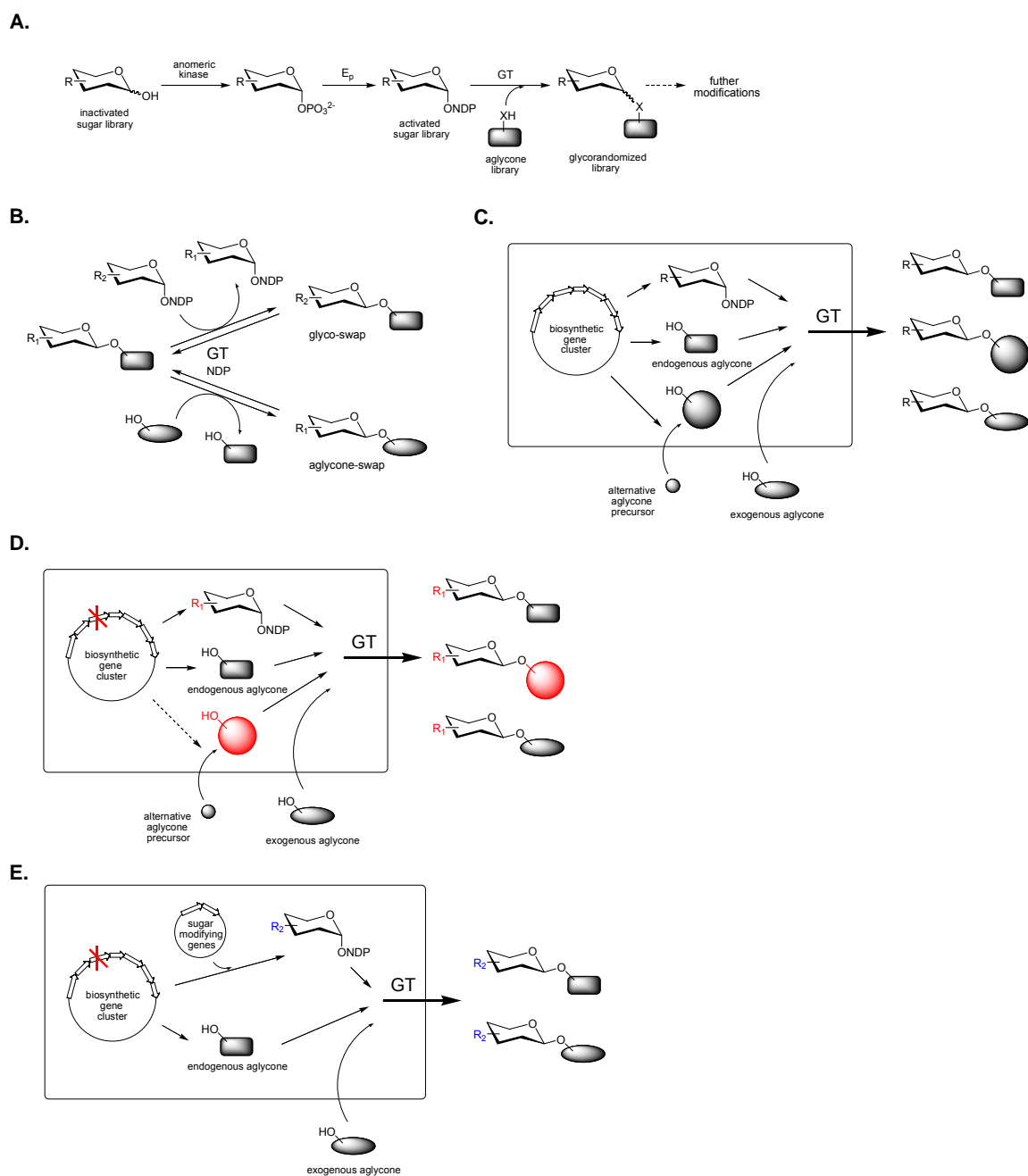


Figure 1-14 Natural product biosynthetic engineering (A) *in vitro* glycorandomization, (B) glycodiversification by reversible GTs, (C) precursor-directed biosynthesis, (D) mutational biosynthesis, (E) combinatorial biosynthesis

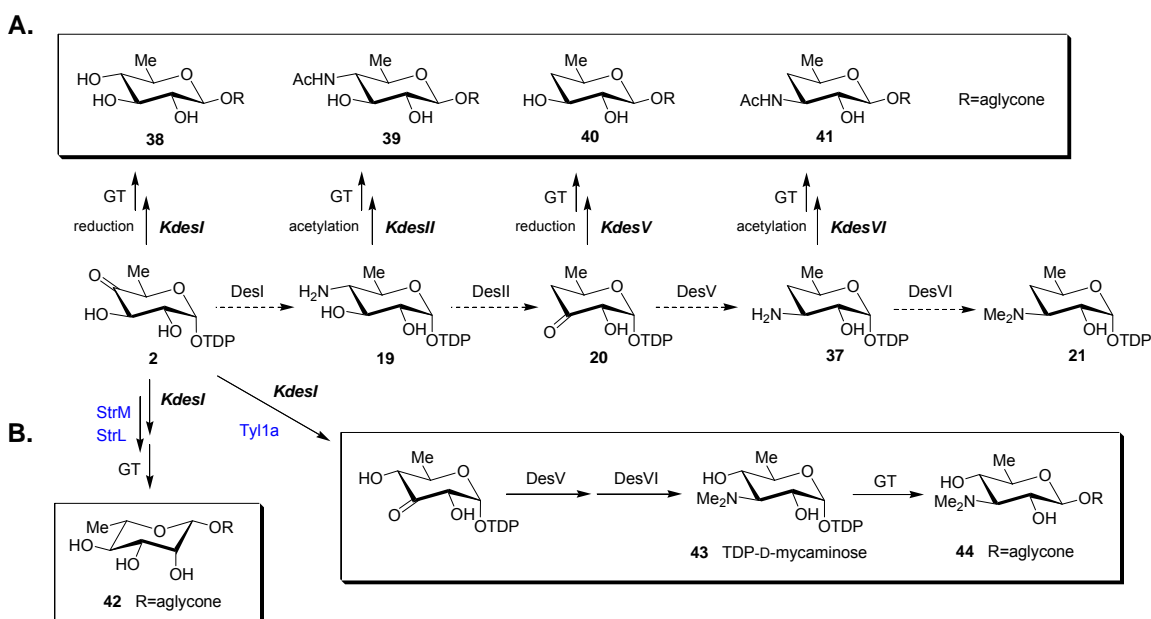


Figure 1-15 Metabolic engineering of TDP-D-desosamine biosynthetic pathway **(A)** mutational biosynthesis, glycodiversification by biosynthetic intermediates **(B)** combinatorial biosynthesis

Clearly, the increasing knowledge regarding sugar biosynthesis pathways in natural product-producing organisms together with the rapidly growing understanding of the biosynthetic enzymes and glycosyltransferases have provided exciting new tools for the generation of glycosylated derivatives of secondary metabolites. The usage of *in vitro* and *in vivo* sugar-biosynthetic engineering approaches, as applied to either glycoside-producing organisms or to non-producing heterologous strains, holds great potential for the structural diversification of glycosylated natural products. The reassembly of nature's biosynthetic machinery has clearly opened up a new area of carbohydrate research, and has expanded natural product glycodiversification for the development of new therapeutic agents.

5. THESIS STATEMENT

Since a significant portion of current drugs are glycosylated natural products, studies of the biosynthesis of unusual sugar residues in nature and the catalytic properties of the natural product glycosyltransferase have attracted much attention in recent years. The advance of modern molecular biological techniques has revolutionized the research of natural product biosynthesis. The work described in this dissertation focuses on the elucidation of an unusual nitro sugar biosynthetic pathway and the characterization of the helper proteins required for the activity of a group of natural product glycosyltransferases.

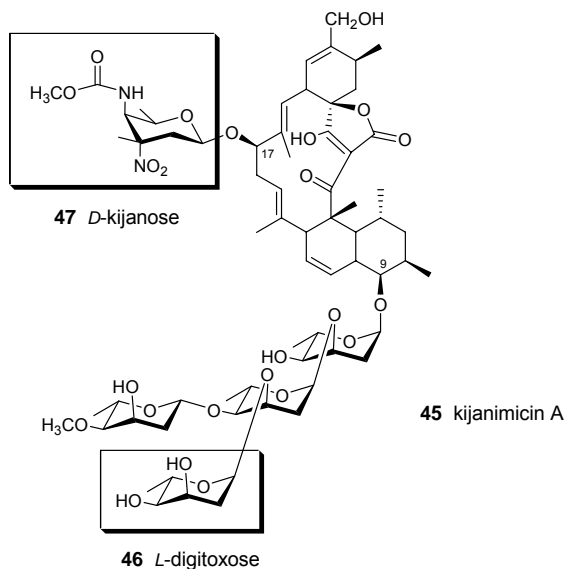
Nitro containing compounds are rare in nature. The attempt to elucidate the nitro sugar biosynthesis in Chapter 2 will not only allow us to decipher nature's strategies for making this unusual functional group, but may also provide important enzymatic tools for drug development in the future. Unveiling the function of auxiliary proteins for glycosyltransferases in Chapter 3 will expand our knowledge about the catalytic properties of macrolide glycosyltransferases, which are essential for glycodiversification applications.

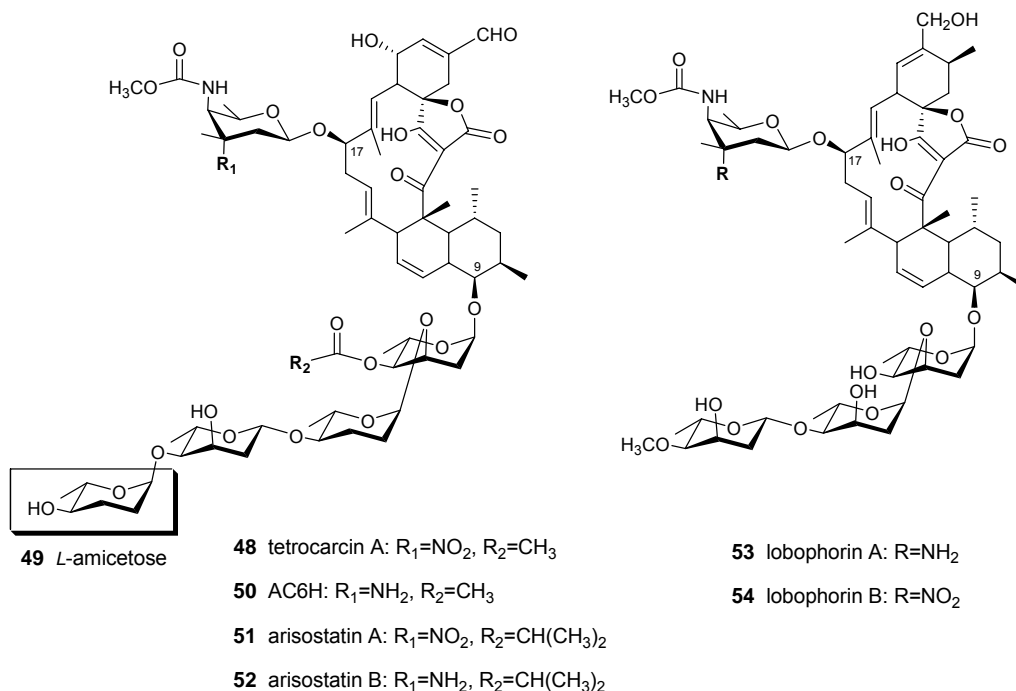
Chapter 2. Biosynthetic Studies of D-Kijanose in Antibiotic

Kijanimicin from *Actinomadura kijaniata*

1. INTRODUCTION

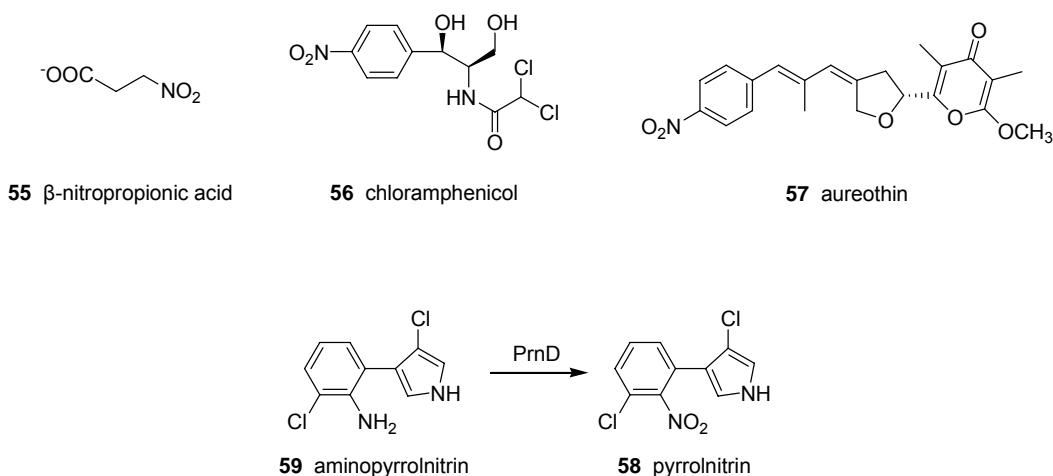
Kijanimicin (**45**) is a member of spirotetronate antibiotic produced from *Actinomadura kijaniata*, an actinomycete bacterium isolated from an African soil sample.⁹⁴ Like other spirotetronate antibiotics, kijanimicin shows antimicrobial activity against Gram-positive bacteria, especially *Bacillus subtilis*, and anaerobes, *Propionibacterium acnes*, but not active against either Gram-negative bacteria or fungi.⁹⁵ It also demonstrates strong antimicrobial activity against rodent malaria *in vivo*. In addition to its antibiotic activities, kijanimicin shows antitumor activities, which commonly occurs in other spirotetronate antibiotics.⁹⁶





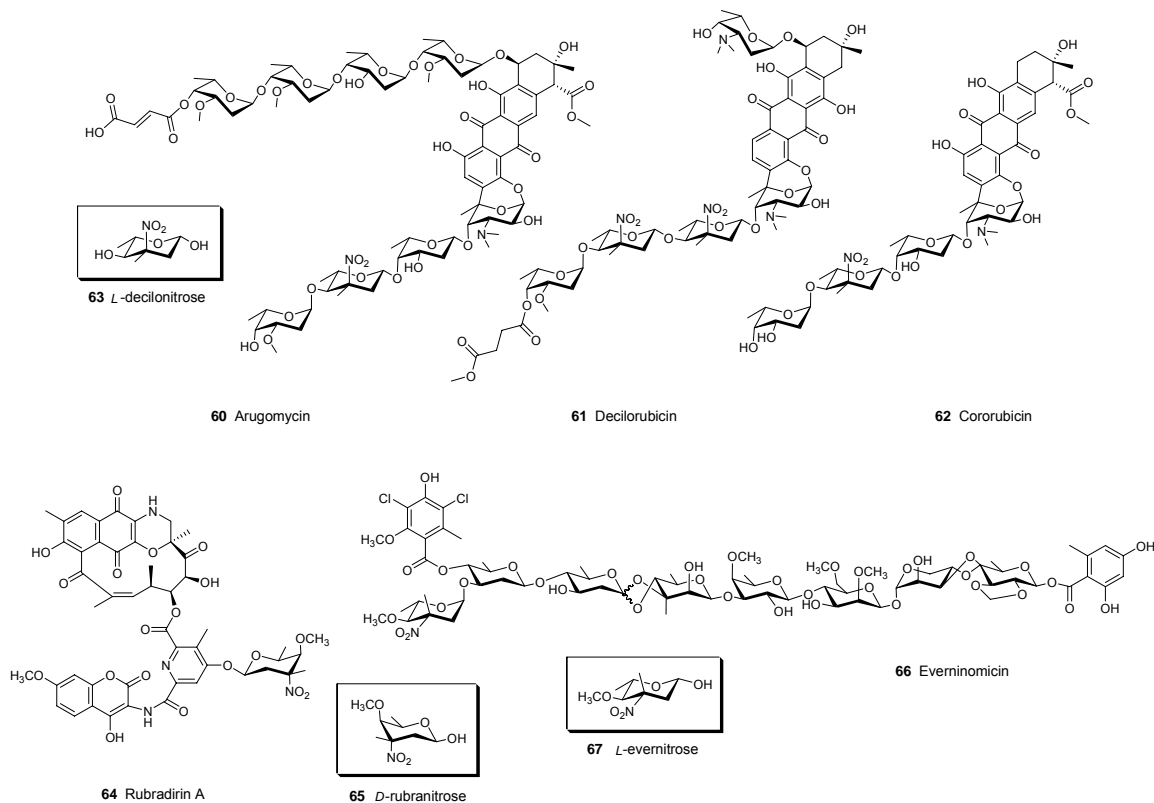
The chemical structure of kijanimicin (**45**) consists of a pentacyclic- tetrone acid core, which is attached by four units of L-digitoxose (**46**) and a rare nitro sugar, 2,3,4,6-tetradeoxy-4-(methoxycarbonylamino)-3-C-methyl-3-nitro-D-xylo-hexopyranose, commonly known as D-kijanose (**47**).⁹⁷⁻⁹⁹ Several kijanimicin-related spirotetronate-type compounds have been identified, and their structures have been determined. Tetrocarcin A (**48**), isolated from *Micromonospora chalicea* KY11091, contains a similar tetrone acid core, a tetra-saccharide unit (two L-digitoxose, two L-amictose (**49**)) at C-9, and the same D-kijanose attached to C-17.¹⁰⁰⁻¹⁰² Another compound, antlermicin A, has exactly the same structure as tetrocarcin A, but from a different bacterial strain, *Micromonospora chalicea* subsp. T-90.¹⁰³ Like kijanimicin,

tetrocarcin shows strong inhibitory activity against *Bacillus subtilis*, moderate activity against *Staphylococcus aureus*, but no activity against Gram-negative bacteria or fungi. Besides antibiotic activity, tetrocarcin also demonstrates antitumor activity against P388 leukemia.¹⁰⁴ Interestingly, a tetrocarcin-related antibiotic, AC6H (**50**), isolated from *Micromonospora carbonaceae* K55-AC6, differs only by an amino group that replaces the nitro group at C-3' of D-kijanose in tetrocarcin A. The alteration of this key functional group difference causes AC6H to have lower antitumor activity.¹⁰⁵ Arisostatin A (**51**) and arisostatin B (**52**), isolated from *Micromonospora* sp. TP-A0316, have similar compositions as tetrocarcin A and AC6H, respectively, where arisostatin A carries the 3'-nitro sugar and arisostatin B carries the 3'-amino sugar. Arisostatin B exhibits lower antibacterial activity and antitumor activity than arisostatin A.^{106, 107} Lobophorins A (**53**) and B (**54**), isolated from a marine actinomycete associating with the brown alga *Lobophora variegata*, have one less L-digitoxose than kijanimicin A. Lobophorins A (amino-) and B (nitro-) do not exhibit significant antibiotic properties. However, both compounds show equally potent anti-inflammatory activities.¹⁰⁸ In several recent studies, tetrocarcin A and arisostatin A were found to induce apoptosis in human tumor cell-lines.¹⁰⁹⁻¹¹² Obviously, these D-kijanosyl spirotetronate compounds possess a broad spectrum of pharmacological potential worthy of further exploitation. The cumulated evidence suggests that the nitro functional group of D-kijanose plays a determinant role in the therapeutic activity.



Only a handful of natural compounds containing nitro groups have been isolated, and even fewer of them have their biosynthetic pathways characterized or key enzymes identified.¹¹³ A fungal metabolite, β -nitropropionic acid (**55**), derived from L-aspartate by the oxidation of the amino to the nitro group in *Penicillium atrovenerum*, is a neurotoxin that blocks the mitochondrial respiratory chain reactions.^{114, 115} However, the amino-oxidation enzyme of β -nitropropionic acid has not been identified yet. Chloramphenicol (**56**), a common antibiotic derived from the bacterium *Streptomyces venezuelae*, possesses a *p*-nitro-benzyl and a dichloroacetyl component in its chemical structure. Although the biosynthetic gene cluster of chloramphenicol has been identified, the oxidation enzyme converting the *p*-amino to *p*-nitro benzyl group is still unknown.¹¹⁶ Aureothin (**57**), an unusual pyranone metabolite from *Streptomyces thioluteus*, has a broad spectrum of biological activities including antitumor, antimicrobial and insecticidal properties. Like chloramphenicol, aureothin possesses a *p*-nitro-benzyl group derived by the oxidation of the corresponding *p*-amino-benzyl group.

Surprisingly, the *N*-oxygenase, AurF, does not show any homology to known oxidoreductases, and neither common motifs nor cofactor-binding sites could be identified by database searches.¹¹⁷ Pyrrolnitrin (**58**), another nitro-group-containing antifungal agent, is produced by several species of soil bacteria. The enzyme catalyzing the oxidation of its precursor, aminopyrrolnitrin (**59**), has been identified and this oxygenase, PrnD, is a [2Fe-2S] Rieske oxygenase.^{118, 119}



Besides the D-kijanose-possessing spirotetronates, there are several other natural products containing unusual nitro-sugars, although their biosynthetic pathways have not been determined. For example, anthracycline antibiotics, composed of a

tetra-hydro-naphthacene-dione core and one to several sugar residues, are chemotherapeutic agents used to treat a broad range of cancers. Some anthracyclines carry these rare nitro-sugar moieties. Arugomycin (**60**), decilorubicin (**61**), and cororubicin (**62**) have similar chemical structures and carry the same unusual nitro sugar, L-decilonitrose (**63**).¹²⁰⁻¹²² Rubradirin A (**64**) is another anthracycline compound which possesses a different nitro sugar, D-rubranitrose (**65**).^{123, 124} Moreover, L-evernitrose (**67**), a stereoisomer of D-rubranitrose (**65**), is found in the oligosaccharide antibiotic, everninomicin (**66**).^{125, 126} From the chemical point of view, L-decilonitrose (**63**), D-rubranitrose (**65**), L-evernitrose (**67**), and D-kijanose (**47**) share structural similarities. Namely, they are all deoxygenated at C-2', C-3', and C-6', and all have a C-methyl group and a nitro group at the C-3' position. Due to their structural similarity, the biosynthetic pathways of these nitro sugars may share some common steps catalyzed by homologous enzymes, especially at the early steps of deoxygenation and C-3' modification.

The kijanimicin (**45**) biosynthetic gene cluster has recently been identified and cloned from the *Actinomadura kijaniata* genome by our research group (unpublished data). The entire gene cluster covers the length of 107.6 kb containing 44 open reading frames (ORFs) (Figure 2-1). Comparing the amino acid sequences of the ORFs to the database, 35 ORFs have been assigned to the kijanimicin biosynthetic genes which include the polyketide synthase genes, the sugar-biosynthetic genes, and several genes responsible for the tailoring and ring-closing of the spirotetronate aglycone core (Table 2-1).

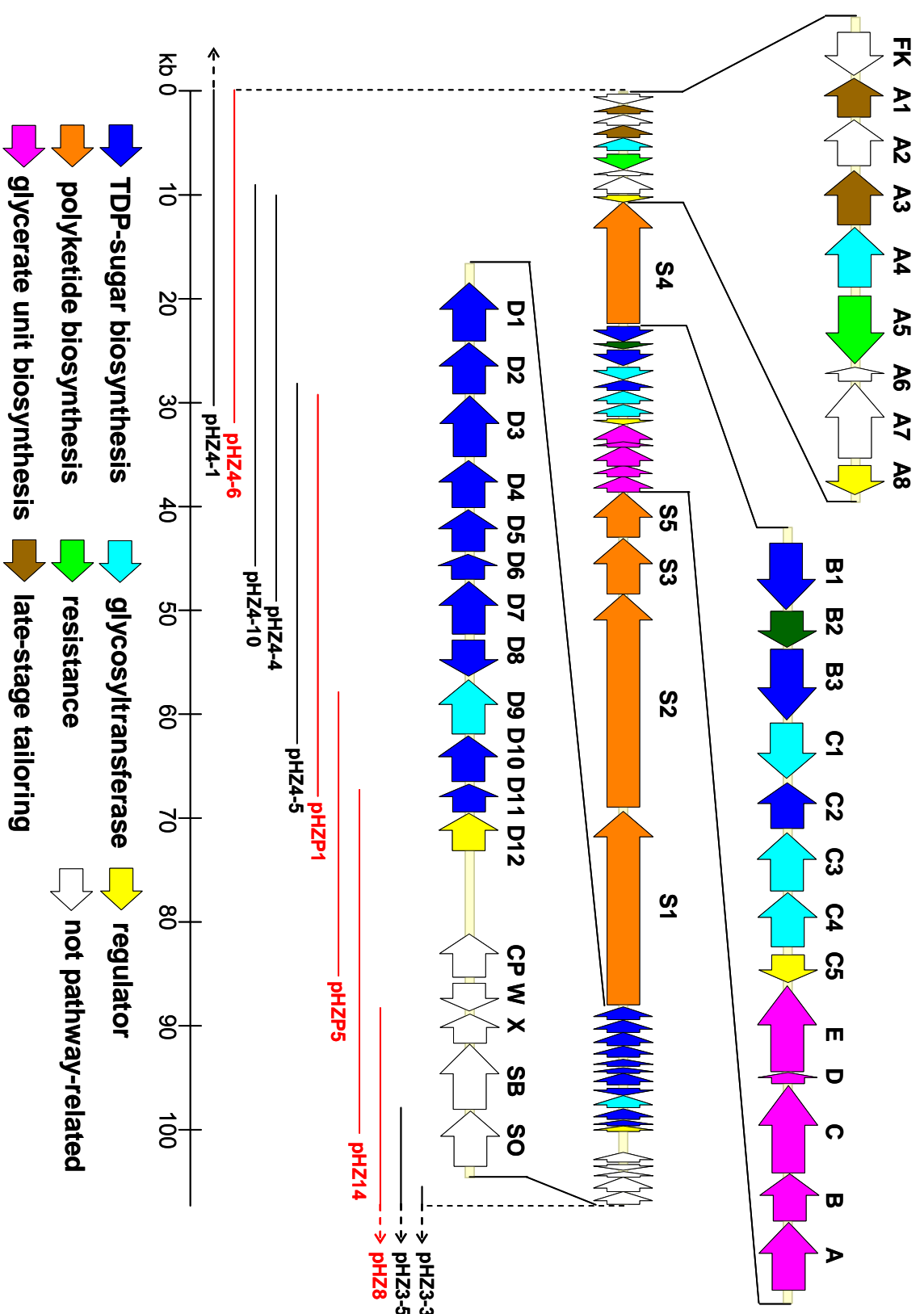


Figure 2-1 The map of kijanimicin biosynthetic gene cluster and carrying cosmid fragments

Gene name	BLAST assigned function	Step catalyzed
kijA1	Sugar-O-methyltransferase	4-O-methylation of terminal digitoxose and/or kijanose?
kijA2	Oxidoreductase/Aldo/ketoreductase	Formation of methylcarboxylamino group of kijanose?
kijA3	P450 monooxygenase	Hydroxylation of aglycone methyl group
kijA4	glycosyltransferase	digitoxosyltransferase
kijA5	Efflux permease	Kjanimicin export
kijA6	Heat shock protein GroES	Not pathway related
kijA7	Heat shock protein GroEL	Not pathway related
kijA8	Tet ^R type regulatory protein	Pathway regulation
kijS4	Polyketide synthase	PKS modules 9, 10
kijB1	Sugar 2,3-dehydratase	Digitoxose, kijanose biosynthesis
kijB2	thioesterase	PKS editing or release of linear polyketide chain
kijB3	FAD-dependent oxidoreductase	Formation of methylcarboxylamino group of kijanose?
kijC1	glycosyltransferase	digitoxosyltransferase
kijC2	Sugar 4-ketoreductase	Digitoxose biosynthesis
kijC3	glycosyltransferase	digitoxosyltransferase
kijC4	glycosyltransferase	digitoxosyltransferase
kijC5	Tet ^R type regulatory protein	Pathway regulation
kijE C-terminus	α/β hydrolase superfamily – putative hydrolase/acyltransferase	Oxidation of glyceryl-KijD to pyruvyl-KijD?
kijE N-terminus	Dihydrolipoamide acyltransferase homolog	Closure of aglycone lactone ring?
kijD	ACP	Glycerate carrier protein
kijC	FkbH homolog	Attachment of 1,3-BPG-derived glycerate to KijD
kijB	Ketoacyl acylcarrier protein synthase III	Attachment of glycerol-derived unit to growing PKS chain?
kijA	FAD-dependent oxidoreductase	Aglycone cyclization to form spirotetronate?
kijS5	Polyketide synthase	PKS Module 11
kijS3	Polyketide synthase	PKS Module 8
kijS2	Polyketide synthase	PKS Modules 4-7
kijS1	Polyketide synthase	PKS Loading, modules 1-3
kijD1	Sugar 3-C-methyltransferase	Kijanose biosynthesis
kijD2	Sugar-3-aminotransferase	Kijanose biosynthesis
kijD3	FAD-dependent oxidoreductase	amine oxidation of kijanose
kijD4	Eod (sugar 4,6-dehydratase)	Digitoxose, kijanose biosynthesis
kijD5	Ep (sugar nucleotidyltransferase)	Digitoxose, kijanose biosynthesis
kijD6	NADPH-dependent flavin reductase	Supplies reduced flavin to KijD3
kijD7	Sugar-4-aminotransferase	Kijanose biosynthesis
kijD8	SAM-dependent methyltransferase	N-methylation of C-4 amine of kijanose or O-methylation of carboxylamino group of kijanose?
kijD9	glycosyltransferase	kijanosyltransferase
kijD10	Sugar 3-ketoreductase	Digitoxose biosynthesis
kijD11	Sugar 5-epimerase	Digitoxose biosynthesis
kijD12	Tet ^R type regulatory protein	Pathway regulation

Table 2-1 Proposed gene functions of ORFs within the kjanimicin gene cluster

With the kijanimicin biosynthetic gene cluster in hand, the biosynthetic pathway of D-kijanose can be proposed based on the assigned enzyme functions and knowledge learned from previous studies of related deoxysugar biosynthesis. In addition, the putative enzymes of D-kijanose biosynthesis can be cloned, overexpressed, and examine their functions *in vitro*. The intended goal to study D-kijanose biosynthesis will not only explore nature's strategy of making nitro-sugars, but will also expand the repertoire of sugar biosynthesis for the engineering of sugar biosynthetic pathways in the future. Pharmaceutically, more secondary metabolites containing nitro-sugars may be synthesized through combinatorial biosynthesis for the treatments of infectious diseases and cancers.

2. EXPERIMENTAL PROCEDURES

General. General experimental procedures for molecular cloning and protein sodium dodecyl sulfate polyacrylamide gel electrophoresis (SDS-PAGE) followed standard laboratory protocols.¹²⁷⁻¹²⁹ Enzymes and DNA size-standard marker used for molecular cloning experiments were purchased from Invitrogen (Carlsbad, CA) or New England Biolabs (Ipswich, MA), except for *pfu* DNA polymerase, which was the product of Stratagene (La Jolla, CA). All reagents for SDS-PAGE and Bio-gel P2 resin were purchased from Bio-Rad (Hercules, CA), with the exception of the prestained protein molecular weight marker, which was purchased from New England Biolabs. The Western-blotting membrane, HybondTM-C Extra, was purchased from Amersham Biosciences (Piscataway, NJ). The antibodies for Western-blotting were purchased from Sigma-Aldrich Chemicals. (St. Louis, MO), and the detecting BCIP/NBT substrate was the product of Promega. (Madison, WI). Amicon Ultra-15 Centrifugal Filter Units, and YM-10 and YM-30 ultrafiltration products were purchased from Millipore (Billerica, MA). Protein dialysis membranes were purchased from Spectrum (Gardena, CA). The protein dyeing reagent for Bradford assay was purchased from BioRad. Antibiotics and chemicals were purchased from Fisher Scientific (Pittsburgh, PA) or Sigma-Aldrich Chemicals. Oligonucleotide primers for cloning were prepared by either Integrated DNA Technologies (Coralville, IA) or Invitrogen (Carlsbad, CA). Growth media components were obtained from Becton Dickinson (Sparks, MD).

Plasmids and Vectors. Cosmid pHZ14, containing the putative D-kijanose biosynthetic cluster from *A. kijaniata*, was used as the template for amplification of *kijD1*,

kijD2, *kijD3*, *kijD6* and *kijD7* by the polymerase chain reaction (PCR). Cosmid pHZ4-6 was used as the template for PCR amplification of *kijB1*. Both of the cosmids were constructed by Dr. Hua Zhang of our group. The *E. coli* protein expression vectors, pET-24b(+) and pET-28b(+) were purchased from Novagen (Madison, WI).

Bacterial Strains. *E. coli* DH5 α from Invitrogen (Carlsbad, CA) was used as the host for routine cloning. *E. coli* BL21 and BL21(DE3) from Novagen (Madison, WI) were used as the hosts for the overexpression of recombinant proteins.

Instrumentation. The pH values were measured using a Corning pH meter 240 from Fisher Scientific. Agarose gel electrophoresis was conducted using a mini-sub cell GT apparatus from Biorad (Richmond, CA) which was powered by either a FB600 or a FB300 power supply from Fisher Scientific. Centrifugation procedures were performed using either an Avanti J-25 or Avanti J-E unit from Beckman-Coulter (Arlington Heights, IL) for large volumes, or using an Eppendorf 5415C microcentrifuge from Brinkmann Instruments (Westbury, NY) for small volumes. Photography of agarose gels was carried out with a Kodak EDAS 290 apparatus connected to a PC running Kodak 1D 3.5 software using a FBTIV-88 transilluminator from Fisher Scientific. PCR was performed using an Eppendorf Mastercycler Gradient from Brinkman Instruments. HPLC separations were performed using a Beckman 366 instrument (Beckman Instruments, Fullerton, CA). Adsorbosphere SAX analytical HPLC column (5 μ , 4.5 \times 250 mm) was obtained from Alltech (Deerfield, IL). Analytical (4 \times 250 mm) and semi-preparative (9 \times 250 mm) CarboPacTM PA1 HPLC columns were obtained from Dionex (Sunnyvale, CA). FPLC was acquired from Amersham Biosciences, and Mono-Q H/R 16/10 FPLC

columns were purchased from Pharmacia (Uppsala, Sweden). Mini-PROTEAN II vertical system used for SDS-PAGE, Mini Trans-Blot Cell used for blotting transfer, GelAir gel drying system, and the accessories and reagents used for SDS-PAGE were products of BioRad. Ultraviolet-visible spectra were obtained using a Beckman DU-650 spectrophotometer. Cell disruption was performed using a Fisher 550 Sonic Dismembrator. DNA sequencing was carried out by the Core Facilities of the Institute of Cellular and Molecular Biology at the University of Texas at Austin. Mass spectra were obtained by the Mass Spectrometry Core Facility in the Department of Chemistry and Biochemistry at the University of Texas at Austin. NMR spectra were acquired on either a Varian Unity 300 or 500 MHz spectrometer, and chemical shifts (δ in ppm) are given relative to those of solvent peaks. Coupling constants are reported in hertz (Hz).

Preparation of Competent Cells. Competent cells were prepared using the rubidium chloride (RbCl) method. Specifically, a single fresh colony of the appropriate *E. coli* strain was used to inoculate 2 mL of Luria-Bertani (LB) liquid medium and the resulting culture was grown overnight at 37 °C with constant shaking at 250 rpm. A 250 μ L aliquot of an overnight culture was transferred to 50 mL of the LB medium in a 250 mL Erlenmeyer flask. Till the cell grew at 37 °C to an OD₆₀₀ of approximately 0.4, the culture was transferred into a pre-chilled polypropylene tube and chilled on ice for 30 min. After centrifugation at $3,000 \times g$ for 12 min at 4 °C, the supernatant was discarded, and the cell pellet was gently resuspended in one-third (15 mL) the original culture volume of ice-cold RF1 solution (100 mM RbCl, 15% glycerol, 50 mM MnCl₂, 30 mM potassium acetate, 10 mM CaCl₂, pH 5.8, filter sterilized by passage through a 0.22 μ m

membrane). After incubation on ice for 15 min, the cell suspension was centrifuged again at $3,000 \times g$, 4 °C for 12 min, and the resulting cell pellet was resuspended in two twenty-fifths (4 mL) of the original culture volume of ice-cold RF2 solution (10 mM RbCl, 10 mM MOPS, 75 mM CaCl₂, 15% glycerol, pH 6.8). The cell suspension was then aliquoted into 100 µL portions in sterilized pre-chilled microcentrifuge tubes and frozen at -80 °C.

PCR Primers. Oligonucleotide primers for cloning were prepared by either Integrated DNA Technologies (Coralville, IA) or Invitrogen (Carlsbad, CA). Two oligonucleotide primers complementary to the sequences at each end of the DNA fragment to be amplified were designed and the appropriate restriction enzyme sites were incorporated when appropriate. Several primer design rules were obeyed. First, each primer must have at least 18 base pairs exactly matching the bases of the template (genome) sequences. Second, the melting temperatures (T_m) of the portion of the primer pair complementary to the target sequence and of the entire primer sequence of the primer pair were matched as closely as possible to ensure efficient annealing throughout the reaction. If restriction enzyme recognition sites were engineered into the primers, a two to four base pair variable sequence was added to the 5' end of the primer, depending on the restriction enzyme. Additionally, primer pairs were checked using NetPrimer[®] available on the PREMIER Biosoft Int. Website (<http://www.premierbiosoft.com/>) to ensure that stable secondary structures, self-dimers and hetero-dimers do not occur in the chosen sequences. The primer pairs for each open-reading frame are listed in Table 2-2. In *kijD7* cloning, the primer with the *NdeI* site was used as the forward primer for both

pET-24b(+) and pET-28b(+) cloning, and the primers with *Xho*I and *Sac*I sites were used as the reverse primers for the pET-24b(+) and pET-28b(+) vectors, respectively.

Gene	Cloning Site	Primer Sequence
<i>kijD1</i>	<i>Nde</i> I	5'- TCG CATATG ACCGGACCGACCGAC -3'
	<i>Eco</i> RI	5'- TG GAATTC TCAGAGCACGCGCACCTC -3'
<i>kijD2</i>	<i>Nde</i> I	5'- GGG CATATG ACGACTCGCGTATGG -3'
	<i>Bam</i> HI	5'- AC GGATCC CGGGTCACAGGTCCGCCA -3'
<i>kijD3</i>	<i>Nde</i> I	5'- GCAC CATATG CCCCCATGGACGGCAC -3'
	<i>Hind</i> III	5'- TCAT AAGCTT TCACCGTGACGTGGGTGTAG -3'
<i>kijD6</i>	<i>Nde</i> I	5'- GCAC CATATG GCGACGCGCCGCGCTG -3'
	<i>Hind</i> III	5'- GGCC AAGCTT ATTCGGTGGTGAACCGC -3'
<i>kijD7</i>	<i>Nde</i> I	5'- AGGT CATATG ATCAACGTAACCCAGC -3'
	<i>Sac</i> I	5'- AGCG GAGCTC TCAGGCGGCCGGGTTCAC -3'
	<i>Xho</i> I	5'- GCCG CTCGAG GGCGGCCGGGTTCACGCCGGG -3'
<i>kijB1</i>	<i>Nde</i> I	5'- GTGA CATATG AGCGCCATCCTCGGCC -3'
	<i>Xho</i> I	5'- CCG CTCGAG CCAGAGAGAACTCAGGCAG -3'

Table 2-2 Primer pairs for cloning the putative D-kijanose biosynthetic genes

PCR Amplification of DNA. Although the procedure used for successful PCR amplification of each DNA fragment varied slightly, a general procedure for primer design and PCR amplification is given here. A polymerase-mediated amplification was routinely carried out in a 0.5 mL thin-walled microcentrifuge tube. A typical 50 μ L reaction mixture consisted of 28 μ L of deionized water, 5.0 μ L of 10 \times *pfu* polymerase buffer, 5.0 μ L of deoxyribonucleotide triphosphate (dNTP) mix (2.5 mM each dNTP), 5.0 μ L of DMSO, 2.5 μ L of each of the primers (10 μ M stock concentration), 1.0 μ L of the

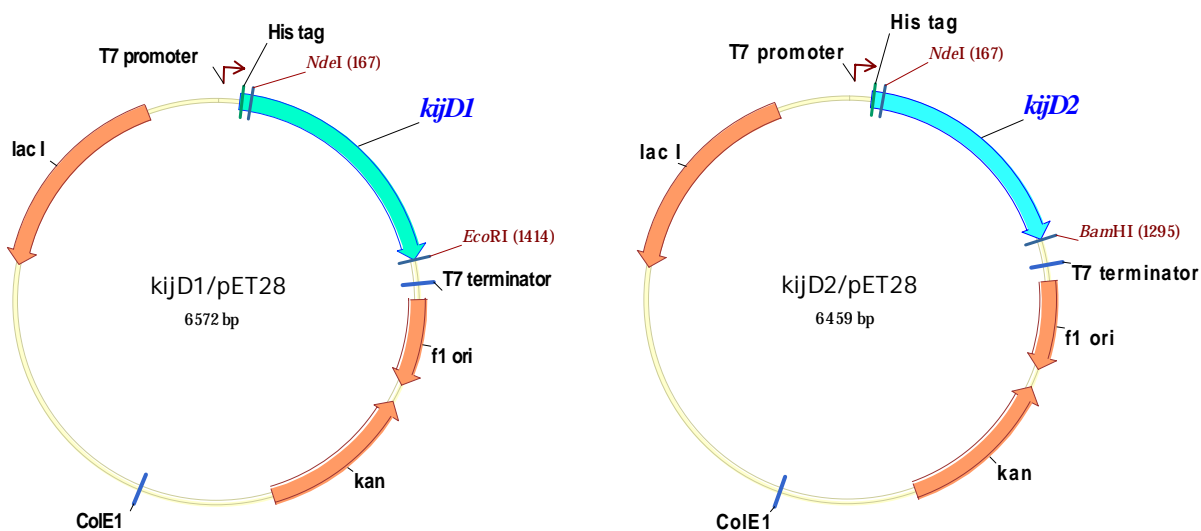
template DNA (approximately 0.1 µg), and 1.0 µL of the cloned *pfu* polymerase (2.5 units, Invitrogen). The reaction mixture was mixed thoroughly by pipette and subjected to the following thermal cycling conditions: (1) 1 cycle of incubation at 95 °C for 5 min; (2) 35 cycles of incubation at 95 °C for 30 s, appropriate annealing temperature for 30 s, and 72 °C for one minute per kilo-bases of target DNA length, where annealing temperature is 3-5 °C lower than the lowest T_m of primers used in the reaction (usually, the annealing temperature is either 55 °C, 58 °C, or 60 °C); (4) 72 °C for 10 min. The tubes were held at 4 °C prior to being removed from the thermal cycler.

Cloning of the Putative D-kijanose Biosynthetic Genes. After PCR amplification, 50 µL of the reaction mixtures were electrophoresed on a 0.8% agarose gel to check the size and yield of the products. The major product of each reaction, which should match the desired size of DNA, was excised from the agarose gel and extracted by the Perfectprep[®] Gel Cleanup kit (Brinkmann, NY). For each purified PCR DNA fragment, 1 µg of PCR product and its cloning vector were both digested with appropriate restriction enzymes at 37 °C for 1 hour. The restriction enzymes and vectors used for each construct are listed in Table 2-3. For the digested vector to be cloned, 0.5 µL of calf intestinal alkaline phosphatase (CIAP; 20 units/µL; Invitrogen, CA) was added to the digesting tube and the reaction tube was incubated for 30 more minutes. After digestion, both PCR product and vector DNA were electrophoresed on a 0.8% agarose gel and excised for purification with Perfectprep[®] Gel Cleanup kit. After purification, the digested PCR product and vector were ligated by DNA ligase. The ligated plasmid containing the PCR-amplified biosynthetic gene was then transformed into *E. coli* DH5α

competent cell by heat-shock. The transformed cells were spread onto LB medium plates containing the appropriate antibiotics and incubated at 37 °C overnight. The newly constructed plasmids carried by the grown colonies were extracted and examined with restriction enzyme digestion and DNA sequencing. The constructed plasmid maps of the putative D-kijanose biosynthetic genes are shown in Figure 2-2.

Plasmid	Gene	Vector	Cloning Site	His ₍₆₎ -tag
kijD1/pET-28	<i>kijD1</i>	pET-28b(+)	<i>NdeI/EcoRI</i>	<i>N'</i> -terminus
kijD2/pET-28	<i>kijD2</i>	pET-28b(+)	<i>NdeI/BamHI</i>	<i>N'</i> -terminus
kijD3/pET-28	<i>kijD3</i>	pET-28b(+)	<i>NdeI/HindIII</i>	<i>N'</i> -terminus
kijD6/pET-28	<i>kijD6</i>	pET-28b(+)	<i>NdeI/HindIII</i>	<i>N'</i> -terminus
kijD7-c/pET-24	<i>kijD7</i>	pET-24b(+)	<i>NdeI/XhoI</i>	<i>C'</i> -terminus
kijD7-n/pET-28		pET-28b(+)	<i>NdeI/SacI</i>	<i>N'</i> -terminus
kijB1-c/pET-24	<i>kijB1</i>	pET-24b(+)	<i>NdeI/XhoI</i>	<i>C'</i> -terminus
kijB1-nc/pET-28		pET-28b(+)	<i>NdeI/XhoI</i>	<i>N',C'</i> -terminus

Table 2-3 Plasmid constructs containing the putative D-kijanose biosynthetic genes



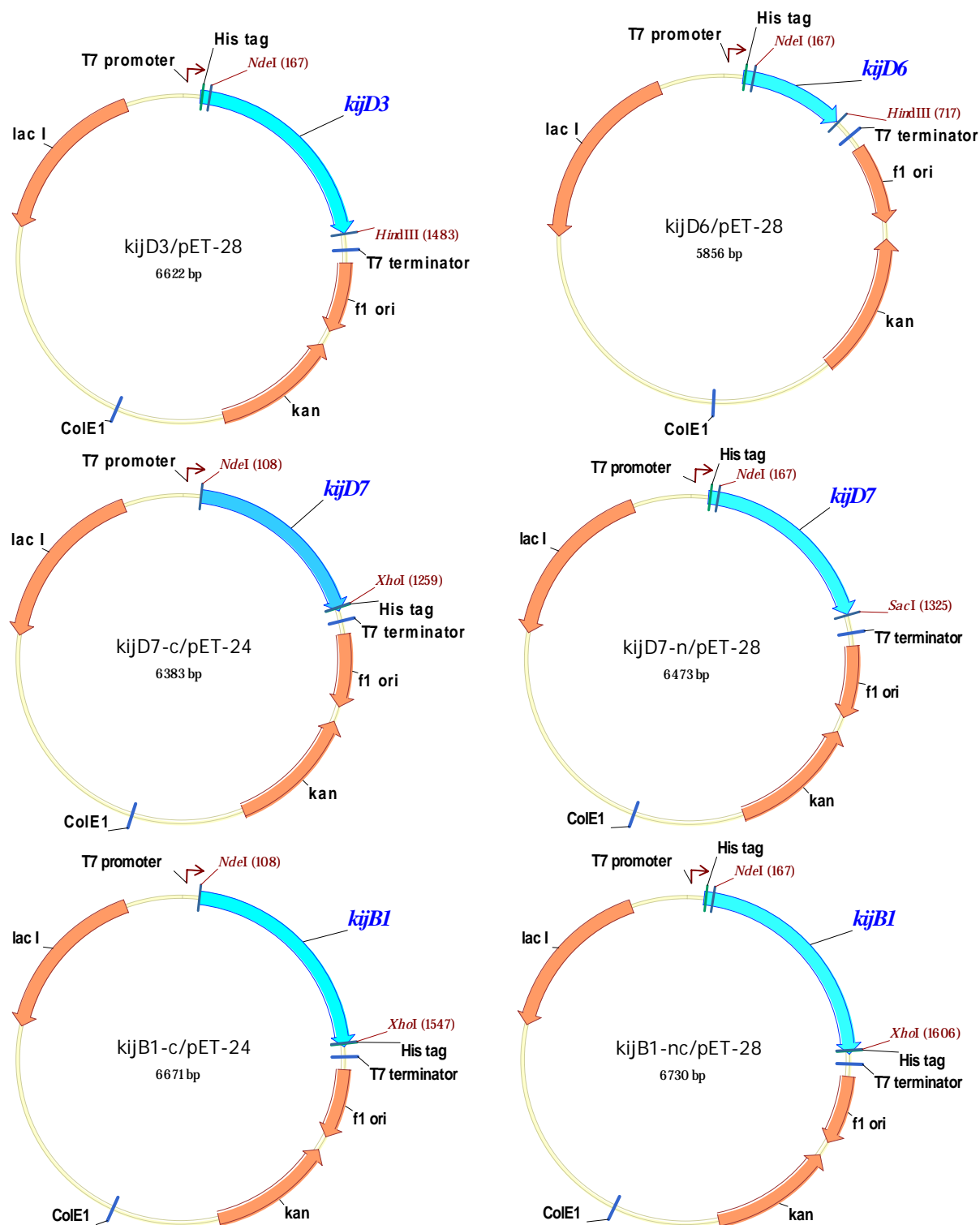


Figure 2-2 Maps of the expression plasmids containing the putative D-kijanose biosynthetic genes

Expression and Purification of the putative D-kijanose Biosynthetic Enzymes.

The general protein expression and purification procedures followed the QIAexpress System protocols.¹³⁰ All protein purification operations were carried out at 4 °C, except for the FPLC step, which was run at room temperature.

Step 1: Growth of E. coli BL21(DE3) host cells carrying the constructs of putative D-kijanose biosynthetic genes. An overnight culture of *E. coli* BL21(DE3)/kijD1/pET-28, grown in 25 mL of Luria-Bertani (LB) medium supplemented with kanamycin (50 µg/mL) at 37 °C, was diluted 250-fold with 6 L of the same medium and incubated at 37 °C until the OD₆₀₀ reached 0.5. Then, IPTG was added to the culture to a final concentration of 0.5 mM, and the culture was allowed to grow for additional 16 hours at 28 °C. The cells were harvested by centrifugation at 4,000 × *g* for 10 min at 4 °C. After discarding the medium, the cell pellets could be directly disrupted by sonication or stored at -80 °C.

Step 2: Crude E. coli Extract Preparation. The harvested cells were thawed, resuspended in 100-150 mL of cell lysis buffer (20% glycerol (w/v), 50 mM sodium phosphate, 150 mM NaCl, 10 mM imidazole, pH 8.0), and disrupted with eight 45 sec sonication bursts (30% intensity of 400 W/20 kHz) with intermittent 1 min cooling periods on ice. Cell lysates were centrifuged at 30,000 × *g* for 30 min at 4 °C, and the supernatants were filtered through a 0.45 µm membrane. The filtered soluble cell lysates were ready for the Ni-NTA resin purification.

Step 3: Ni-NTA Affinity Chromatography. The total soluble cell lysate was added 10 mL of Ni-NTA slurry, and the mixture was incubated for 1 hr with gentle shaking at 4 °C. The total mixture was then loaded onto an empty liquid chromatography column. In an alternative procedure, the crude cell lysate was loaded onto a column pre-packed with 10 mL Ni-NTA resin which was pre-equilibrated with 50 mL lysis buffer (20% glycerol (w/v), 50 mM sodium phosphate, 150 mM NaCl, 10 mM imidazole, pH 8.0). The cell lysate was allowed to flow through the resin by gravity and the flow-through lysate was collected. After collecting the flow-through lysate, the column was washed with 30 mL of lysis buffer and then 50 mL of washing buffer (20% glycerol (w/v), 50 mM sodium phosphate, 150 mM NaCl, 20 mM imidazole, pH 8.0). The washing buffer flowed through the resin was also collected. After washing, the resin-bound protein was eluted with 25 mL of elution buffer (20% glycerol (w/v), 50 mM sodium phosphate, 150 mM NaCl, 250 mM imidazole, pH 8.0). The unbound lysate, flowed-through washing buffer, and the final elution fractions were checked by SDS-PAGE (12% acrylamide gel) with Coomassie blue staining and Western Blotting with anti-His-tag monoclonal antibody.

Step 4: FPLC-MonoQ chromatography of KijD2 Protein. The KijD2 elute obtained from step 3 was further purified by FPLC with a MonoQ HR (16/10) column using buffers A (20 mM Tris-HCl, pH 7.5) and B (20 mM Tris-HCl, 500 mM NaCl, pH 7.5). The elution gradient started from 10% buffer B at 15 min to 100% buffer B at 55 min. The flow rate was 5.0 mL/min and the detector was set at 280 nm. The KijD2 elute peak around the 70% buffer B was collected.

Analysis of Poly-Histidine-Tagged Recombinant Protein with Western Blotting.

After SDS-PAGE was complete, the polyacrylamide gel was removed carefully and equilibrated in transfer buffer (25 mM Tris-HCl, 192 mM glycine, 20% (v/v) methanol, pH 8.3) at room temperature for 10 min with gentle shaking. The equilibrated gel and blotting membrane were assembled into the gel-transferring sandwich and set onto the Mini Trans-Blot Cell apparatus. The protein transfer was performed at 100 V for 1 h with cooling. After transfer, the membrane with immobilized proteins was rinsed with TBST buffer (100 mM Tris-HCl, 0.9% (w/v) NaCl, 0.1% (v/v) Tween 20, pH 7.5), and then blocked with 5% non-fat milk/TBST buffer (w/v) at room temperature for 1 h. The blocked membrane was hybridized with mouse monoclonal anti-polyHistidine antibody (3,000 \times dilution in 5% non-fat milk/TBST) at room temperature for 1 h or at 4 °C overnight. After washing three times with TBST buffer, the membrane was incubated with alkaline-phosphatase-conjugated anti-mouse IgG Fc-specific secondary antibody (30,000 \times dilutions in 5% non-fat milk/TBST) at room temperature for 45 min with gentle agitation. The membrane was then washed three times with TBST buffer, and the immobilized poly-histidine-tagged protein was detected with BCIP/NBT color development substrate in alkaline phosphatase buffer (100 mM Tris-HCl, 100 mM NaCl, 5 mM MgCl₂, pH 9.5).

Concentrating Purified Proteins. The protein eluates, from either Ni-NTA or FPLC-MonoQ chromatography, were concentrated with Amicon Ultra-15 Centrifugal Filter Units (Membrane NMWL, 10,000 kDa) until the total volume of the elutes was reduced to ~5 mL. The centrifugation operations were carried out at 4 °C

PLP-reconstitution of KijD2 and KijD7 and Protein Dialysis. The concentrated protein eluates (5-10 mL) were loaded into the dialysis membrane tube (MWCO: 12-14,000 kDa) and dialyzed against 1 L of potassium phosphate buffer (50 mM KPi, 20% glycerin, pH 7.5) at 4 °C. For putative aminotransferases KijD2 and KijD7, 1 mM of pyridoxal 5'-phosphate (final concentration) was added to the protein eluates and incubated at 4 °C for 1 h with gentle shaking before dialysis. The dialysis buffer was changed with fresh buffer at least three times, and for each round, the dialysis was performed with gentle stirring for at least 6 h. After dialysis, protein concentrations were determined by either Bradford assay¹³¹ with bovine serum albumin (BSA) as the standard, or the UV absorbance at 280 nm. The proteins were aliquoted into 1 mL fractions and stored at -80 °C.

Transamination Half-Reactions of KijD2 and KijD7. The half-reaction mixture contained 80 µM protein (KijD2 or KijD7), 1 mM L-amino acid (glutamine, glutamic acid or alanine) in 50 mM potassium phosphate buffer (pH 7.5). The mixture was incubated at 30 °C for 3 h before spectro-photoscanning by UV-Vis spectrophotometer.

Enzymatic Synthesis of TDP-D-glucose (I). Preparation of TDP-D-glucose from thymidine and glucose-1-phosphate was followed the two-stage, "one-pot" reaction procedure developed previously by our group.^{132, 133} In the first stage, a mixture containing 54 mg thymidine, 165 mg phosphoenolpyruvate (PEP), and 8 mg ATP was dissolved in 50 mM Tris-HCl (pH 7.5) with 25 mM MgCl₂. To this substrate mixture was added the triple enzyme mixture of 25 µM thymidine kinase (TK), 25 µM thymidylate kinase (TMK), 25 µM nucleoside diphosphate kinase (NDK), and 1,000 units

of rabbit muscle pyruvate kinase (PK). The resulting reaction mixture was incubated at 37 °C for 16 h, generating thymidine triphosphate (TTP). After removing the enzymes by filtrating through an Amicon YM-10 membrane, the filtrate was mixed with 97 mg of D-glucose-1-phosphate and the pH value was re-adjusted to 7.5. Then, α -D-glucose-1-phosphate thymidyltransferase (RfbA) from *S. enterica* LT2 was added to the mixture to give a final concentration of 25 μ M. The mixture was incubated for 2 h at 37 °C, and filtered through an Amicon YM-10 membrane again to remove the RfbA enzyme. The crude product, TDP-D-glucose (**1**), was purified with Bio-Gel P2 resin at 4 °C.

A Bio-gel P2 column (~500 mL gel, 25 mm \times 100 cm) was packed and washed with water. After sample loading, the column was eluted at a flow rate of 10 mL/hr with water as the eluant. The elute fractions (8 mL/fraction) were collected, and were screened by UV absorbance at 267 nm. The fractions containing TDP-D-glucose eluted between 350 and 500 mL. The desired fractions were pooled, and then lyophilized. The identity and purity of the product were verified by ^1H NMR spectroscopy and mass spectrometry. The ^1H NMR (300 MHz, D_2O) spectrum of TDP-D-glucose was δ 1.79 (3H, s, 5''-Me), 2.23 (2H, m, 2'-H), 3.29-3.41 (3H, m, 2-H, 3-H, 4-H), 3.58 (1H, m, 3'-H), 3.63-3.74 (2H, m, 5-H, 6-H), 4.04 (1H, m, 4'-H), 4.49 (2H, m, 5'-H), 5.46 (1H, dd, J = 3.6, 3.3, 1-H), 6.20 (1H, t, J = 7.0, 1'-H), 7.60 (1H, s, 6''-H). Low-resolution ESI-MS calculated for $\text{C}_{16}\text{H}_{25}\text{N}_2\text{O}_{16}\text{P}_2^{-1}$ ($\text{M} - \text{H}^+$) m/z 563.08, found m/z 563. The lyophilized TDP-D-glucose weighted 131 mg (88% yields) of about 85% purity, and the major impurity was glucose-1-phosphate.

Preparation of Enzymes used in the Synthesis of TDP-4-keto-6-deoxy-D-glucose

(2). The TK, TMK, and NDK used in TTP synthesis were prepared as described by Takahashi et al.¹³³ Rabbit muscle pyruvate kinase was purchased from Sigma-Aldrich as a 400-800 units/mg ammonium sulfate precipitate. This ammonium sulfate precipitate was re-dissolved in ddH₂O to a concentration of 2500 units/mL, dialyzed against 50 mM sodium phosphate buffer, 300 mM NaCl, pH 8.0, to remove ammonium sulfate, and stored at -80 °C.

RfbA was prepared as follows. The *rfbA* gene was amplified from *Salmonella enterica* serovar *Typhimurium* LT2 genomic DNA by PCR. The primer pair used for PCR was 5'-CGGGATCCGAAGGAGATATATAATGAAAACGCGTAAGGGC-3' and 5'-CTTGCATGCCTGCAGTTAATGATGATGATGATGTAAACCTTTCACCATC-3', containing engineered *Bam*HI and *Pst*I restriction sites (*italic*), respectively. The PCR-amplified DNA was then purified, digested with *Bam*HI and *Pst*I, and ligated into *Bam*HI/*Pst*I digested pUC18 vector. The resulting plasmid construct was used to transform *E. coli* BL21(DE3) for protein expression. RfbA overexpression was achieved by growth of the transformed host in 3 liters LB media containing 100 µg/mL ampicillin at 37 °C overnight. The recombinant RfbA protein was purified from the harvested cells by Ni-NTA affinity chromatography in the same manner as that used for the purification of D-kijanolose biosynthetic proteins. After purification, the purified RfbA was concentrated, dialyzed, and its concentration was determined by the identical methods used for D-kijanolose biosynthetic proteins.

RfbB, the TDP-D-glucose 4,6-dehydratase, used in the synthesis of

TDP-4-keto-6-deoxy-D-glucose (**2**) was prepared in the following manner. The *rfbB* gene was amplified from *Salmonella enterica* serovar *Typhimurium* LT2 genomic DNA by PCR. The PCR primer pair was 5'-**GGAATTC**GAAGGAGATATATAATG-GTGAAGATACTTATTACTGG-3' and 5'-CG**GGATCCTT**AATGATGATGATGATG-CTGGCGTCCTTCATAGTTC-3', containing engineered *Eco*RI and *Bam*HI restriction sites (*italic*), respectively. The PCR-amplified product was purified, digested with *Eco*RI and *Bam*HI, and then ligated into *Eco*RI/*Bam*HI digested pUC18 vector. The RfbB/pUC18 construct was used to transform *E. coli* BL21(DE3) for RfbB expression. Protein overexpression was carried out by growing the transformed host in 3 liters LB media containing 100 µg/mL ampicillin at 37 °C overnight. The RfbB purification, concentration, dialysis, and quantitation were performed in the same manner as RfbA.

HPLC Activity Assay for TylX3 and KijB1. A reaction mixture (50 µL) of 10 µM KijB1 and 1 mM TDP-4-keto-6-deoxy-D-glucose (**2**) in 50 mM potassium phosphate buffer (pH 7.5) was incubated at 30 °C for 1 h. After incubation, the reaction mixture was filtered through a Microcon YM-10 membrane to remove enzyme, and the filtrate was kept on ice until HPLC analysis. HPLC analysis was performed by injecting 20 µL of each sample into the Adsorbosphere strong anion-exchange (SAX) analytical column with a linear gradient from 50 to 500 mM potassium phosphate buffer (pH 3.5) at 1 mL/min flow rate for 25 min. The HPLC detector was set at 267 nm. The retention times of each compound were 5.5 min for maltol (**7**), 8.5 min for TDP-D-glucose (**1**), 9 min for TDP-4-keto-6-deoxy-D-glucose (**2**), and 10.5 min for TDP, based on retention times for the pure standard compounds applied to the same analysis program.

HPLC Coupled Activity Assay for KijB1 and KijD2. A reaction mixture (45 μ L) of 30 μ M PLP-reconstituted KijD2, 1 mM TDP-4-keto-6-deoxy-D-glucose (**2**), and 10 mM L-glutamate (pH 8.0) in 50 mM potassium phosphate buffer (pH 7.5) was incubated at 30 °C for 10 min. Then, 3 μ M KijB1 was added to the mixture to make the total volume 50 μ L. The final reaction mixture was incubated at 30 °C for 1 h. After incubation, the reaction mixture was filtered through a Microcon YM-10 membrane to remove enzyme, and the filtrate was kept on ice until HPLC analysis. HPLC analysis was performed by injecting 20 μ L of each sample to the Adsorbosphere strong anion-exchange (SAX) analytical column with a linear gradient from 50 to 500 mM potassium phosphate buffer (pH 3.5) at 1 mL/min flow rate for 25 min. The HPLC detector was set at 267 nm. The retention times of each compound were 4.8 min for TDP-3-amino-2,3,6-trideoxy-4-keto-D-*threo*-hexopyranose (**68**, Figure 2-4), 5.5 min for maltol (**7**), 8.5 min for TDP-D-glucose (**1**), 9 min for TDP-4-keto-6-deoxy-D-glucose (**2**), and 10.5 min for TDP, based on retention times for the pure standard compounds applied to the same analysis program. The product conversion rate was calculated by integrating the peak area of the product on the HPLC trace and dividing by the original substrate peak area.

Large Scale Preparation of KijB1 Decomposition Products and KijD2 Product with HPLC. A 4 mL reaction mixture of 12.5 μ M RfbB and 5 mM TDP-D-glucose (**25**) in 50 mM potassium phosphate buffer (pH 7.5) was incubated at 37 °C with gentle shaking for 2 h. After the RfbB reaction, 50 μ M reconstituted KijD2 (final concentration), 50 μ M PLP (final concentration), and 50 mM L-glutamate (pH 8.0, final

concentration) were added to the mixture and incubated at 30 °C with gentle shaking for 10 min. Then, 5 μ M KijB1 was added into the mixture to make the total volume of 5 mL. The final reaction mixture was incubated at 30 °C with gentle shaking for 2.5 h. After incubation, the reaction mixture was filtered through a Microcon YM-10 membrane to remove enzyme, and the filtrate was aliquoted into 1 mL fractions, frozen, and stored at -80 °C until HPLC analysis. HPLC analysis was performed using a semi-preparative Dionex CarboPac PA1 HPLC column with 200 μ L of sample for each injection. The sample was eluted by a gradient of water as solvent A and 500 mM ammonium acetate (pH \sim 7.0) as solvent B, where the gradient ran from 10 to 20% B over 5 min, then 20 to 40% B over 20 min, 40 to 50% B over 5 min, 5 min wash at 50% B, following 100% B wash for 15 min, and re-equilibration at 10% B for 15 min. The flow rate was 5 mL/min, and the detector was set at 267 nm. The retention times of each compound were 2.6 min for maltol (**7**), 11.0 min for KijD2 product, TDP-3-amino-2,3,6-trideoxy-4-keto-D-*threo*-hexopyranose (**68**), 23.0 min for TMP, 38.5 min for TDP-D-glucose (**1**), 39.0 min for TDP-4-keto-6-deoxy-D-glucose (**2**), and 55.5 min for TDP. The identity of the products was verified based on the standard compounds analyzed under the same HPLC condition. The eluates corresponding to compounds **7**, **68**, and TDP were collected, kept on ice, and immediately sent for high-resolution ESI mass spectrometry. High resolution ESI-MS of **7**: calculated for $C_6H_6O_3^{+1}$ ($M + H^+$) 126.03115, found 126.0315; TDP: calculated for $C_{10}H_{15}N_2O_{11}P_2^{+1}$ ($M + H^+$) 401.01456, found 401.0147; **68**: calculated for $C_{16}H_{24}N_3O_{13}P_2^{-1}$ ($M - H^+$) 528.07899, found 528.0780.

HPLC Coupled Activity Assay for KijD1, KijD3 plus KijD6, or KijD7. A stock reaction mixture (150 μ L) of 30 μ M PLP-reconstituted KijD2, 1 mM TDP-4-keto-6-deoxy-D-glucose (**2**), and 10 mM L-glutamate (pH 8.0) in 50 mM potassium phosphate buffer (pH 7.5) was incubated at 30 $^{\circ}$ C for 10 min. For KijD1 activity test, 30 μ M KijD1 and 10 mM *S'*-adenosylmethionine were added to the above mixture. For KijD3 plus KijD6 assay, 30 μ M KijD3, 30 μ M KijD6 and 10 mM NADPH were added to the stock mixture. For KijD7 activity assay, 30 μ M PLP-reconstituted KijD7 was added into the stock mixture. Then, for all of the above assays, 3 μ M KijB1 was added into each mixture to make the total volume of 200 μ L. The final reaction mixture was incubated at 30 $^{\circ}$ C and 50 μ L aliquots of each reaction mixture was taken out after incubation for 2, 3, 4, and 6 h. Each fraction of the reaction mixtures was filtered through a Microcon YM-10 membrane to remove enzymes, and the filtrate was kept on ice or frozen at -80 $^{\circ}$ C until HPLC analysis. HPLC analysis was performed by injecting 20 μ L of sample to the analytical Dionex CarboPac PA1 HPLC column. The sample was eluted by a gradient of water as solvent A and 500 mM ammonium acetate (pH \sim 7.0) as solvent B, where the gradient ran from 10 to 20% B over 5 min, then 20 to 40% B over 20 min, 40 to 50% B over 5 min, 5 min wash at 50% B, following 100% B wash for 15 min, and re-equilibration at 10% B for 15 min. The flow rate was 1 mL/min, and the detector was set at 267 nm.

3. RESULTS AND DISCUSSION

Analysis of Kijanimicin Biosynthetic Gene Cluster and Assignment of D-Kijanose Biosynthetic Pathway. Based on the studies of unusual sugar biosynthesis carried out in recent years, we have learned that the strategies of catalytic enzymes and the biosynthetic pathways are usually evolutionarily conserved among various unusual sugars and their producing bacteria.^{18, 134-137} Like many other deoxysugars, the biosynthesis of D-kijanose, a 2,3,4,6-tetradeoxy-hexose, starts from D-glucose-1-phosphate with the formation of nucleotidyl-activated TDP-D-glucose (**1**) and TDP-4-keto-6-deoxy-D-glucose (**2**), a common precursor of most C-6 deoxysugars. The thymidylation of D-glucose is catalyzed by D-glucose-1-phosphate thymidyltransferase (E_p), also known as TDP-D-glucose synthase, which is encoded by the *kijD5* gene (Figure 2-1, Table 2-1). The subsequent C-6 deoxygenation of TDP-D-glucose is catalyzed by the TDP-D-glucose 4,6-dehydratase (E_{od}), encoded by *kijD4*, which belongs to the short-chain dehydrogenase/reductase (SDR) family. This enzyme uses the active-site bound NAD^+ cofactor to oxidize the hydroxyl group at C-4 of **1**. Then the mechanism is followed by C5-C6 dehydration and C-6 reduction leading to the formation of TDP-4-keto-6-deoxy-D-glucose (**2**). The primary sequence of KijD4 shows 61.8% identity to TylA2 found in the tylosin biosynthetic pathway and 54.5% identity to StrE isolated from the streptomycin biosynthetic pathway.^{138, 139} Both TylA2 and StrE are known TDP-D-glucose 4,6-dehydratase. In fact, the kijanimicin gene cluster was initially screened with the probe of a conserved region of *tylA2*, which was cloned from the TDP-D-mycaminose biosynthetic gene cluster of *S. fradiae*. By detailed

inspection of KijD4 amino acid sequence, the conserved Tyr155 and Thr131 residues involved in C-4 oxidation can be easily found, and also Asp132 and Glu133 serving as the acid and base catalysts, respectively, for the C-6 dehydration (Figure 2-3).¹⁴⁰⁻¹⁴²

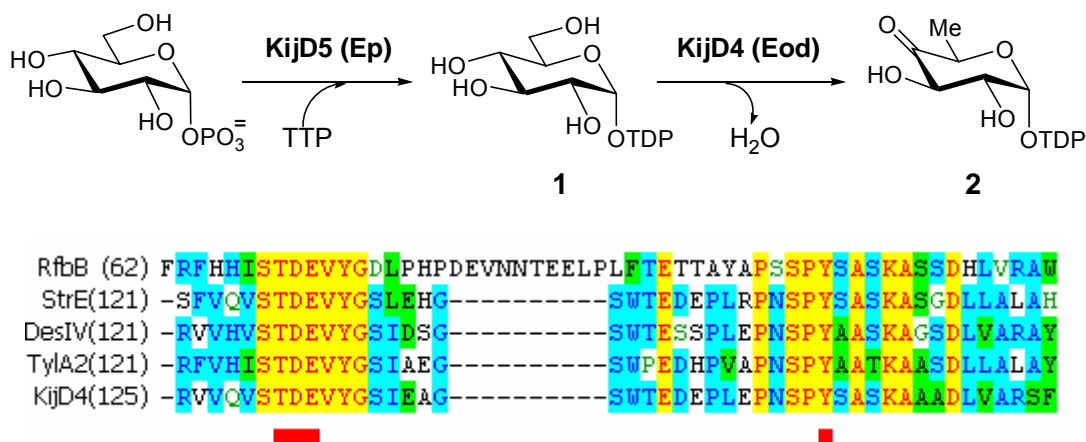


Figure 2-3 Proposed reaction scheme of KijD5 and KijD4 (**top**); Partial sequence alignment of various TDP-D-glucose 4,6-dehydratases (**bottom**)

Like other 2,6-dideoxysugars, the subsequent step after C-6 deoxygenation is C-2 deoxygenation, which is catalyzed by another dehydratase, the TDP-4-keto-6-deoxyglucose 2,3-dehydratase. This enzyme is encoded by the *kijB1* gene in the kijanimicin cluster (Table 2-1). KijB1 shows 44.2% sequence identity to TylX3 and 41.8% identity to EryBVI, both of which are 2,3-dehydratases involved in L-mycarose biosynthesis in the tylosin and erythromycin pathways, respectively.^{19, 143} D-kijanose contains a C-4 amino group and a C-3 nitro group, which is probably derived from an amino group. As expected, there exist only two putative aminotransferase genes, *kijD2* and *kijD7*, in the kijanimicin gene cluster. Transamination of a keto sugar

catalyzed by a pyridoxal 5'-phosphate (PLP)-dependent transaminase is a common mechanism for C-N bond formation in aminosugar biosynthesis.^{18, 135, 136} Previous studies on L-epivancosamine biosynthesis have shown that the C-3 aminotransferase, EvaB, acts after C-2 deoxygenation catalyzed by EvaA to produce TDP-2,3,6-trideoxy-3-amino-4-keto-D-*threo*-hexopyranose (**68**).²¹ Similarly, in the case of D-rubranitrose biosynthesis, the C-3 transamination is catalyzed by RubN4, following the C-2 deoxygenation catalyzed by the 2,3-dehydratase, RubN3.¹⁴⁴ We proposed that the reaction subsequent to the 2,3-dehydration in D-kijanose biosynthetic pathway should be the same as that for the formation of L-epivancosamine and D-rubranitrose (Figure 2-4). Compared to other PLP-dependent sugar aminotransferases in the database, KijD2 shows more similarity to the C-3 aminotransferase, while KijD7 is closer to the C-4 aminotransferase (Figure 2-5). So, KijD2 is most likely the C-3 aminotransferase that converts the KijB1 product (**5**) into **68**.

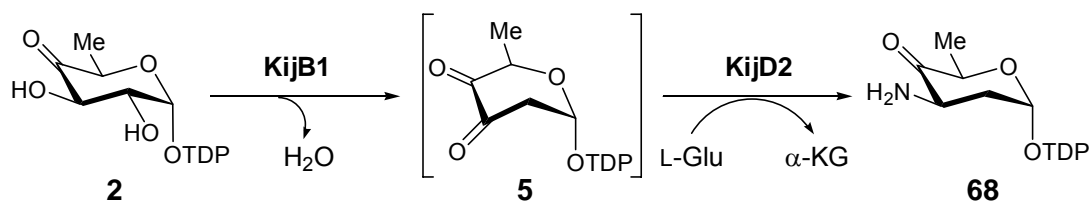


Figure 2-4 Proposed reaction scheme for KijB1 and KijD2

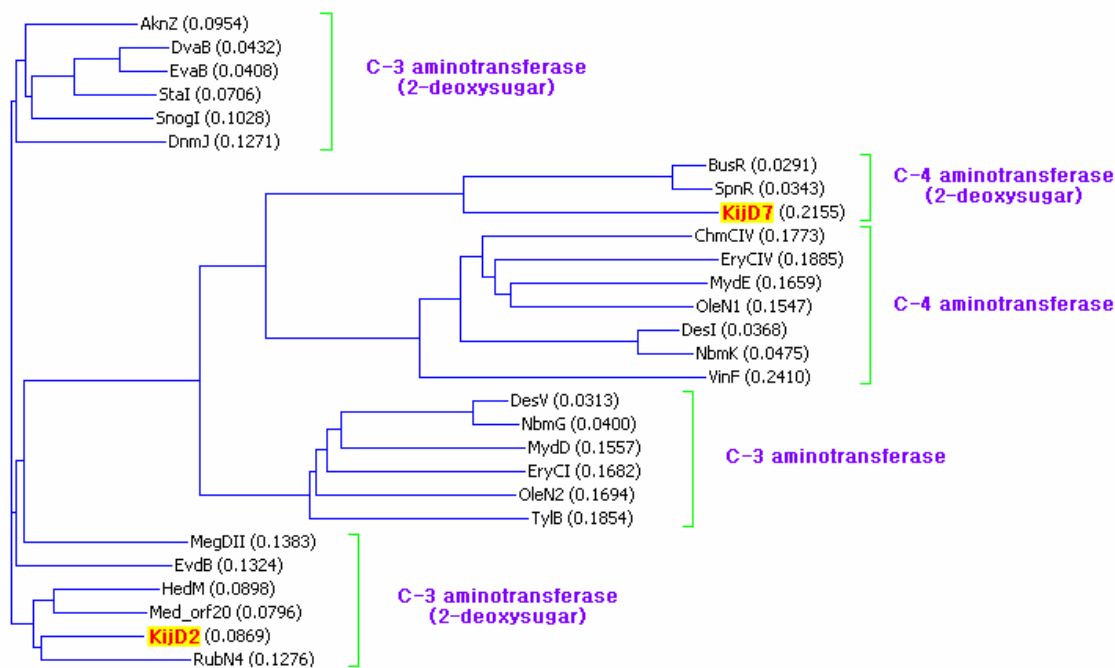
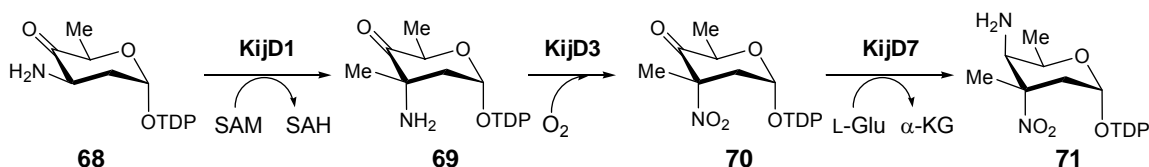


Figure 2-5 Phylogenetic tree of deoxysugar aminotransferases and their proposed functions

The next step of D-kijanose biosynthesis is likely the C-3 C-methyltransfer catalyzed by KijD1, an *S*-adenosylmethionine (SAM)-dependent C-methyltransferase. The addition of a methyl-branch chain to sugars using SAM as the methyl-donor is a common reaction found in sugar metabolism.^{135, 136} KijD1 shows 67.0% sequence-identity with EvaC, the enzyme that converts **68** to TDP-3-amino-3-*C*-methyl-2,3,6-trideoxy-4-keto-D-*erythro*-hexopyranose (**69**) during the biosynthesis of L-epivancosamine.²¹ It should be noted that TylC3, the C-3 methyltransferase involved in the biosynthesis of L-mycarose, catalyzes the transmethylation reaction to the stereochemically opposite position and shows only 28.3% identity to KijD1. Thus, KijD1 most likely catalyzes the same reaction as EvaC.



Based on the structure of D-kijanose, the next biosynthetic step after KijD1 reaction could be either C-3 amino-oxidation or C-4 aminotransfer. From this point on, we enter an unexplored area since neither experimental data nor hypothesized pathway exists in the literatures for nitro sugar biosynthesis. However, when we carefully compare the kijanimicin gene cluster with the other two identified clusters of nitro-sugar-possessing compounds, rubradirin (**64**) and everninomicin (**66**), we can find a unique tri-gene sub-cluster in all three genomes (Figure 2-6).^{145, 146} In the kijanimicin cluster, the three genes are kijD1, kijD2 and kijD3, whose assigned functions are C-3 methyltransferase, C-3 aminotransferase, and a flavin-dependent oxidoreductase, respectively. In the rubradirin and everninomicin clusters, the same three homologous genes are also clustered together (Figure 2-6). The oxidoreductases, KijD3, RubN8 and EvdC, show high sequence homology (48% identity, 85.5% similarity), and no similar protein can be found in other identified sugar biosynthetic clusters, for example, L-epivancosamine. Based on the observations above and the lack of other oxidases common to all three clusters, we propose that KijD3, RubN8, and EvdC are the oxidases responsible for the oxidation of the C-3 amino group of TDP-3-amino-3-C-methyl-2,3,6-trideoxy-4-keto-D-*erythro*-hexopyranose (**69**) to a nitro

group. Moreover, the tri-gene sub-cluster, which is conserve in these three nitro-sugar clusters, may be transcribed as one mRNA because there is no intergenic gap between the consecutive genes. This also implies that these three enzymes, C-3 aminotransferase, C-3 methyltransferase and amino-oxidase, may work consecutively in all three biosynthetic pathways, converting **5**→**68**→**69**→**70**. It is worthy to note that the spirotetronate antibiotics arisostatin B (**52**) and lobophorin A (**53**) have 3-amino-D-kijanose rather than 3-nitro-D-kijanose. This might suggest either that amine oxidation occurs after glycosyltransfer or that these kijanosyl-transferases are promiscuous and capable of accepting both amino- and nitro-forms of TDP-D-kijanose as the substrate. However, the high degree of sequence identity among KijD3 homologues in spite of the marked structural differences among the aglycones of **45**, **52**, and **53** makes the latter possibility more likely.

The putative NAD(P)H-dependent flavin reductase, KijD6, which is located near KijD3 in the cluster, may act cooperatively with KijD3 to regenerate reduced flavin during amino oxidation. However, homologues of KijD6 are absent in the everninomicin and rubradirin clusters, so KijD6 may not be a part of the KijD3 amine oxidation system. Next, the C-4 aminotransferase KijD7 is predicted to convert **30** to **31**. As the aminotransferases alignment shown in Figure 2-5, KijD7 is highly similar to SpnR (57% identity, 69% similarity), the 2,6-dideoxysugar C-4 aminotransferase involved in D-forosamine biosynthesis in the spinosyn biosynthetic pathway of *Saccharopolyspora spinosa*.¹⁴⁷

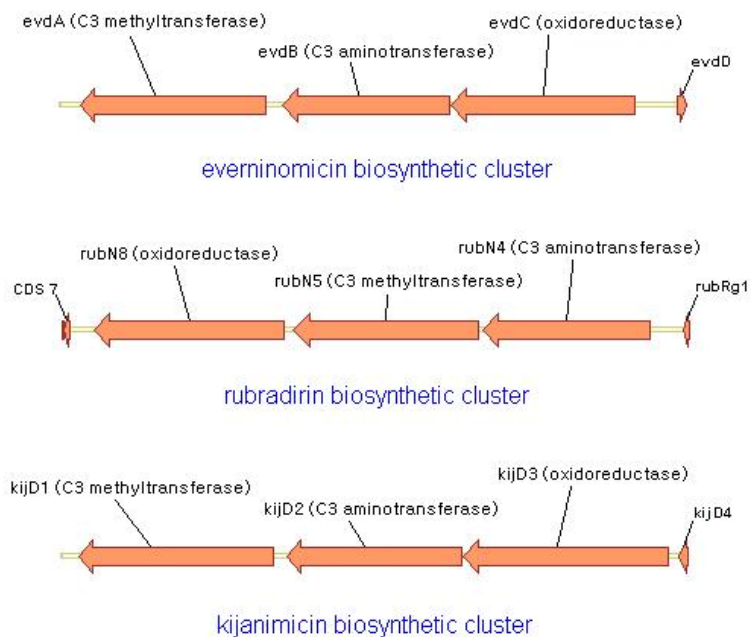
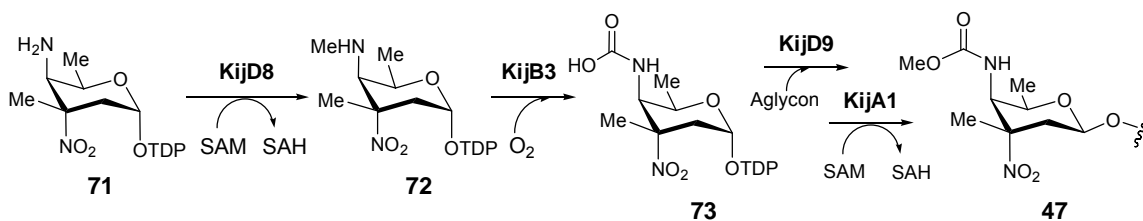


Figure 2-6 The tri-gene (C-3 aminotransferase, C-3 methyltransferase, and amine-oxidase) sub-clusters in three biosynthetic gene clusters of C-3-nitro-sugar containing compounds



Since there is no similar structure and related reports on the biosynthesis of C-4 methylcarbamate moiety, it is not apparent what types of enzymatic activities might be required to construct this functional group of D-kijanose (**47**). Its formation could occur on a TDP-sugar intermediate, such as **71**, or via a series of tailoring steps after the sugar

precursor has been attached to the aglycone. It is straightforward to expect formylation of the C-4 amine of **71** to be the first step in this tailoring pathway. However, gene alignment failed to show any putative *N*-formyltransferase in the kijanimicin cluster. In view of the remaining unassigned genes in the kijanimicin cluster and basic biosynthetic logic, we speculate that formation of the methylcarbamate might be a collaborative effort of three enzymes. The methyltransferase, KijD8, could be responsible for *N*-methylation of the C-4 amine of **71**, resulting in **72**. The flavin-dependent oxidoreductase, KijB3, may then oxidize the methyl group to a carboxylate group forming **73**. Finally, the putative sugar *O*-methyltransferase KijA1 may catalyze the last step to generate D-kijanose (**47**). Since most sugar *O*-methyltransfer steps occur after glycosyltransfer in natural product pathways, it is possible that methylation of the C-4 carboxylamino moiety may occur in this manner.

There exist five putative glycosyltransferases (GTs) encoded in the kijanimicin gene cluster, KijA4, KijC1, KijC3, KijC4, and KijD9, in accordance with the presence of five sugar residues in the structure of kijanimicin (**45**). Sequence comparison of these GTs reveals that KijD9 is significantly different from the other four GTs, suggesting that it likely catalyzes attachment of D-kijanose (**47**) or its precursor to the C-17 hydroxyl group of the aglycone, kijanolide.

Cloning, Expression and Purification of KijB1 and KijD2 Proteins. To study D-kijanose biosynthesis *in vitro*, we need to clone and express the putative biosynthetic enzymes. First, we decided to examine the activities of the putative 2,3-dehydratase and C-3 aminotransferase. The genes of *kijB1* was cloned into pET-24b(+) and pET-28b(+)

vectors to make *C'*-terminal His₍₆₎-tagged and *N',C'*-terminal double His₍₆₎-tagged *kijB1* constructs, respectively. Both constructs were used to transform the *E. coli* protein expressing host, BL21(DE3), for protein over-expression. However, only the *kijB1-nc/pET-28* plasmid expressed the recombinant KijB1 protein (Figure 2-7). The estimated molecular weight of the over-expressed KijB1 from the SDS-PAGE result is consistent with the calculated KijB1 molecular weight (56,552 Da). The KijB1 expression strain was then grown in a 6-liters culture scale. After cell harvest, the recombinant KijB1 was extracted and purified with Ni-NTA affinity resin to obtain a total amount of 50.4 mg protein with ~80% purity.

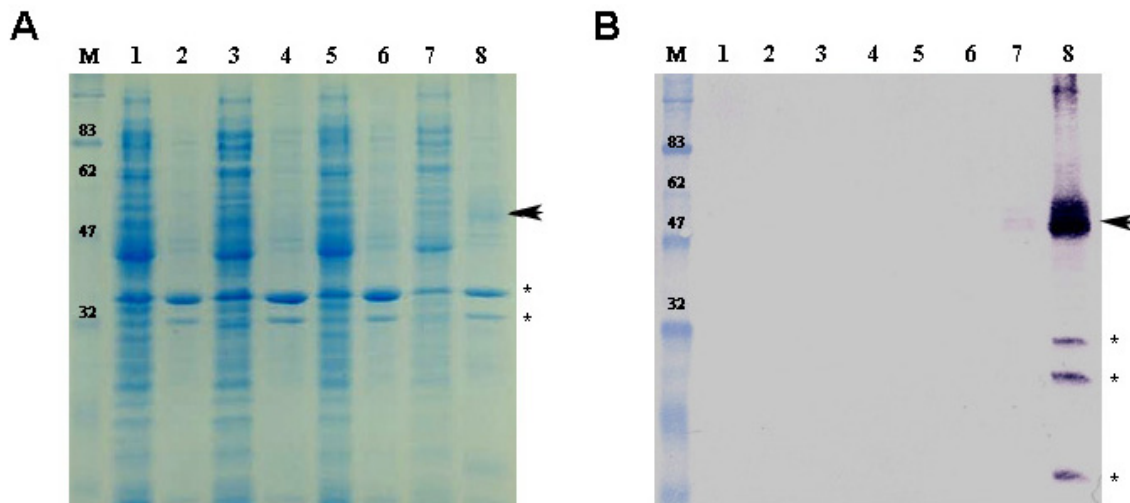


Figure 2-7 The expression and purification of KijB1. (A) Coomassie blue staining; (B) Western blotting; M, protein molecular weight marker; lane 1-2, pET-24 vector only; lane 3-4, *kijB1-c/pET-24*; lane 5-6, pET-28; lane 7-8, *kijB1-nc/pET-28*; lane 1,3,5,7, insoluble fractions of cell extracts; lane 2,4,6,8, soluble fractions of cell extracts; Arrow head, KijB1 recombinant protein; star, unrelated proteins.

The putative deoxysugar C-3 aminotransferase gene, *kijD2*, was cloned into pET-28b(+) with an *N'*-terminal His₍₆₎-tagged. The recombinant KijD2 was successfully expressed in *E. coli* BL21(DE3) host and purified from a large-scale culture by two chromatographic steps (Figure 2-8). The first was the Ni-NTA affinity chromatography, and the second one was the FPLC-MonoQ anion-exchange chromatography. The final yield of KijD2 was 37 mg (~80% purity) from 6 liters of culture. The calculated molecular weight of the recombinant KijD2 is 43,194 Da.

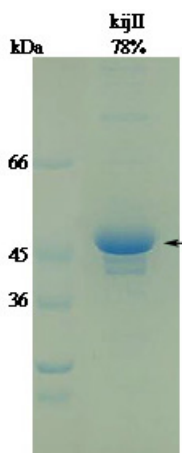


Figure 2-8 SDS-PAGE of KijD2 after FPLC-MonoQ purification. Arrow head, KijD2 recombinant protein.

Reconstitution of KijD2 with Pyridoxal 5'-Phosphate. KijD2 is predicted as a PLP-dependent C-3 aminotransferase. The KijD2 eluate purified by Ni-NTA affinity chromatography displayed a light yellow color which indicates the presence of the PLP cofactor. However, the yellow color disappeared after the purification by FPLC/MonoQ column. On the basis of our previous experience dealing with another PLP-dependent sugar transaminase, TylB, we decided to reconstitute KijD2 with PLP by adding the coenzyme to the purification eluate during the dialysis process.¹⁴⁸ The UV-Vis spectrum

of KijD2 after reconstitution showed the existence of conjugated PLP which shows a λ_{max} at 420 nm (Figure 2-9).

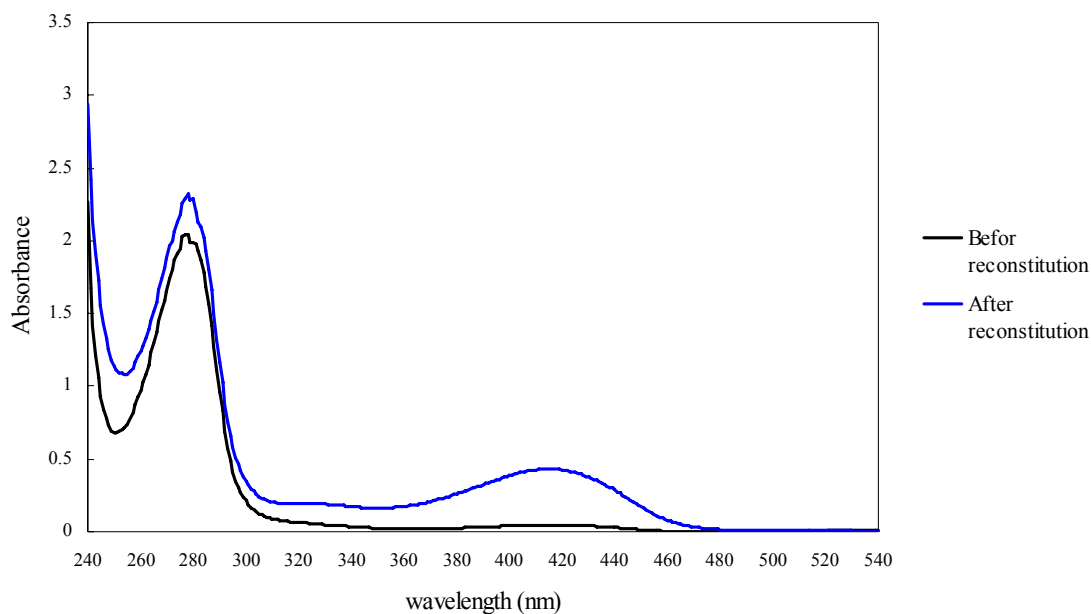


Figure 2-9 Pyridoxal-5'-phosphate reconstitution of KijD2

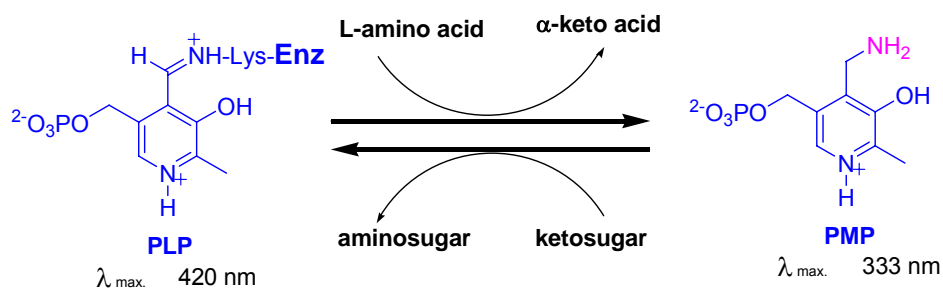


Figure 2-10 Transamination reaction of PLP-dependent aminotransferase.

Testing the Transamination Activity of KijD2 with Different Amino Donors.

The transamination catalyzed by PLP-dependent enzymes can be divided into two

half-reactions. The first step is transferring the amino group from an amino acid donor to PLP generating PMP, followed by a second step of transferring the amino group from PLP to an acceptor (Figure 2-10). After PLP-reconstitution, KijD2 was tested for its capability to carry out the first half-transamination reaction with three different amino donors, L-glutamic acid, L-glutamine, and L-alanine (Figure 2-11). The recombinant KijD2 showed efficient transamination of PLP to pyridoxamine 5'-phosphate (PMP) when using L-glutamate and L-alanine as the amino donors. When KijD2 was incubated with L-glutamine, the conversion of PLP to PMP was about 60% under the same conditions. Thus, either L-glutamate or L-alanine can be used as the amino donor in KijD2 activity assay.

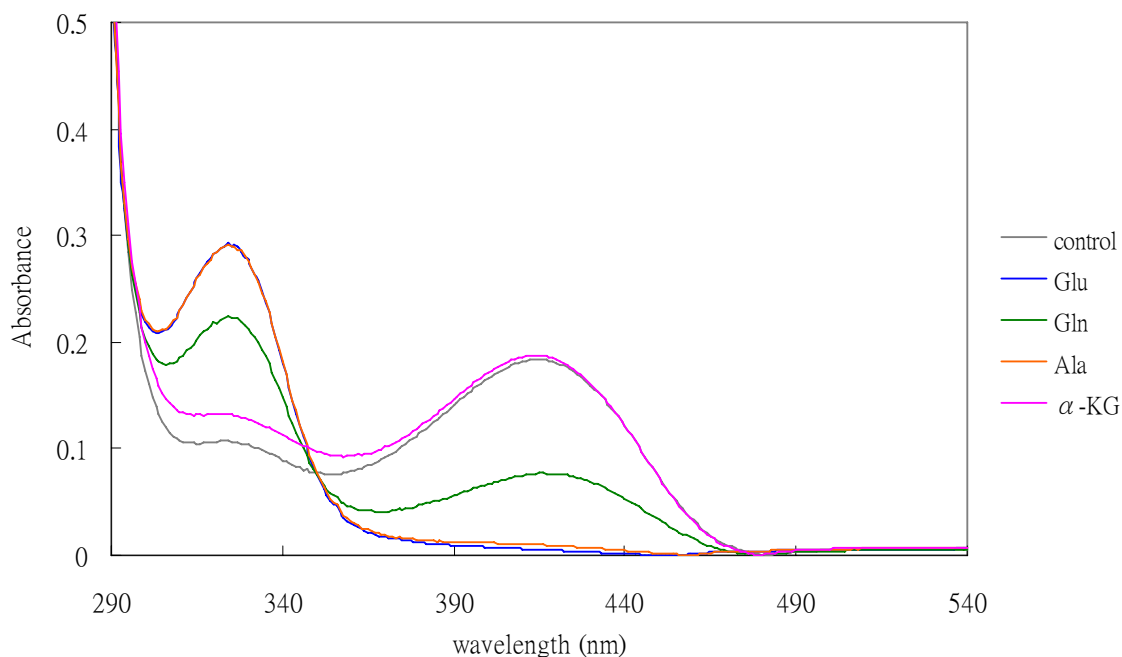
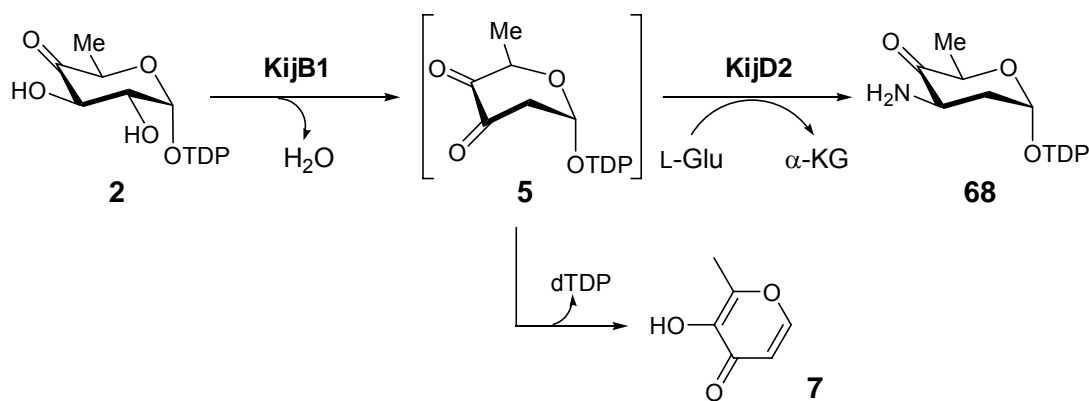


Figure 2-11 Transamination reaction of PLP-dependent aminotransferase, KijD2. (control reaction, no amino acid added; α -KG, α -ketoglutarate)

Activity Assay of KijB1 and KijD2. For *in vitro* characterization of KijB1 and KijD2, we prepared the substrate, TDP-4-keto-6-deoxy-D-glucose (**2**), using enzymatic synthesis from thymidine and D-glucose-1-phosphate.^{132, 133} Incubation of the substrate with KijB1 was carried out as described in the Experimental Section. A reference reaction using TylX3 instead of KijB1 was also performed. HPLC analysis of the KijB1 reaction showed the same result as the TylX3 reaction (Figure 2-12, trace 2, 3).¹⁹ Due to the instability of KijB1 (TylX3) product, TDP-3,4-diketo-2,6-dideoxy-D-hexopyranose (**5**), the two new UV-absorption peaks were predicted to be the decomposed products, maltol (**7**, retention time = 5.5 min) and TDP (retention time = 10.5 min).^{19, 20} The two side products were later purified by preparative HPLC (Figure 2-13) and verified by high-resolution ESI-MS (Figure 2-14 A, B).



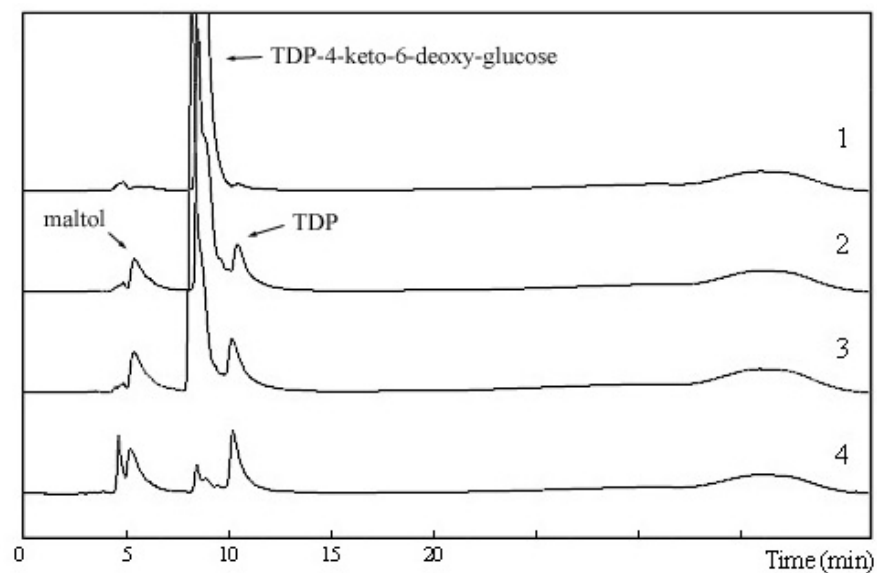


Figure 2-12 HPLC traces of KijB1 and KijD2 reactions analyzed using a SAX column. **1**, TDP-4-keto-6-deoxy-D-glucose (**2**); **2**, (**2**) + TylX3; **3**, (**2**) + KijB1; **4**, (**2**) + KijB1 + KijD2 + L-glutamate.

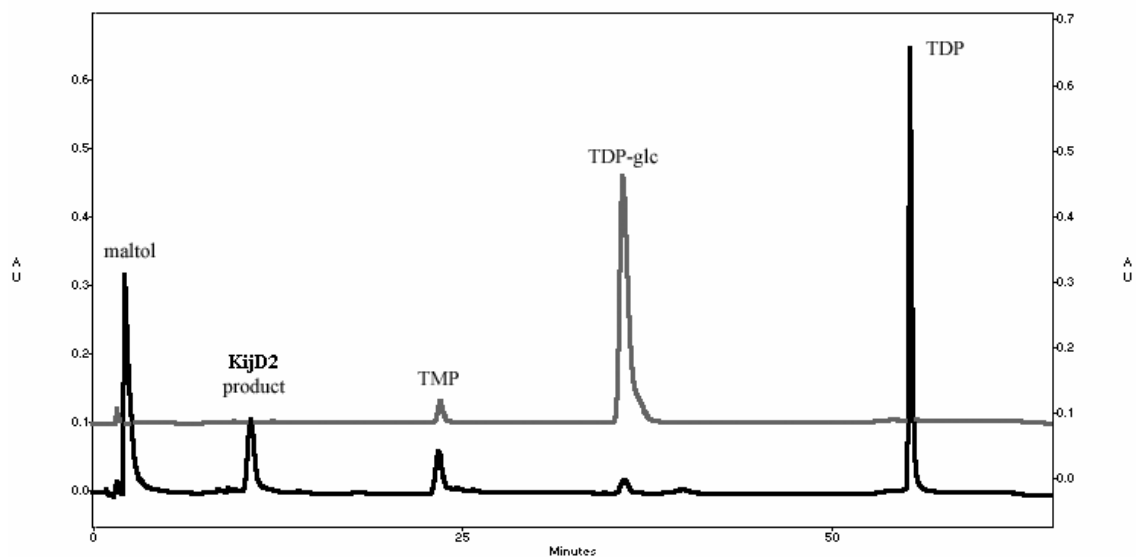


Figure 2-13 HPLC traces of large-scale KijB1/KijD2 coupled reaction analyzed using Semi-preparative Dionex column. **Top**, substrate TDP-D-glucose (**1**); **bottom**, (**1**) + RfbB + KijB1 + KijD2 + L-glutamate.

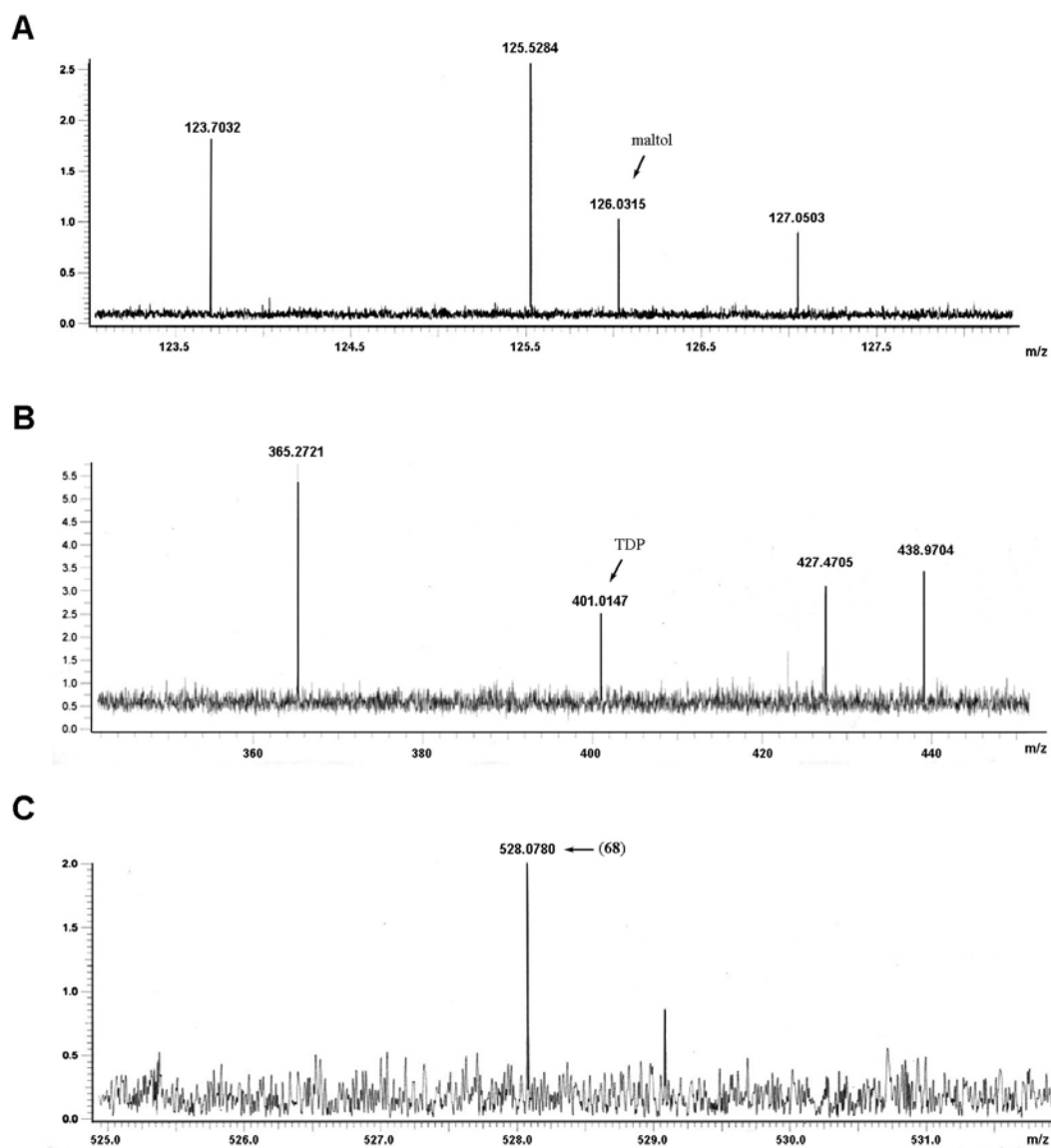


Figure 2-14 High-resolution ESI-MS/MS of maltol (A), TDP (B), and KijD2 product (C).

The enzymatic activity of KijD2 was monitored by a coupled reaction of KijB1 and KijD2 with L-glutamate as the amino donor. A new peak (retention time = 4.8 min)

appeared in the trace of HPLC analysis (Figure 2-12, trace 2, 4), which corresponds to TDP-2,3,6-trideoxy-3-amino-4-keto-D-*threo*-hexopyranose (**68**) previously identified in the study of L-epivancosamine biosynthesis.²¹ The conversion of **2** to **68** was about 22% under the incubation condition. The new compound, KijD2 product, was also purified by preparative HPLC (Figure 2-13) and verified by high-resolution ESI-MS (Figure 2-14 C).

Cloning, Expression and Purification of KijD1, KijD3, KijD6 and KijD7 Proteins. On the basis of the proposed D-kijanose biosynthetic pathway, the enzymes in action after C-3 transamination step should be sequentially the C-3 methyltransferase (KijD1), the amino-oxidase (KijD3 + KijD6), and the C-4 aminotransferase (KijD7). The recombinant proteins of these enzymes were prepared by cloning the encoding genes into pET-28b(+) vector to make *N'*-terminal His₍₆₎-tagged constructs which were then expressed in the *E. coli* host, BL21(DE3). For KijD7, we also constructed the kijD7-c/pET-24 plasmid to express the *C'*-terminal His₍₆₎-tagged KijD7 protein. The recombinant strains were grown in 6-liter cultures, except for the strain expressing KijD6 which was grown in a 3-liter culture. After harvest, the desired proteins were purified by Ni-NTA affinity chromatography. The calculated molecular weights of the recombinant proteins are 47,738 Da (KijD1), 48,400 Da (KijD3), 21,066 Da (KijD6), 43,880 Da (*N'*-His₍₆₎-tagged KijD7), and 42,782 Da (*C'*-His₍₆₎-tagged KijD7), matching the corresponding bands on SDS-PAGE (Figure 2-15). The yields of the recombinant proteins are 102.1 mg/6 L culture (KijD1, >95% pure), 61.6 mg/6 L culture (KijD3), 59.8 mg/3 L culture (KijD6), and 125 mg/6 L culture (*C'*-His₍₆₎-tagged KijD7, ~80% pure).

As the PLP-dependent aminotransferase KijD2, KijD7 was also reconstituted with PLP during the dialysis procedure.

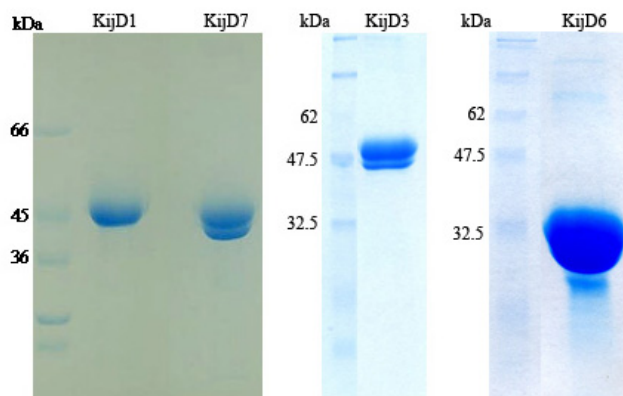


Figure 2-15 SDS-PAGE of Ni-NTA purified KijD1, KijD3, KijD6, and C'-His₍₆₎-tagged KijD7.

Activity Assay of KijD1, KijD3, KijD6, and KijD7. Based on the biosynthesis of L-epivancosamine and our gene alignment prediction, the next reaction after C-3 transamination for D-kijanose biosynthesis should be catalyzed by KijD1, the C-3 C-methyltransferase. Since the yield and stability of the KijD2 product (**68**) are low, we did not purify **68** to test the subsequent enzyme reactions. Instead, we used **2** as the starting material in the coupled reaction with KijB1 and KijD2 to examine the activity of the target enzyme. However, the coupled reactions with KijD1, KijD3 plus KijD6, or KijD7 were all unsuccessful. No new product was detected by HPLC analysis.

Transamination Activity of KijD7 Using Different Amino Donors. KijD7 was predicted to be another PLP-dependent aminotransferase, transferring the amino group from an L-amino acid to the C-4 position of the sugar. To test this, we examined its

transamination half-reaction from different amino acid donors to PLP (Figure 2-10) as we did with KijD2. Interestingly, the recombinant KijD7 can carry out transamination converting PLP to PMP using either L-glutamate, L-glutamine, or L-alanine as the amino donor (Figure 2-16).

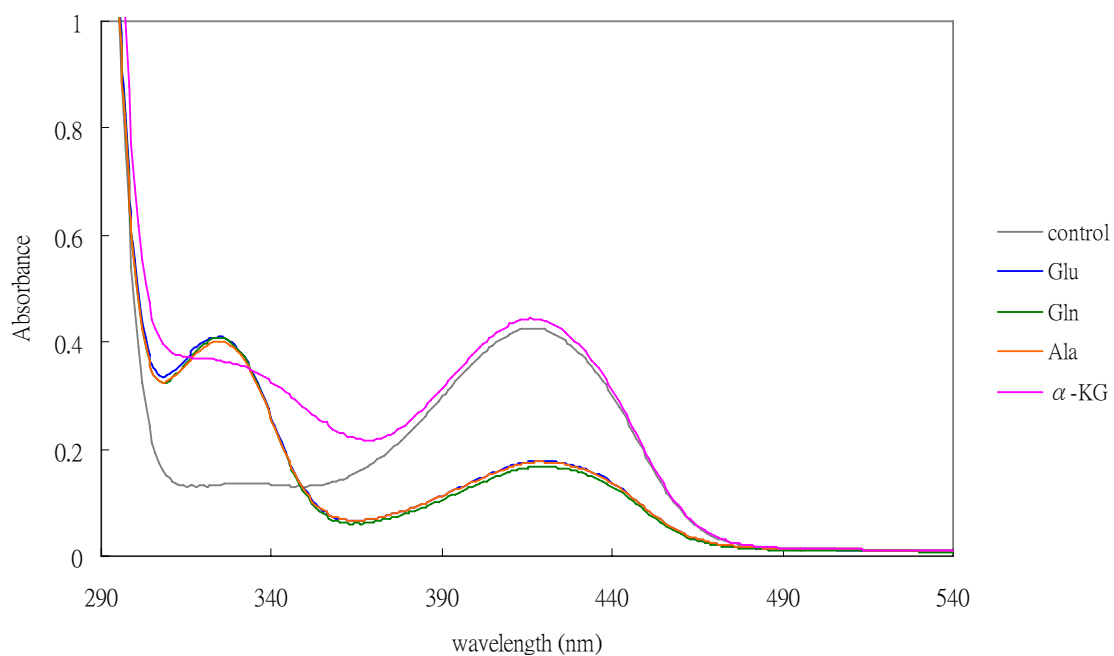


Figure 2-16 Transamination reaction of PLP-dependent aminotransferase, KijD7. (control reaction, no amino acid added; α -KG, α -ketoglutarate)

4. CONCLUSION

Few natural products contain a nitro group in their chemical structures. D-Kijanose is an unusual nitro sugar found in several antibiotics and anti-tumor compounds. Here, we presented the first attempt to elucidate the biosynthetic pathway of D-kijanose in an antibiotic and anti-tumor agent, kijanimicin, from *Actinomadura kijaniata*. From the sequence of D-kijanose biosynthetic gene cluster, we proposed a reasonable biosynthetic pathway of D-kijanose. Moreover, we proved the first two steps of this pathway, C-2 deoxygenation and C-3 transamination, are catalyzed respectively by KijB1 and KijD2 *in vitro*. With the other biosynthetic enzymes in hand, the complete biosynthetic pathway should finally become clear.

Chapter 3. Macrolide Glycosyltransferases and Their Auxiliary Proteins

1. INTRODUCTION

Many bioactive natural products isolated from microorganisms are glycosylated with various unusual sugar residues. These sugar moieties, in many cases, contribute to biological activities of these compounds.^{2, 149} A vast majority of these unusual sugars belong to the 6-deoxyhexose family, whose biosynthesis involves two common steps: the nucleotidyl activation and the sugar 4,6-dehydration. The resulting 4-keto-6-deoxyhexose could undergo further alterations and modifications including additional deoxygenation, ketoreduction, transamination, *C*-, *O*-, or *N*-methylation, and epimerization. Subsequent transfer of the nucleotidyl sugars to the aglycones via *O*-, *N*-, or *C*-linkage is catalyzed by the glycosyltransferase (GT), a process which usually occurs at the late stage of the natural product biosynthesis pathway. Sometimes, several tailoring modifications after glycosylation are required to complete the biosynthesis.

Decades of research on the biosynthesis of glycosylated natural products have made significant advance in our understanding of the common characteristics of GTs and the glycosylating reactions as summarized in Section 2 of Chapter 1. Particularly notable are the macrolide antibiotics, which contain many different unusual deoxy- and/or amino-sugars that are essential for the antibiotic activity. Most of these sugar moieties are transferred to their aglycone acceptors by inverting glycosyltransferases. These GTs

generally have GT-B folds and most of them belong to the GT-2 subfamily according to the CAZy classification.⁶⁶ As reviewed in Chapter 1, natural product glycosyltransferases generally show substrate flexibility toward both sugar donors and receptors. This flexibility can be attributed to the disordered conformation of the substrate-binding pocket between the two domains found in the GT-B fold.⁷¹

Recently, several natural product glycosyltransferases were found to require specific accessory proteins for efficient glycosylation. This was first discovered in 2004 for the D-desosaminyl glycosylation in the pikromycin/methymycin biosynthetic pathway found in *Streptomyces venezuelae* by Dr. Svetlana A. Borisova from our research group (Figure 3-1A).¹⁵⁰ The desosaminyl glycosyltransferase, DesVII, by itself converts only 3% aglycone (**35**) to the glycosylated product *in vitro*, compared to the 92% conversion in the presence of the accessory protein, DesVIII, under the identical reaction conditions. The requirement of DesVIII for glycosylation was further substantiated by the fact that glycosylated compounds were produced by the *desVIII* knock-out mutant of *S. venezuelae* in which *desVII* was intact.^{151, 152} Similar glycosylations requiring both GT and a helper protein were also discovered in a few other macrolide biosynthetic pathways. In the biosynthesis of aclacinomycin A from *S. galilaeus*, the GT AknS requires the helper protein AknT to transfer L-deoxyfucose to the aglycone, aklavinone (Figure 3-1B).¹⁵³ TylM2, the D-mycaminosyl transferase in the tylosin biosynthetic pathway from *S. fradiae* (Figure 3-1C), and MycB, the D-desosaminyl transferase of mycinamicin biosynthesis from *Micromonospora griseorubida* (Figure 3-1D), both require helper proteins, TylM3 and MydC, respectively, to generate the desired glycosides in a

heterologous expression system.¹⁵⁴

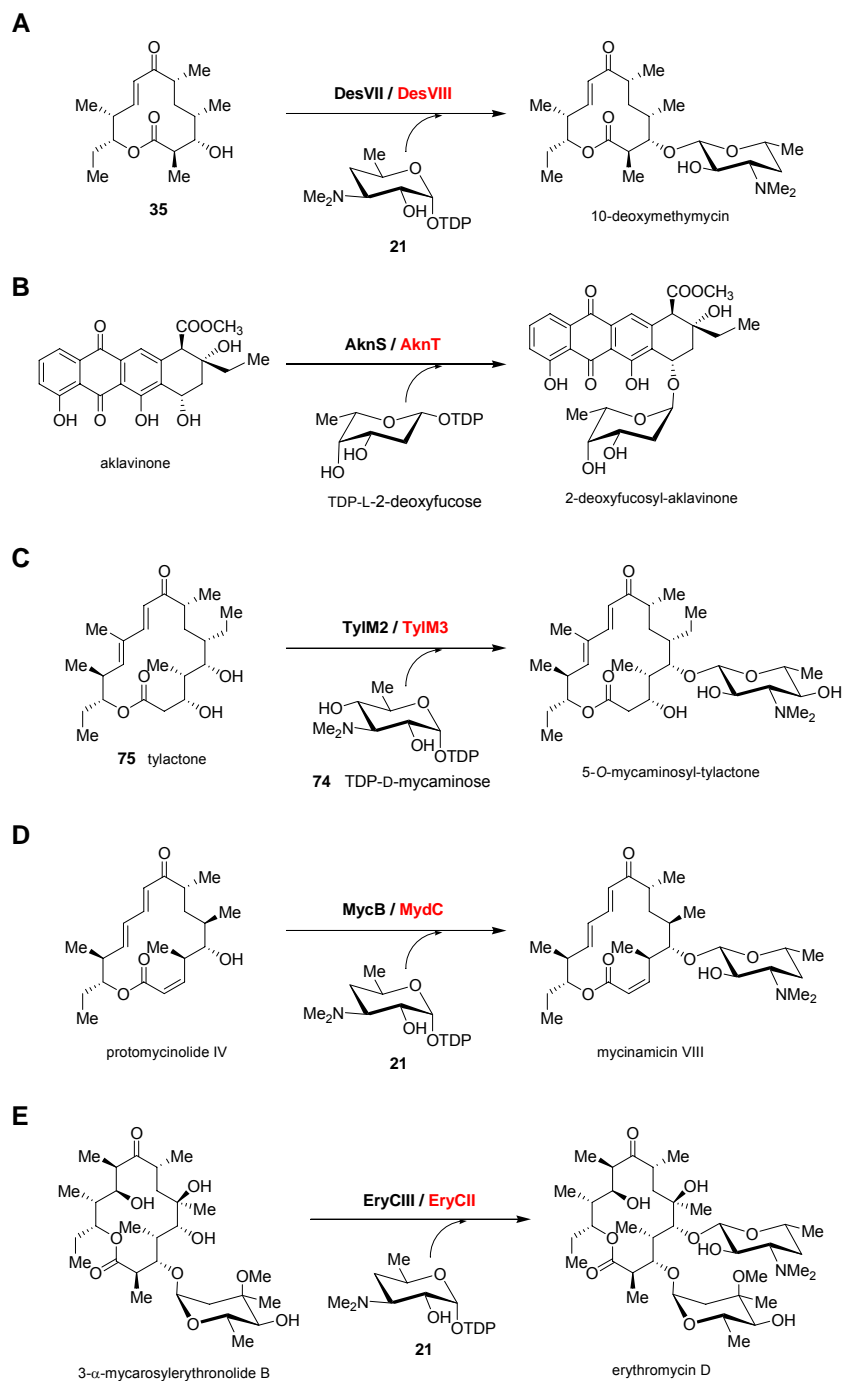
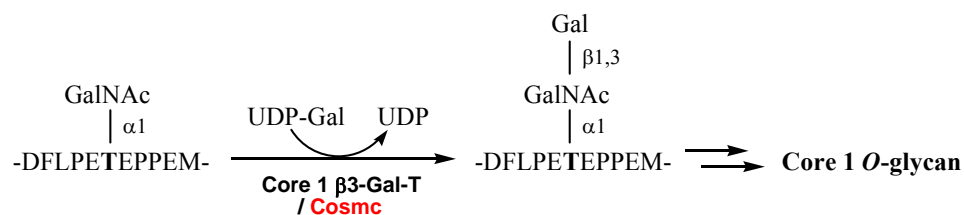


Figure 3-1 Glycosylation reactions that require both glycosyltransferases and the specific auxiliary proteins (red).

EryCIII, which catalyzes the glycosylation of D-desosamine in the erythromycin biosynthetic pathway from *Saccharopolyspora erythraea*, was active in the presence of its own helper protein, EryCII, or AknT, the helper protein for AknS in aclacinomycin A biosynthesis (Figure 3-1E).¹⁵⁵ This result suggested that a glycosylation helper protein may be replaced by other homologous proteins from different biosynthetic pathways even if their sugar substrates are different. It was reported that overexpression of EryCIII in *E. coli* to obtain soluble and active protein was possible only when coexpressed with the GroEL/ES chaperone complex. However, the purified EryCIII protein was unstable and lost activity within hours of isolation.¹⁵⁶ Interestingly, when EryCIII was coexpressed with EryCII, it was not only soluble and fully active but also retained activity for at least two months, even when the helper protein was removed.¹⁵⁵ All of these results suggest that the glycosylation auxiliary protein may act like a protein chaperone, which assists the folding of a disordered glycosyltransferase and can be replaced by other chaperone proteins.

The glycosyltransferase chaperone does not just exist in the natural product biosynthesis. In human *O*-glycan biosynthesis, the core 1 β 3-galactosyltransferase, which transfers galactose from UDP-galactose to the 3-hydroxyl group of *N*-acetylgalactose of the Tn antigen, also requires a specific chaperone protein, Cosmc, for its proper folding and activity.¹⁵⁷ The human Cosmc gene is X chromosome-linked, and its abnormality causes the autoimmune disease, Tn syndrome, due to the incomplete glycosylation of the membrane protein on patients' blood cells.¹⁵⁸



Several such protein-specific chaperones have been identified in nature.^{159, 160} Some of these interact with target proteins to stabilize an intrinsically unstable folding intermediate.¹⁶¹ Current results suggest that the glycosyltransferase-specific chaperone (helper protein) is required for the activation of GT, but is not required for the catalytic mechanism. The helper proteins are replaceable by other homologous chaperones, or inefficiently by other cellular stress-response chaperones. The precise mechanism and function of these GT-specific helper proteins awaits further study, the results of which may provide valuable information for future glycosyltransferase research, disease etiology and drug development.

2. EXPERIMENTAL PROCEDURES

General. General experimental procedures for molecular cloning and protein sodium dodecyl sulfate polyacrylamide gel electrophoresis (SDS-PAGE) followed general laboratory manuals.¹²⁷⁻¹²⁹ Most materials used for the experiments described in this chapter have already been mentioned in the Experimental Procedures section of Chapter 2. The experimental procedures of yeast two-hybrid assay followed the instruction manual of ProQuest™ Two-Hybrid System from Invitrogen (Carlsbad, CA) and miscellaneous protocols for yeast two-hybrid assay.^{127, 162} Salmon sperm DNA, purchased from Sigma-Aldrich (St. Louis, MO), was used as the carrier DNA for yeast transformation. The replica plating device, velvets and Whatman® 541 filter papers for yeast two-hybrid assay were purchased from Fisher Scientific (Pittsburgh, PA). The 0.45 µm NYTRAN® filter membrane used for X-gal assays was obtained from Schleicher & Schuell (Keene, NH) and the X-gal (5-bromo-5-chloro-3-indolyl-β-D-galactoside) was purchased from Sigma-Aldrich Chemicals. The chemical ingredients, 3AT (3-amino-1,2,4-triazole) and 5-FOA (5-fluoroorotic acid), added to the plate medium for yeast two-hybrid assays, were also purchased from Sigma-Aldrich. S-protein agarose for S-Tag protein pull-down assay was purchased from Novagen (Madison, WI). The Glutathione-agarose prepacked column for the purification of GST-DesVII and the monoclonal anti-maltose binding protein antibody were also Sigma-Aldrich products. General methods and protocols for *Streptomyces* strains experiments were from the guidelines of *Streptomyces* genetics by Kieser et. al.¹⁶³ Growth media components were acquired from Becton Dickinson (Sparks, MD) and Sigma-Aldrich Chemicals.

QuikChange Multi-Site Directed Mutagenesis Kit was purchased from Stratagene (La Jolla, CA). Analytical thin-layer chromatography (TLC) was applied on 0.25 mm Polygram Sil G/UV₂₅₄ plates obtained from Macherey-Nagel (Easton, PA).

Instrumentation. Most instrumentation used for the experiments described in this Chapter are listed in the Experimental Procedures section of Chapter 2. Analytical C₁₈ HPLC column was purchased from Varian (Palo Alto, CA), while the preparative C₁₈ HPLC column was obtained from Alltech (Deerfield, IL).

Plasmids and Vectors. The low-copy-number *E. coli*/yeast shuttle vectors, pDBLeu and pEXP-AD502, as part of the ProQuest™ Two-Hybrid System were obtained from Invitrogen (Carlsbad, CA). Cosmid pLZ4,⁴² carrying the complete D-desosamine biosynthetic cluster, was used as the template for amplification of all desired genes and gene fragments from *S. venezuelae*. Cosmid pHJL309, generously provided by Dr. Eugene Seno of Eli Lilly Research Laboratories, was used as the template for PCR amplification of *tylM2* and *tylM3*. Cosmid pMG160, kindly provided by Dr. Fumio Kato at Toho University, Japan, was used as the template for PCR amplification of *mydC* and *mycB*. The *Streptomyces/E. coli* shuttle vector, pCM1d, was constructed by Dr. Charles E. Melançon, III from our group.¹⁶⁴ Another *Streptomyces* expression vector, pAX702, modified from pDHS702 was provided by Dr. David Sherman at the University of Michigan.¹⁶⁵ The pHc29 plasmid for the expression of DesVII-C-His protein was constructed by a previous group member, Dr. Huawei Chen. The pDesVIII-MalEpET plasmid for the expression of MalE-DesVIII fusion protein was provided by Dr. Svetlana A. Borisova from our group.¹⁶⁶ The *E. coli* protein expression vectors, pET-21b(+),

pET-29 and pET-41a(+) were purchased from Novagen (Madison, WI), and MalE-pET vector was constructed and provided by Dr. Peng Gao from our group.

Bacterial and Yeast Strains. *E. coli* DH5 α and BL21(DE3) strains used for work described in this Chapter are identical to those described in the Experimental Procedures section of Chapter 2. *E. coli* BL21-CodonPlus[®](DE3) strain was purchased from Stratagene (La Jolla, CA). *E. coli* S17-1 was the donor strain used in *S. venezuelae* conjugal transfer experiments.¹⁶⁷ *S. venezuelae* (ATCC 15439), *S. narbonensis* (ATCC 19790), *S. erythraea* (ATCC 11635), *S. peucetius* (ATCC 29050), *S. antibioticus* (ATCC 11891) and *Micromonospora megalomicea* subsp. *nigra* (ATCC 27598) were obtained from the American Type Culture Collection (Manassas, VA) as freeze-dried samples, which were reconstituted according to the instructions from ATCC. *S. venezuelae* Kdes mutant was constructed and provided by Dr. Svetlana A. Borisova from our group. The yeast strain MaV203 (*MAT α* , *leu2-3,112*, *trp1-901*, *his3 Δ 200*, *ade2-101*, *gal4 Δ* , *gal80 Δ* , *SPAL10::URA3*, *GAL1::lacZ*, *HIS3_{UAS GAL1}::HIS3@LYS2*, *can1^R*, *cyh2^R*) and five control strains (A-E) for the two-hybrid assay were included in the ProQuest™ Two-Hybrid System purchased from Invitrogen (Carlsbad, CA).¹⁶²

Culture Media. Luria broth (LB) for *E. coli* culture, YPAD medium and Synthetic Complete (SC) medium for yeast culture were prepared following the recipes shown in the general laboratory manuals.^{127, 129, 162} To prepare SC plates containing 3-AT and 5-FOA, the SC medium was autoclaved, cooled to approximately 65 °C, and the appropriate amount of 3-AT or 5-FOA powder was added. The mixture was stirred to dissolve, and then poured into plates without further pH adjustment. Tryptone soya

broth (TSB) for the cultures of *Streptomyces* strains was made following the recipe from the general guidelines of *Streptomyces*.¹⁶³ AS1 plates were made by dissolving 1 g of yeast extract, 0.2 g of L-alanine, 0.5 g of L-arginine, 5 g of soluble starch, 2.5 g of NaCl, 10 g of Na₂SO₄, and 15 g of agar in 1 L of deionized water, adjusting pH to 7.5, and autoclaving. After autoclaving, the medium was supplemented with MgCl₂ to a final concentration of 10 mM and then poured into the plates.¹⁶⁸ For *Streptomyces* sporulation, SPA agar was prepared by dissolving 1 g of yeast extract, 1 g of beef extract, 2 g of tryptone, 10 g of glucose, trace amount of FeSO₄, and 15 g of agar in 1 L of deionized water and autoclaving. SGGP media was made of a mixture of 4 g of peptone, 4 g of yeast extract, 4 g of casamino acids, 2 g of glycine, and 0.25 g of MgSO₄•7H₂O dissolved in 1 L of deionized water, and autoclaved. After autoclaving, 20 mL of 50% (w/v) sterile glucose and 10 mL of 1 M KH₂PO₄ were added to the media. The *M. megalomicea* growth medium, ATCC #172 broth (either as a liquid or solid), was prepared as follows: a mixture of 10 g of glucose, 20 g of soluble starch, 5 g of yeast extract, 5 g of N-Z Amine, and 1 g of CaCO₃ were dissolved in 1 L of distilled water and autoclaved to make liquid media. For solid media, extra 15 g of agar was added in the mixture. For *Streptomyces venezuelae* secondary metabolite production, seed medium was prepared by adding 20 g of glucose, 15 g of soybean flour, 5 g of CaCO₃, 1 g of NaCl, and 2 mg of CoCl₂•6H₂O to 1 L of deionized water, then adjusting the pH to 7.2 and autoclaving. The vegetative medium was prepared by adding 20 g of glucose, 30 g of soybean flour, 2.5 g of CaCO₃, 1 g of NaCl, and 2 mg of CoCl₂•6H₂O to 1 L of deionized water, then adjusting the pH to 7.2, and autoclaving.

Growth and Maintenance of M. megalomicea. *M. megalomicea* was grown in ATCC #172 broth at 29 °C with shaking. A spore suspension of *M. megalomicea* was prepared for long-term storage by growth on #172 broth agar for 1 week at 29 °C. After the cells changed color completely from orange to black, the surface of the plate was overlaid with a sterile 20% glycerol solution and spores were gently suspended in the solution by rubbing the surface of the plate with a sterile cotton swab. Spore suspension was collected from the plate and stored at -80 °C.

Isolation of M. megalomicea Genomic DNA. To isolate the genomic DNA, 50 mL liquid culture of *M. megalomicea* was grown in #172 broth at 29 °C with shaking at 250 rpm for 7 days. The mycelium was harvested by centrifugation at $1,000 \times g$ at 4 °C for 10 min. After carefully removing the medium, the mycelium pellet was washed once with 10 mM EDTA (pH 8.0) in 10% sucrose. The mycelium was digested with 2 mg/mL lysozyme in 3 mL TES buffer (25 mM Tris-HCl, 25 mM EDTA, 0.3 M sucrose, pH 8.0) at 37 °C for 10 min. The lysozyme-treated mycelium was disrupted by mixing gently with 4 mL of $2 \times$ Kirby mix, which contains 2% SDS, 12% sodium 4-aminosalicylate, 0.1 M Tris-HCl (pH 8.0), and 6% equilibrated phenol (pH 8.0). Then, 8 mL of phenol/chloroform/isoamyl alcohol (50:50:1) was added to the cell lysate and thoroughly mixed. After centrifugation at $1,500 \times g$ for 10 min, the aqueous (upper) layer was transferred to a new tube and mixed with 3 mL of phenol/chloroform/isoamyl alcohol (25:24:1) and 0.6 mL of 3 M sodium acetate. The lysate mixture was centrifuged, transferred again, and 0.6 volumes of isopropanol were added. The genomic DNA was spooled with a sealed Pasteur pipette, and washed with 70% ethanol.

The genomic DNA pellet was air dried, redissolved in TE buffer, and stored at -20 °C.

Preparation of Competent Cells. The procedure used to prepare *E. coli* competent cells is detailed previously in the Experimental Procedures section of Chapter 2.

PCR primers and PCR Amplifications. The basic rules of designing oligonucleotide primers and the general procedure for PCR amplification of DNA fragments were described in the Experimental Procedures section of Chapter 2. For those PCR amplifications using genomic DNA as the template, the genomic DNA was digested by restriction enzymes before PCR. To prepare the digested genomic DNA, 10 µg of genomic DNA was digested with *Bam*HI restriction enzyme at 37 °C overnight, except *S. antibioticus* (ATCC 11891) genomic DNA which was digested with *Eco*R I. After digestion, the genomic DNA fragments were extracted by phenol/chloroform/isoamyl alcohol (25:24:1) to remove the enzyme, alcohol-precipitated, and re-dissolved in water for PCR.^{127, 129} The digested genomic DNA from *S. erythraea* (ATCC 11635), *S. peucetius* (ATCC 29050), and *Micromonospora megalomicea* subsp. *nigra* (ATCC 27598) were used as the templates for *eryC2* (*eryC3*), *dnrQ*, and *megD1* (*megD6*), respectively. With the genes to be cloned into the yeast two-hybrid fusion plasmids, the PCR primers were designed for translational in-frame fusion to the N'-terminal DNA-Binding (DB) or Activation (AD) domain. For pDBLeu vector cloning, *Nhe*I and *Spe*I were chosen to be the two cloning sites, and their recognition sequences were designed into the 5'-end of the forward and reverse primers, respectively. For pEXP-AD502 vector cloning, *Eco*RI and *Bgl*II were the two cloning sites designed

into the 5'-end of the forward and reverse primers, respectively. The primer sequences used for cloning into the yeast two-hybrid plasmids were listed in Table 3-1.

For constructing the *S. venezuelae* expression plasmid pCM37, Table 3-2 lists the primer pairs used to amplify the D-desosamine biosynthetic genes. The primers were designed to retain the original genomic sequence, which contains the authentic ribosome-binding sites (RBSs), except for the insertion of an *NdeI* restriction site between the *desII* and *desIII* genes to disrupt a putative transcription terminator. The primers listed in Table 3-3 were used to amplify the glycosyltransferases (GTs) and helper proteins, constructed using the pAX702 vector. All primers were designed to amplify the genes including their original RBSs. GT primers contain an *XbaI* site in the forward primers, and a *HindIII* site in the reverse primers. Helper protein primers contain the *NdeI* and *XbaI* sites in the forward and reverse primers respectively, except the *dnrQ* forward primer which contains an *EcoRI* site instead of an *NdeI* site. Because the lack of obvious RBSs in the 5'-untranslated regions of *nbmC* and *dnrQ*, we incorporated an artificial RBS in their forward primers (Table 3-3, underlined). For cloning purposes, the authentic *EcoRI* site just in front of the start codon of *eryC2* (Table 3-3, underlined) was disrupted by a point mutation (⁻²T→⁻²C). The digested genomic DNA from *S. narbonensis* (ATCC 19790), *S. antibioticus* (ATCC 11891) and *Micromonospora megalomicea* subsp. *nigra* (ATCC 27598) were used as the templates for *nbmC* (*nbmD*), *oleP1*, and *megC2*, respectively.

Gene	Vector	Primer Sequence
<i>des7</i>	pDBLeu	5'- CAC GCTAGC ATGCGCGTCCTGCTGACC -3'
		5'- GTGC ACTAGT GTGCCGGGCGTCGGCCGGCG -3'
<i>tylM2</i>	pDBLeu	5'- GAAA GCTAGC ATGCGCGTACTGCTGACC -3'
		5'- GTGG ACTAGT CCTTTCCGGCGCGGATCG -3'
<i>tylM3</i>	pDBLeu	5'- CCCG GCTAGC GTGAACACGGCAGCCGGCCC -3'
		5'- ACTA ACTAGT CTCGGGGACATACGGGGCGA -3'
<i>mycB</i>	pDBLeu	5'- AGTG GCTAGC ATGCGCGTGCTGCTGACC -3'
		5'- TCGA ACTAGT TCAGCGCGCTGGCCCCGGTG -3'
<i>eryC3</i>	pDBLeu	5'- GGTA GCTAGC ATGCGCGTCGTCTTCTCC -3'
		5'- GCGT ACTAGT TCATCGTGGTTCTCTCCTTC -3'
<i>megD1</i>	pDBLeu	5'- AGGA GCTAGC ATGCGCGTCGTGTTTTCATC -3'
		5'- GTGG ACTAGT TCATCGCGGCAGGTGCGGC -3'
<i>ACP domain</i>	pDBLeu	5'- TATA GCTAGC ACGGTGTCCCGTCCCAGC -3'
		5'- CCGC ACTAGT GGTGTTACGGGGGCCGAG -3'
<i>TE domain</i>	pDBLeu	5'- AGAT GCTAGC ATGTCCGGGGCCGACACC -3'
		5'- CCGC ACTAGT CTTGCCCCGCCCCCTCGATG -3'
<i>des8</i>	pEXP-AD502	5'- G GAATTC TGACCGACGACCTGACGGG -3'
		5'- GA AGATCT AGGAGCTGCTGACCGGGAC -3'
<i>tylM3</i>	pEXP-AD502	5'- G GAATTC TGAACACGGCAGCCGGCCCC -3'
		5'- TT AGATCT CGGGGACATACGGGGCGA -3'
<i>tylM2</i>	pEXP-AD502	5'- GGCA GAATTC TGC GCGTACTGCTGACCTG -3'
		5'- CCGC AGATCT CTACCTTTCCGGCGCGGATCG -3'
<i>mydC</i>	pEXP-AD502	5'- AGAA GAATTC TGACGAGTGACGAGCAGG -3'
		5'- CCGG AGATCT TCAGGCGCTGATCGGCAC -3'
<i>eryC2</i>	pEXP-AD502	5'- GG GAATTC TGACCACGACCGATCGCGCC -3'
		5'- GGT AGATCT AGAGCTCGACGGGGCAGC -3'
<i>megD6</i>	pEXP-AD502	5'- GAGC GAATTC TGGCAGTTGGCGATCGAAG -3'
		5'- TTCT AGATCT ACAGCTCGACCGGGCAACG -3'
<i>dnrQ</i>	pEXP-AD502	5'- AGCA GAATTC TGCCCACACCCACGTCCGC -3'
		5'- TCCC AGATCT ACTTCTGGGCCAGCCGCAGC -3'

Table 3-1 PCR primer pairs of genes used for cloning into the yeast two-hybrid plasmids

Gene(s)	Cloning Site	Primer Sequence
<i>des1-2</i>	<i>EcoRI</i>	5'- GGCC GAATTC TTCCCGGATCGGCGAATC -3'
	<i>NdeI</i>	5'- GGAATT CATATG GCCCTCAGGTGGGGGGATCGTG -3'
<i>des3-4</i>	<i>NdeI</i>	5'- GGGC CATATG GTCCGGCCGGGCCCTCGGTG -3'
	<i>BglII</i>	5'- TGGT AGATCT CGCCGGCCCGGCCGC -3'
<i>des4-5</i>	<i>BglII</i>	5'- GGCG AGATCT ACCACATCGGCGGCGGCCTG -3'
	<i>XbaI</i>	5'- CTAG TCTAGA CGGCCTGCTGGGTCTACC -3'
<i>des6</i>	<i>XbaI</i>	5'- GGCC TCTAGA CTCCGAAAGACCGAAAGCAGGAG -3'
	<i>HindIII</i>	5'- CTCT AAGCTT GGTGCACCCGGGACG -3'

Table 3-2 Primer pairs for constructing pCM37

Other primer pairs for constructing *E. coli* expression vectors are listed in Table 3-4. To design the 5'-primer for the Des7-pET41 construct, the *DesVII* coding sequence must be fused in-frame with GST-tag and S-Tag on the pET-41a(+) vector.

To change the rare arginine codons in genes encoding TyIM2 and TyIM3, we applied the PCR reactions to make the multiple mutagenesis (Figure 3-2). The primers for these multiple mutagenesis reactions are listed in Table 3-5. The PCR strategy to construct the four arginine codon-exchanged *TyIM3cx* was first to amplify the five fragments of *TyIM3* that contain new arginine codons and 24-bp overlapping regions at their both ends. The consecutive fragments were then joined to one continuous DNA fragment using overlap extension PCR. After the third-round of PCR to join the final two fragments (Figure 3-2, F6, F7), the complete four-codon-exchanged *TyIM3cx* was amplified, and subsequently digested with *NdeI/HindIII* for inserting into the pET-28b(+) vector. The same strategy was used to exchange the first two arginine codons of *TyIM2*

to make *TylM2cx*. The two codon-exchanged constructs were used as the PCR templates for cloning *TylM2cx/pET-21* and *TylM3cx/pET-29*.

GT	Primer Sequence
<i>des7</i>	5'- GGCC TCTAGA CAAGGAAGGACACGACG -3'
	5'- GCGC AAGCTT AGATACAGGGGTGAGGC -3'
<i>mycB</i>	5'- GCAG TCTAGA GGAAGGAGTGACGACG -3'
	5'- GGGC AAGCTT AGAGTCGATCAAGGTCAG -3'
<i>nbmD</i>	5'- GCCC TCTAGA CAAGGAAGGACACGACG -3'
	5'- GGGG AAGCTT GGAGATCAGTGGTGAGG -3'
Helper Protein	Primer Sequence
<i>des8</i>	5'- GGAATT CATATG CGAAGGAGCGGCGAAG -3'
	5'- GCGG TCTAGA GGTGTCTCAGGAGCTGC -3'
<i>mydC</i>	5'- GGCGTGG CATATG GTGACCGACAGATTCACC -3'
	5'- GCGC TCTAGA CATCGTCGTCACTCCTTCC -3'
<i>nbmC</i>	5'- GATCTCA CATATG <u>GGAGGG</u> CCACGGTGACCGACGAC -3'
	5'- GGGGCG TCTAGA GGTGGGGAGGTTCGGAAC -3'
<i>tylM3</i>	5'- GGAATT CATATG ATGACCGAACACGCCTCC -3'
	5'- GCAC TCTAGA CCAGTGCCCTTCTCACTCG -3'
<i>megD6</i>	5'- GAGTCTG CATATG ACAGTCTTCAATCC -3'
	5'- GACC TCTAGA TTCTTCCTCTACAGC -3'
<i>eryC2</i>	5'- CCGG CATATG CGGAGGGAAT <u>CC</u> ATGACCACGACCGATCG -3'
	5'- GCCG TCTAGA GTTACCTCAGAGCTCGAC -3'
<i>dnrQ</i>	5'- GGGG GAATTC <u>GGAGGG</u> ACAGTGTGAGGAGCACGACGATG -3'
	5'- GGGG TCTAGA ACGCCGTCACGAGCACCTTCATGGGGTCAC -3'
<i>megC2</i>	5'- GTCAGTG CATATG GGAGAGGGCATGAACACGAC -3'
	5'- GCTCAG TCTAGA GGCACCTCAGAGTTCGACC -3'
<i>oleP1</i>	5'- GCAGTGA CATATG CCGATCCCCCTCAGG -3'
	5'- GCGC TCTAGA ACGCGATGCTCATGC -3'

Table 3-3 PCR primer pairs (**top**, 5'-forward; **bottom**, 3'-reverse) for cloning glycosyltransferases and helper proteins

Construct	Cloning Site	Primer Sequence
Des7-pET41	<i>NcoI</i>	5'- GCTA CCATGG GCGTCCTGCTGACCTCGTTC -3'
	<i>XhoI</i>	5'- GGC CTCGAG TCAGTGCCGGGCGTCGGCCGGCG -3'
TylM2-pET28	<i>NdeI</i>	5'- CCG CATATG CGCGTACTGCTGACC -3'
	<i>HindIII</i>	5'- ATGG AAGCTT CTACCTTTCCGGCGCGGA -3'
TylM2cx-pET21	<i>NdeI</i>	5'- CCG CATATG CGCGTACTGCTGACC -3'
	<i>HindIII</i>	5'- GGCG AAGCTT ACGTTCCGGCGCGGATCGGGACC -3'
TylM3cx-pET29	<i>NcoI</i>	5'- AGCC CCATGG ACACGGCAGCCGGCCCGACC -3'
	<i>HindIII</i>	5'- AGTG AAGCTT TCACTCGGGGACATACGG -3'

Table 3-4 Primer pairs for constructing *E. coli* protein expression plasmids

Construction of Plasmids for E. coli Expression. All the molecular cloning procedures are the same as described in the Experimental Procedures of Chapter 2. The GST-DesVII expression plasmid, Des7-pET41, was constructed by inserting the *DesVII* coding sequence between *NcoI/XhoI* restriction sites of the pET-41a(+) vector. For the TylM2-pET28 expression plasmid, the PCR product of *TylM2* was cloned into the *NdeI/HindIII* restriction sites of pET-28b(+). TylM3-pET28 was constructed in the same manner as TylM2-pET28 by our group member Christopher J. Thibodeaux. To construct the *TylM3cx* into MalE-pET vector, the codon-exchanged *TylM3cx* fragment was cut from the plasmid TylM3cx-pET28 with *NdeI/HindIII*, and insert into MalE-pET vector pretreated with the same restriction enzymes. The two coexpression plasmids, TylM2cx/pET-21 and TylM3cx/pET-29, were made by inserting the PCR products of TylM2cx and TylM3cx into the *NdeI/HindIII* sites of pET-21b(+) and the *NcoI/HindIII* sites of pET-29b(+), respectively (Figure 3-3).

Primer #	Sequence
TylM2cx	
up	5'- CCG CATATG CGCGTACTGCTGACC -3'
R1-f	5'- GCCTGGGCCCCTG <u>CGT</u> GCGGCCGGACAC -3'
R1-r	5'- GTGTCCGGCCGC <u>ACG</u> CAGGGCCCAGGC -3'
R2-f	5'- CACCGCACTCCAC <u>CGT</u> AACGGCCGGTCC -3'
R2-r	5'- GGACCGGCCGTT <u>ACG</u> GTGGAGTGC GTG -3'
down	5'- ATGG AAGCTT CTACCTTCCGGCGCGGA -3'
TylM3cx	
up	5'- AGAG CATATG AACACGGCAGCCGGCC -3'
R1-f	5'- CGCGCCGGACGC <u>CGT</u> CTCCAATCACC -3'
R1-r	5'- GGTGAGTTGGAG <u>ACG</u> GCGTCCGGCGCG -3'
R2-f	5'- CGGCCCCCGGAC <u>CGT</u> GAGGAGCGAGAC -3'
R2-r	5'- GTCTCGCTCCTC <u>ACG</u> GTCCGGGGGCGG -3'
R3-f	5'- CGCCTGGAGAGC <u>CGT</u> GTGGCACGCGAG -3'
R3-r	5'- CTCGCGTGCCAC <u>ACG</u> GCTCTCCAGGCG -3'
R4-f	5'- GGCCGGTCTG <u>CGT</u> GCGCTCGCCG -3'
R4-r	5'- CGGCGAGCGC <u>ACG</u> CAGACCGGCC -3'
down	5'- AGTG AAGCTT TCACTCGGGGACATACGG -3'

Table 3-5 Primer pairs for PCR-based multiple mutagenesis of *TylM2cx* and *TylM3cx*. The new arginine codon for mutagenesis was underlined, and the bold-labeled sequences are restriction sites for cloning.

Expression and Purification of the Recombinant Proteins from E. coli BL21(DE3).

All general *E. coli* protein expression procedures are identical to those described in the Experimental Procedures section of Chapter 2. The Des7-pET41 expression plasmid was transformed into *E. coli* BL21(DE3) strain. The transformed strain was incubated in LB media at 37 °C till the OD₆₀₀ reached 0.4. Then, after adding 0.1 mM IPTG, the culture was allowed to grow at 16 °C overnight, and the cells were harvested by

centrifugation. After harvesting, the cell pellet was resuspended in PBS buffer (150 mM NaCl, 10 mM potassium phosphate, pH 7.4) followed by sonication and centrifugation to collect the soluble cell lysate. The crude cell lysate was filtered through an 0.45 μ m filter and Triton X-100 was added to a final concentration of 1% (v/v). The filtered lysate was then loaded onto a glutathione-agarose prepacked column, pre-equilibrated with PBS buffer, under gravity flow. After washing the column with four column volumes of PBST (PBS containing 1% Triton X-100), the GST-DesVII was eluted with freshly prepared elution buffer (10 mM reduced glutathione in 50 mM Tris-HCl, pH 7.5). The eluted GST-DesVII was then dialyzed against 50 mM potassium phosphate buffer, pH 7.5, with 20% glycerol. The calculated molecular weight of GST-DesVII was 78095 Da. For DesVII-C-His and MalE-DesVIII expression and purification, all the procedures followed the same protocol listed in Dr. Borisova's thesis.¹⁶⁶ The GST and MalE proteins were expressed in *E. coli* BL21(DE3) with the empty vectors pET-41a(+) and pMalE-pET, respectively. The expression and purification methods were the same as those of GST-DesVII and MalE-DesVIII. The calculated molecular weight of MalE-DesVIII was 86471 Da.

For the expression of TylM2-pET28 by BL21(DE3), a 6-liter culture in LB medium with 50 μ g/mL kanamycin was performed at 37 °C until the OD₆₀₀ reached 0.4. Then, 0.5 mM IPTG was added to the culture to induce TylM2 overexpression. The expression conditions used for *N'*-His-TylM2 was either at 16 °C for 3 days or at 37 °C for 24 h. The purification procedures of *N'*-His-TylM2 by Ni-NTA affinity chromatography and FPLC-MonoQ chromatography were the same as those stated in the

Experimental Procedures section of Chapter 2. Similar procedures were also used to overexpress and purify the *N*'-His-TylM3 from the plasmid TylM3-pET28, except the expression host was BL21-CodonPlus[®] (DE3) and the expression conditions used were at 16 °C for 3 days.

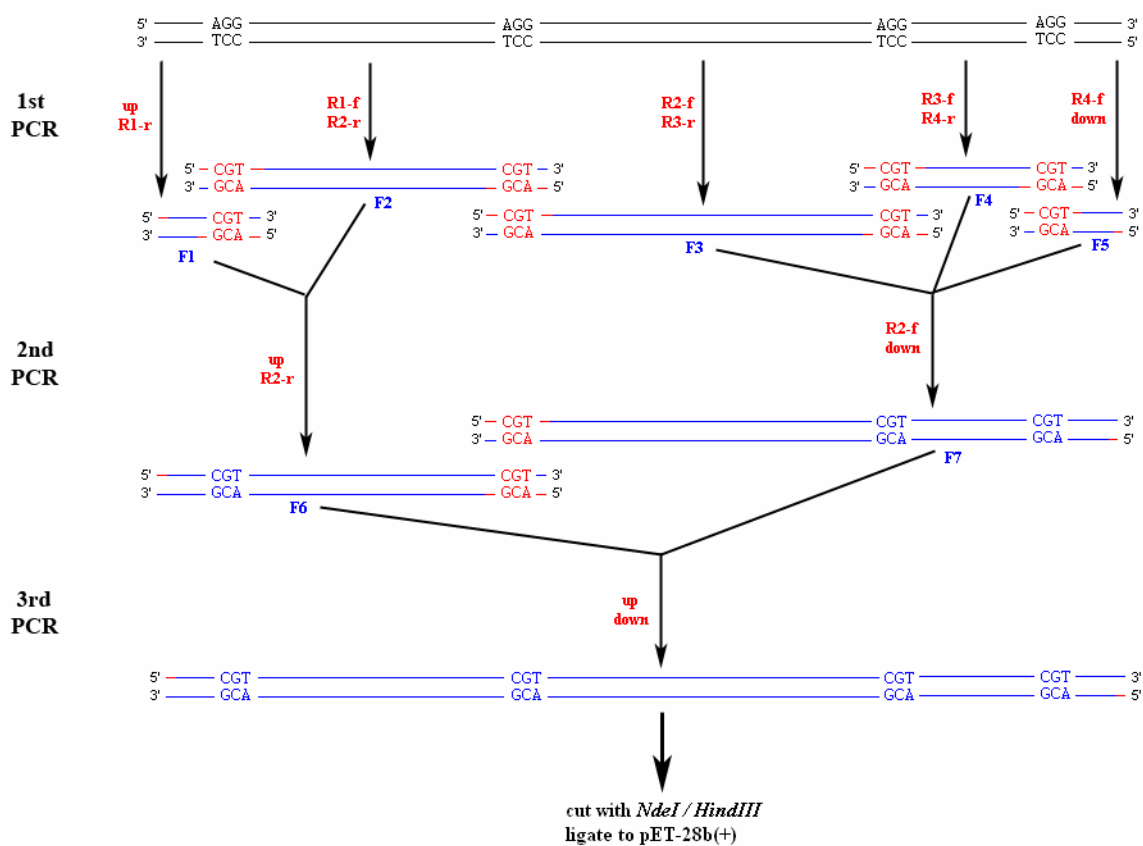


Figure 3-2 The PCR procedures to make TylM3cx construct. The primer pairs used for each PCR are listed besides the arrow.

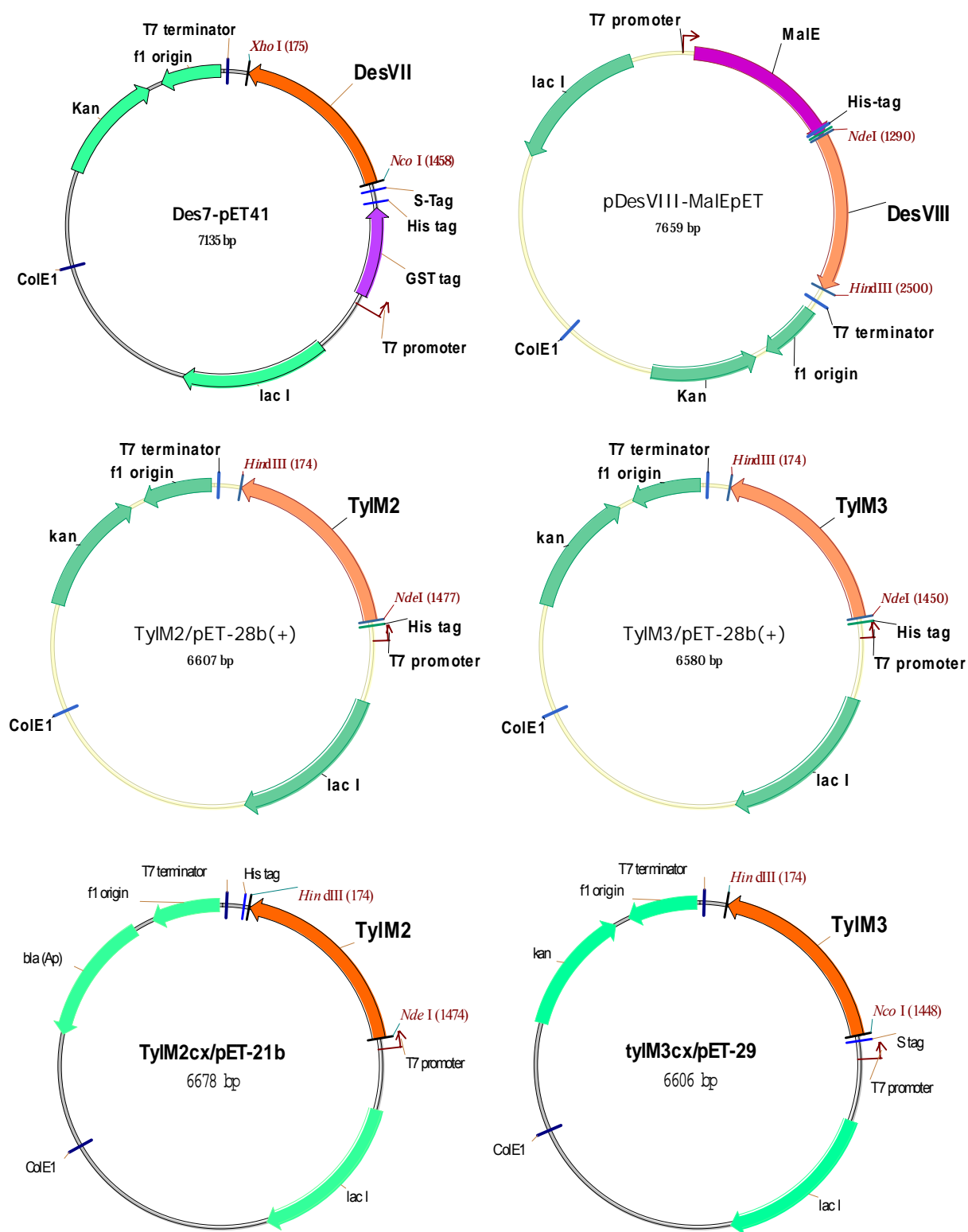


Figure 3-3 Plasmid Maps for *E. coli* Overexpressions of Glycosyltransferases and Helper

Proteins

The expression of codon exchanged TylM2cx and TylM3cx in BL21(DE3) followed the same protocols used for TylM2-pET28, except the IPTG concentration for induction was 0.3 mM. The expression temperature and time for TylM2cx were 37 °C overnight or 16 °C for 2 days when expressing TylM3cx. For the overexpression of MalE-TylM3cx, 3 liters of culture medium was incubated at 16 °C for 3 days. After purification of the fusion protein by Ni-NTA affinity chromatography, the dialyzed MalE-TylM3cx was treated with Tev protease and using Ni-NTA affinity chromatography again to remove the His-tagged MalE. The unbound TylM3cx in the flow-through fraction was collected, dialyzed, and concentrated again for activity assay.

To purify TylM2cx and TylM3cx under denaturing conditions, the culturing, harvesting and lysate-preparing procedures were the same as the purification under the native conditions, except the lysis buffer was different (100 mM NaH₂PO₄, 10 mM Tris-HCl, 8 M urea, pH 8.0). After the centrifuge, the denaturing lysates (100-150 mL) were collected and mixed with 10 mL Ni-NTA slurry and mix gently by shaking for 1 h at room temperature. Then, the lysate-resin mixture was loaded into a chromatography column, and the flow-through fraction was collected. After washing twice with washing buffer (100 mM NaH₂PO₄, 10 mM Tris-HCl, 8 M urea, pH 6.3), the denatured protein was eluted with 30 mL elute buffer (100 mM NaH₂PO₄, 10 mM Tris-HCl, 8 M urea, pH 4.5). The collected eluate of denatured protein was concentrated later with YM-10 Centricon™ to ~5 mL volume for renaturing dialysis procedure. The concentrated protein eluates (5-10 mL) were loaded into the dialysis membrane tube (MWCO:

12-14,000 kDa) and dialyzed against series of 1 L dialysis buffer at 4 °C (Table 3-6). The renaturing protein was incubated in each buffer for 12 h with slow stirring. After dialysis, the renatured protein were subjected to concentration determination and then stored at -80 °C.

Buffer #	Composition
1 st	50 mM potassium phosphate, 6 M urea, 5% glycerol (pH 7.5)
2 nd	50 mM potassium phosphate, 5 M urea, 5% glycerol, 0.1% Triton X-100 (pH 7.5)
3 rd	50 mM potassium phosphate, 4 M urea, 10% glycerol, 0.1% Triton X-100 (pH 7.5)
4 th	50 mM potassium phosphate, 3 M urea, 10% glycerol, 0.1% Triton X-100 (pH 7.5)
5 th	50 mM potassium phosphate, 2 M urea, 15% glycerol, 0.1% Triton X-100 (pH 7.5)
6 th	50 mM potassium phosphate, 1 M urea, 15% glycerol, 0.1% Triton X-100 (pH 7.5)
7 th	50 mM potassium phosphate, 20% glycerol, 0.1% Triton X-100 (pH 7.5)
8 th	50 mM potassium phosphate, 20% glycerol, 0.1% Triton X-100 (pH 7.5)

Table 3-6 Buffer compositions of sequential dialysis buffers used for TylM2cx and TylM3cx renaturation.

For the coexpression of TylM2cx and TylM3cx in one cell, the two constructed plasmids, TylM2cx/pET-21 and TylM3cx/pET-29, were co-transformed into *E. coli* expression host BL21(DE3) using heat-shock method and the positive transformants were selected with ampicillin and kanamycin. The positive transformants were also verified by plasmid extraction to examine the co-existence of two different plasmids. Then, the positive strain was cultured in 3 liter LB medium at 18 °C for 18 h with 0.3 mM IPTG induction to coexpress the TylM2 and TylM3 proteins. After cell harvest, the purification procedures were the same as those used for other His-tagged proteins.

In Vitro S-tag Pull-down Assay. A precipitation mixture containing 100 μ L S-protein agarose beads (Novagen) and 50 μ g of each protein to be tested was prepared and incubated at room temperature on an orbital shaker for 30 min. After incubation, the mixture was centrifuged at $500 \times g$ to pellet the agarose beads with bounded proteins. Then, the supernatant was discarded and the agarose beads pellet was washed 3 times with the binding buffer (20 mM Tris-HCl, pH 7.5, 150 mM NaCl, 0.1% Triton X-100). The washed agarose beads were then resuspended with SDS-PAGE loading buffer, boiled, and the eluate was loaded onto SDS-PAGE for Western-Blotting. The procedure of Western-Blotting was similar to the one described in the Experimental Procedures section of Chapter 2, except the anti-maltose binding protein (MBP) antibody in addition to the anti-polyHistidine antibody were used as the primary antibodies.

In Vitro Glycosylation Assay of TylM2/TylM3. The basic assay method followed the glycosylation assay of TDP-D-desosamine (**21**) developed in our lab and the product analysis employed Thin-Layer Chromatography (TLC).¹⁶⁶ The reaction mixture contained 0.5 mM ty lactone (**75**), 0.5 mM TDP-sugar (TDP-D-desosamine (**21**) or TDP-D-mycaminose (**74**)), 5 mM $MgCl_2$, and 0.5 μ M of each enzyme (TylM2 with or without TylM3) in 50 mM Tris-HCl buffer (pH 7.5). TDP-D-mycaminose (**74**) and TDP-D-desosamine (**21**) were obtained from Dr. Svetlana A. Borisova, and their preparations were described in her thesis.¹⁶⁶ Ty lactone (**75**) was kindly provided by the Eli Lilly and Company (Indianapolis, IN). The reaction was incubated at 29 $^{\circ}C$ with shaking, and quenched by adding an equal volume of chloroform at the end of 2 h and 16 h after incubation. After quenching, the mixture was centrifuged to detain the

chloroform extract, which was then concentrated to a volume of 50 μL by heating at 37 $^{\circ}\text{C}$. The extract was spotted on a TLC plate (10-20 μL per spot), developed with the chloroform : methanol (9:1) solvent system, and visualized by vanillin staining (0.75% vanilla, 1.5% (v/v) H_2SO_4 in methanol).

Construction of Fusion Plasmids for Yeast Two-Hybrid Assay. The DNA manipulations used to construct yeast two-hybrid fusion plasmids were similar to the procedures outlined in the Experimental Procedures section of Chapter 2, except the restriction enzymes (explained in *Primer Design*) were different. The maps of two example constructs, Des7/pDBLeu and Des8/pEXP-AD502, are shown in Figure 3-4.

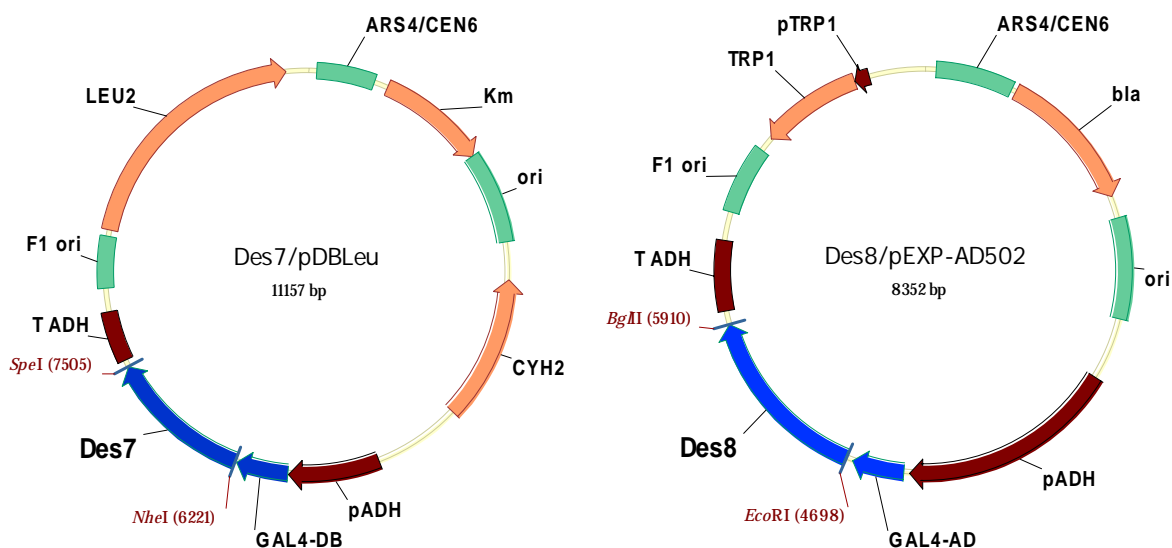


Figure 3-4 Plasmid Maps of the Yeast Two-Hybrid Expression System

*Construction of *S. venezuelae* Expression Plasmids.* The expression plasmids pCM37 was constructed by transferring the *desI-desVI* genes into the pCM1d vector

(Figure 3-5, left). The *desI-II* genes were inserted between the *EcoRI* and *NdeI* sites. The *desIII-V* genes were separated into two PCR fragments using a *BglII* site located in *desIV*, and cloned in between the *NdeI* and *XbaI* sites. The *desVI* gene was cloned into the *XbaI* and *HindIII* sites.

The construction of GT plus helper protein plasmids entailed the insertion of a GT and a helper protein between the *XbaI/HindIII* and *NdeI/XbaI* sites of pAX702 vector, respectively (Figure 3-5, right). In the case of *dnrQ* as the helper protein, *EcoRI* and *XbaI* were the restriction sites used for the cloning.

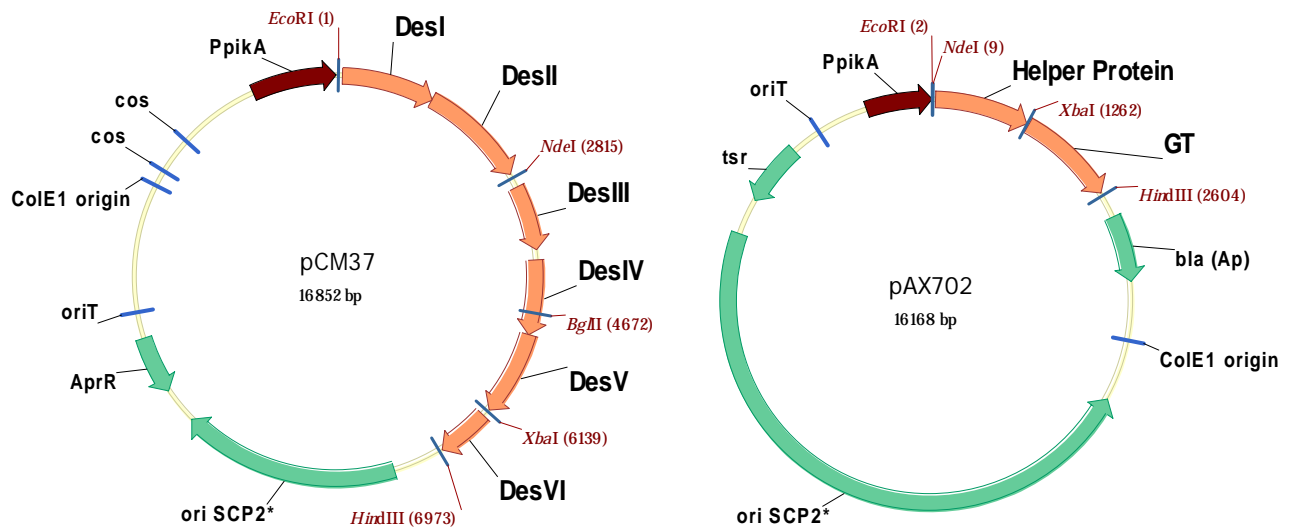


Figure 3-5 Plasmid maps of pCM37 and GT/Helper protein-pAX702

Introducing DNA into Yeast Cells. For *Saccharomyces cerevisiae*, fresh yeast competent cells were prepared for every transformation using the lithium acetate method.^{127, 162} A single yeast MaV203 colony was inoculated into 5 mL YPAD medium

and grown overnight at 30 °C with shaking. The overnight culture was transferred to 500 mL YPAD and grew at 30 °C until OD₆₀₀ reached 0.4. The yeast cells were harvested with centrifugation at 3,000 × g for 5 min at room temperature. The harvested cell pellet was then washed with 50 mL sterile water and centrifuged again. The cell pellet was then washed again using 50 mL TE/LiAc solution, containing 0.1 M lithium acetate (pH 7.5), 10 mM Tris-HCl (pH 7.5), and 1 mM EDTA. After the wash, the yeast pellet was resuspended with 2 mL TE/LiAc solution. To transform the cells, a mixture of 200 µL fresh competent cell, 0.1 mg freshly boiled carrier DNA, and 100 ng each of the two plasmids (pDBLeu-X and pEXP-AD502-Y) was prepared and then 1.2 mL PEG/LiAc solution, which contains 0.1 M lithium acetate (pH 7.5), 10 mM Tris-HCl (pH 7.5), 1 mM EDTA, and 40% (w/v) PEG 3350, was added. The final mixture was incubated at 30 °C for 30 min, followed by a heat-shock at 42 °C for 15 min. After the heat-shock, the transformation yeast was centrifuged and then spread on the Synthetic Complete (SC) medium without leucine and tryptophan. The SC plates were incubated at 30 °C for 2 days until colonies appeared. With each of the different pDBLeu-X or pEXP-AD502-Y plasmids, an empty pEXP-AD502 or pDBLeu vector, respectively, was co-transformed as the negative control.

Yeast Two-Hybrid Assays Using Replica Plating. After yeast transformation, two different colonies from each transformation were inoculated on a single SC-Leu-Trp plate along with two colonies each from Yeast Control Strains A-E. This plate was incubated for ~18 h at 30 °C and set as the master plate for replica plating. After incubation, the master plate was gently pressed with a light, consistent pressure onto a piece of

autoclaved velvet, transferring only a slight haze of cells and avoiding cell clumps on the velvet. Then, SC-Leu-Trp-His plates containing 3AT (3-amino-1,2,4-triazole) at concentrations of 10, 25, 50, 75, and 100 mM, an SC-Leu-Trp-Ura plate, an SC-Leu-Trp+0.2% 5-FOA (5-fluoroorotic acid) plate, and a YPAD plate were gently pressed onto this “inoculated” velvet to transfer the colonies or patches. Immediately following replica plating, the cells on the selection plate were replica cleaned or “diluted” by pressing a fresh piece of autoclaved velvet onto the surface with a greater amount of pressure than replica plating. The replica plates were replica cleaned again after the initial 24-hr incubation at 30 °C, and incubated for another 24 to 48 h. The growth conditions of colony patches on the SC replica plates were carefully compared to the Control Strains A-E and the negative control colonies.

X-gal Assay of Yeast Two-Hybrid Tests. After replica cleaning and incubation, a 90 mm nylon membrane was placed on the surface of the replica YPAD plate for 1 min. The nylon membrane was carefully removed and completely immersed in liquid nitrogen for 20-30 s. The membrane was removed from the liquid nitrogen and placed on top of pre-soaked Whatman[®] filter paper with colonies-side up in an empty Petri dish. The Whatman[®] filter paper was soaked with the solution containing 10 mg X-gal/100 µL *N,N*-dimethyl formamide (DMF), 60 µL 2-mercaptoethanol and 10 mL Z-buffer (0.1 M sodium phosphate, 10 mM KCl, 1 mM MgSO₄, pH 7.0). The Petri dish containing the nylon membrane was covered and incubated at 37 °C for over 24 h or until the appearance of blue color. Results from the colonies carrying the testing constructs were compared to the results from Yeast Control Strains A-E and the negative control strains.

Conjugal Transfer of Expression Plasmids from E. coli to S. venezuelae Kdes mutant. The method for these experiments followed the methods published by Bierman et al.¹⁶⁹ with minor modifications.¹⁷⁰ All *S. venezuelae* cultures were grown in glass tubes containing glass beads. A 1 mL aliquot of *S. venezuelae Kdes* mutant (recipient) mycelia stock was inoculated into 9 mL of Tryptone soya broth (TSB) containing kanamycin (50 µg/mL) and grown at 29 °C for 18 h. In parallel, *E. coli* S17-1 competent cells (donor) were transformed with the expression plasmids in preparation for conjugal transfer, and transformants were plated on the LB agar with appropriate antibiotics. For pCM37 transformation, apramycin (50 µg/mL) and streptomycin (10 µg/mL) were contained in the LB plates; and for constructs involving the pAX702 vector, ampicillin (50 µg/mL) and streptomycin (10 µg/mL) were used. Next, 2 mL aliquots of the recipient culture were reinoculated into 18 mL of TSB with kanamycin (50 µg/mL) and allowed to grow for another 18 h at 29 °C. Before reinoculation, the mycelial culture was briefly vortexed to avoid clumping. In parallel, 2 positive *E. coli* S17-1 colonies (donor) were inoculated into 2 mL of TSB containing the same antibiotics as the LB plates, and grown at 37 °C overnight with shaking. Subsequently, 1 mL of the recipient culture was again transferred into 9 mL of TSB with kanamycin and grown for 3 h at 29 °C. Meanwhile, 20 µL of *E. coli* S17-1 cultures (donor) were transferred to 2 mL of fresh TSB with antibiotics as stated previously. Both donor and recipient cells were pelleted by centrifugation and washed twice with fresh TSB to remove antibiotics. After wash, the recipient and all donor cells were resuspended in 2 mL TSB separately. For each conjugal transfer, three ratios (9:1, 1:1, and 1:10) of donor to recipient cell

mixtures were prepared. Three to five aliquots of 100 μ L each donor/recipient mixtures were spread on freshly prepared AS1 agar plates. The plates were incubated at 29 °C for at least 18 h before overlaying with 2 mL of the appropriate antibiotic mixture. For every conjugation plate, nalidixic acid (500 μ g/mL) and kanamycin (500 μ g/mL) must be included in the antibiotics mixture. When performing pCM37 conjugal transfer, apramycin (500 μ g/mL) was added in the mixture. Both apramycin (500 μ g/mL) and thiostrepton (500 μ g/mL) were added while transferring pAX702-derived plasmids. The plates were incubated at 29 °C for 5 to 7 days until small recombinant *S. venezuelae* colonies (positive transformants) appeared.

Preparation of Spore Suspensions and Frozen Mycelia of S. venezuelae Strains. Wild type *S. venezuelae* and its mutant strains were stored for long-term as spore suspensions in 20% glycerol at -80 °C. Colonies of *S. venezuelae* strains were first streaked onto SPA plates containing the appropriate antibiotics and incubated for 5-7 days at 29 °C until the cells turned gray or black (sporulation). After the cell color changed, 2 mL of sterile 20% glycerol solution was overlaid on the surface of the plates and spores were gently suspended in the solution by rubbing the surface of the plate with a sterile cotton swab. Spore suspension was collected and filtered through a sterile pipette tip loosely packed with cotton wool and stored at -80 °C.

To prepare frozen mycelia of *S. venezuelae* strains, a 25 μ L aliquot of frozen spore suspension was inoculated into 25 mL of SGGP medium containing the appropriate antibiotics, and allowed to grow for 28 h at 29 °C with shaking. After mycelia grew from spores and the culture exhibited turbidity, the whole cultures were transferred to 50

mL conical tubes and centrifuged at room temperature for 10 min at $1,700 \times g$. The SGGP medium was discarded after centrifugation and the mycelial pellet was washed twice with 15 mL of sterile 10.3% sucrose. The washed mycelial pellet was resuspended in 10 mL of sterile 10.3% sucrose and stored in 2 mL aliquots at $-20\text{ }^{\circ}\text{C}$.

Small-scale Isolation of Metabolites Produced by S. venezuelae Strains and Analysis by Thin-Layer Chromatography. The *S. venezuelae* strains were grown under conditions favoring the formation of 12-membered ring macrolides.¹⁷¹ For small-scale cultures, a 25 μL aliquot of frozen spore suspension or fresh culture from an SPA plate colony was inoculated into 5 mL seed medium with the appropriate antibiotics, and grown at $29\text{ }^{\circ}\text{C}$ with shaking for 48 h or until the culture was turbid. The culture was vortexed briefly to disrupt mycelial clumps, and 500 μL of the seed culture was transferred to 20 mL of the vegetative medium. The vegetative culture was grown at $29\text{ }^{\circ}\text{C}$ with shaking for another 48-60 h or until the culture turned dark brown. The culture was centrifuged at $4,000 \times g$ for 15 min at room temperature to remove the mycelia and insoluble media components. The supernatant was retained and adjusted to pH 9.5 with 10 M KOH, and then extracted with an equal volume of chloroform. The media/chloroform mixture was vigorously agitated, and then centrifuged to separate the aqueous and the chloroform layer. The chloroform fraction that contains the secondary metabolites was transferred to a glassware container for rotary evaporation. After the crude extract, usually yellow in color, was obtained, it was re-dissolved with 300 μL chloroform and subjected to Thin-Layer Chromatography (TLC) and further analysis.

The TLC analysis was performed with a 9:1 or 4:1 chloroform/methanol solvent

system. The *S. venezuelae* secondary metabolites on the TLC plates were visualized by vanillin staining followed by heating or under short wavelength UV light. Vanillin staining solution was prepared by dissolving 0.75% (w/v) vanillin powder in methanol with 1.5% (v/v) concentrated sulfuric acid. After vanillin stain, the 12-membered-ring aglycone 10-deoxymethynolide (**35**) appeared in dark blue color, methymycin (**23**) and other 12-membered ring macrolides hydroxylated at C-10 in olive green color, and neomethymycin (**76**) and other 12-membered ring macrolides hydroxylated at C-12 in orange color. Small-scale preparative TLC of *S. venezuelae* extracts was performed by the same method as the analytical TLC, except the vanillin staining was only applied to the edges of the TLC plate. After staining two edges, the unstained silica corresponding to the compound of interest was scraped off the TLC plate. This scraped silica gel was then ground and extracted three times with 100 μ L of 4:1 chloroform/methanol solvent, and the solution was concentrated for mass spectrometry analysis or dried for storing.

HPLC Analysis of the Crude Extracts from S. venezuelae Strains. The *S. venezuelae* metabolite extracts were prepared as described in the small-scale TLC assay. The dried extracts were dissolved in 1 mL of 50% acetonitrile containing 50% aqueous 14 mM triethylamine (pH 2.5). Depending on the extract concentration, a 20 or 100 μ L aliquot of the solution was injected into the analytical HPLC C₁₈ column. The HPLC solvent system and time program used were identical to those reported in previous studies.^{164, 166} Buffer A was 57 mM ammonium acetate, and Buffer B was acetonitrile. HPLC running program began with isocratic elution using 25% Buffer B for 10 min, then Buffer B was increased to 40% for 20 min, followed by 100% Buffer B for 10 min to

clean the column. The column was then re-equilibrated with 25% Buffer B for 20 min. The detector was set at 235 nm for detection of 12-membered-ring aglycones and their glycosylated derivatives.

LC-MS Quantitative Analysis of Crude Extracts from S. venezuelae Strains. The *S. venezuelae* metabolite extracts were prepared as described in the small-scale TLC assay. The dried extracts were dissolved in 0.5 mL of acetonitrile and were then subjected to liquid chromatography coupled to an electrospray ionization-mass spectrometer (LC-ESI-MS, performed by the Mass Spectrometry Core Facility in the Department of Chemistry and Biochemistry at the University of Texas at Austin). LC was performed with a Finnigan Surveyor system (Thermo Fisher Scientific, Waltham, MA), equipped with a 50 × 2.1 mm Thermo Hypersil GOLD (3 μm) column. Compounds were eluted with a gradient of 5–100% acetonitrile in water at a flow rate of 0.5 ml/min for 10 min, followed by a wash with 100% acetonitrile wash for another 10 min. The eluant was directly injected into the ESI interface of a LTQ XL™ Linear Ion Trap Mass Spectrometer (Thermo Fisher Scientific). Mass spectrometric data were acquired in the positive-ion mode while scanning for the specific masses of **35** (calculated M.W. 297.3), **23** (calculated M.W. 470.5), and **76** (calculated M.W. 470.5). The extent of glycosylation, or glycosylation ratio, from each sample extract was calculated with the equation of $[(\mathbf{23}+\mathbf{76})/(\mathbf{35}+\mathbf{23}+\mathbf{76})]$ using the peak intensity obtained from the LC–MS spectrum. For each mutant strain, the data were averaged from three separate cultivations and extractions.

3. RESULTS AND DISCUSSION

Testing the Protein-Protein Interactions with Yeast Two-Hybrid Assay. Due to the requirement of helper proteins for some macrolide glycosylation, the two-protein glycosylation system indicates possible interactions between the GTs and the helper proteins. We chose the yeast two-hybrid system to test this hypothesis. The two-hybrid system is an *in vivo* yeast-based system that identifies the interaction between two proteins (X and Y) by reconstituting an active transcription factor.¹⁷² The active transcription factors are formed as a dimer between two fusion proteins, one of which contains a DNA-Binding Domain (DB) fused to the first protein of interest (DB-X) and the other, an Activation Domain (AD) fused to the second protein of interest (AD-Y). The DB-X:AD-Y interaction could reconstitute a functional transcription factor that activates chromosomally-integrated reporter genes driven by promoters containing the relevant DB binding sites (Figure 3-6). When a selectable marker such as *HIS3* is used as a reporter gene, two-hybrid-dependent transcription activation can be monitored by cell growth on plates lacking histidine, thereby providing a means to detect protein-protein interactions genetically. In our experiments, we used ProQuest™ Two-Hybrid System from Invitrogen (Carlsbad, CA) that applied three reporter genes, *HIS3*, *lacZ*, and *URA3*, to avoid false-positive results.¹⁷³

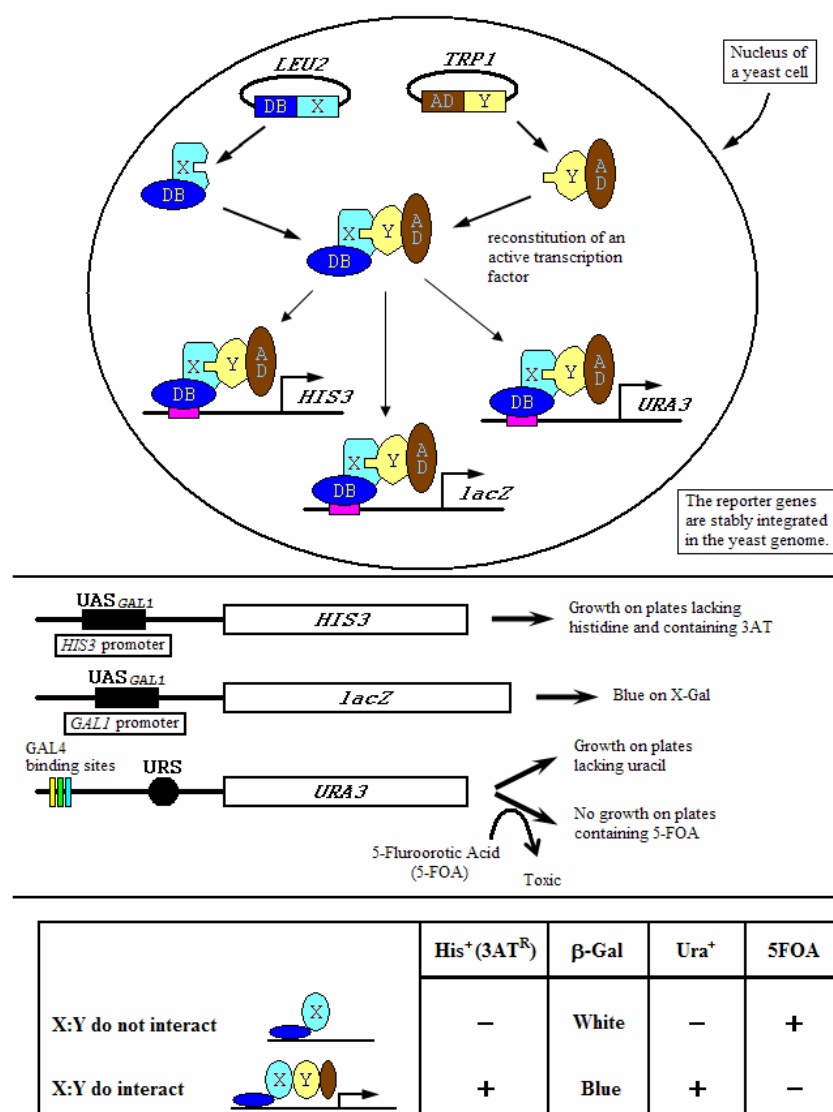


Figure 3-6 Yeast Two-Hybrid System Assays (adapted from Reference 162)

Basically, we made DB constructs fused with all the GTs and AD constructs fused with the helper proteins. Then, we co-transformed not only the original pairs of the GT and helper protein but also different cross-combinations of non-native pairs of GTs and helper proteins. We tested these non-native GT/helper protein pairs to examine the

homology and specificity between different homologous proteins. From the assay results listed in Table 3-7 (#1-31), only the DB-des7:AD-des8 pair exhibited all three reporter gene expressions. Furthermore, their interaction is weak based on the comparison to the control strains (Figure 3-7, #4). The constructs of DB-des7, DB-tylM2 and DB-megD1 showed self-activation of the *HIS3* reporter gene. This self-activation was also exhibited in the expression of the *lacZ* gene for DB-megD1 construct (Table 3-7, #2, 11, 23). *HIS3* encodes imidazole glycerol phosphate dehydratase, an enzyme involved in the sixth step of histidine biosynthesis. This enzyme can be specifically inhibited in a dose-dependent manner by 3-amino-1,2,4-triazole (3AT). The MaV203 strain expresses a basal level of *HIS3*, and even slight increases in the expression can be detected using the SC plates containing different concentrations of 3AT. Thus, the stronger expression of *HIS3* on DB-des7:AD-des8 co-transformant than the DB-des7 self-activation suggested that DesVII interacts with DesVIII. As observed with Yeast Control Strain B, intermediate levels of *URA3* expression could result in both cell growth inhibition on 0.2% 5-FOA and insufficient *URA3* gene product to allow growth on SC plates lacking uracil. The 5-FOA-sensitive and *Ura3*-negative phenotype often indicated that the protein pairs interact weakly as we observed in the result of the DB-des7:AD-des8 co-transformant. Besides the BD-GT:AD-helper protein tests, we also wanted to test the possible interactions between the helper protein and the domain of polyketide synthase (PKS). We chose PikAIII ACP and TE domains of pikromycin PKS and examined their interactions with the helper protein DesVIII of desosaminyl glycosylation (Table 3-7,

#32-35). To rule out the possibility that the negative results were caused by improper folding and structural hindrance of the two fusion proteins, we swapped the fusion domains of TylM2 and TylM3 to examine their alternative interactions. However, DB-tylM3:AD-tylM2 did not show any expression of the three reporter genes (Table 3-7, #36-38).

Strain # (DB-X) × (AD-Y)		Reporter genes (assays)				Interaction
		His ⁺ (3AT ^R)	β-Gal	Ura ⁺	5FOA	
Control A (no insert DNA)		-	W	-	+	No
Control B (human RB × E2F1)		+	B	-	Δ	Weak
Control C (fly DP × E2F)		++	B+	++	-	Strong
Control D (rat cFos × mouse cJun)		++	B+	+	Δ	Strong
Control E (yeast GAL4)		+++	B+	++	-	Very strong
1	DB × AD	-	W	-	+	-
2	DB-des7 × AD	+	W	-	+	-
3	DB × AD-des8	-	W	-	+	-
4	DB-des7 × AD-des8	++	B	-	Δ	Weak
5	DB-des7 × AD-tylM3	+	W	-	+	No
6	DB-des7 × AD-eryC2	+	W	-	+	No
7	DB-des7 × AD-megD6	+	W	-	+	No
8	DB-des7 × AD-dnrQ	+	W	-	+	No
9	DB-des7 × AD-mydC	+	W	-	/	No
10	DB × AD-dnrQ	-	W	-	/	-
11	DB-tylM2 × AD	+	W	-	+	-
12	DB-tylM2 × AD-des8	+	W	-	+	No
13	DB-tylM2 × AD-tylM3	+	W	-	+	No
14	DB-tylM2 × AD-eryC2	+	W	-	+	No
15	DB-tylM2 × AD-megD6	-	W	-	+	No
16	DB × AD-tylM3	-	W	-	+	-

17	DB-eryC3 × AD	-	W	-	+	-
18	DB-eryC3 × AD-des8	-	W	-	+	No
19	DB-eryC3 × AD-tylM3	-	W	-	+	No
20	DB-eryC3 × AD-eryC2	-	W	-	+	No
21	DB-eryC3 × AD-megD6	-	W	-	+	No
22	DB × AD-eryC2	-	W	-	+	-
23	DB-megD1 × AD	++	B-	-	+	-
24	DB-megD1 × AD-des8	++	B-	-	+	No
25	DB-megD1 × AD-tylM3	++	B-	-	+	No
26	DB-megD1 × AD-eryC2	++	B-	-	+	No
27	DB-megD1 × AD-megD6	++	B-	-	+	No
28	DB × AD-megD6	-	W	-	+	-
29	DB-mycB × AD	-	W	-	/	-
30	DB-mycB × AD-mydC	-	W	-	/	No
31	DB × AD-mydC	-	W	-	/	-
32	DB-TE × AD	-	W	-	+	-
33	DB-TE × AD-des8	-	W	-	+	No
34	DB-ACP × AD	-	W	-	+	-
35	DB-ACP × AD-des8	-	W	-	+	No
36	DB-tylM3 × AD	-	W	-	/	-
37	DB-tylM3 × AD-tylM2	-	W	-	/	No
38	DB × AD-tylM2	-	W	-	/	-

Table 3-7 Yeast Two-Hybrid Assay Results (W, white; B, blue; B+, strong blue; B-, light blue; Δ, mediate inhibition; slash, no 5-FOA assay)

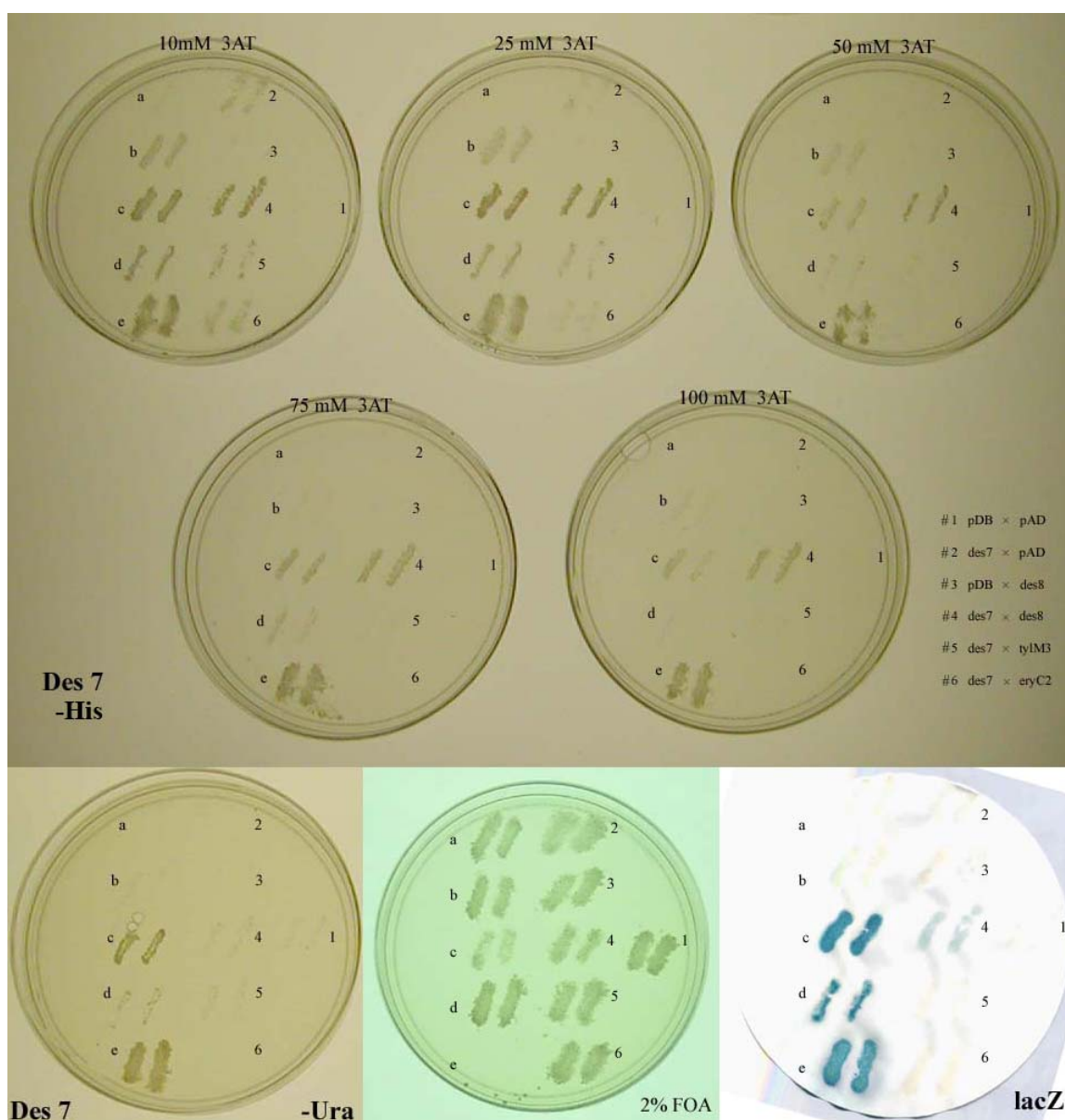


Figure 3-7 Yeast Two-Hybrid System Assays for Sample #1-6

In Vitro DesVII-DesVIII Interaction Test with S-tag Pull-down Assay. The protein-protein interaction of DesVII (GT) and DesVIII (helper protein) was observed in the *in vivo* yeast two-hybrid system. To further verify their interaction and rule out the

possibility of artifacts due to the heterologous expression system, we expressed and purified GST-S·Tag-DesVII and the maltose binding protein (MBP)-DesVIII fusion protein to perform the pull-down assay using the S-protein agarose beads which specifically bind to the S·Tag fusion protein. As the result shown in Figure 3-8, MBP-DesVIII (arrowhead) was co-precipitated with GST-S·Tag-DesVII (arrow, blotted against anti-polyHistidine primary antibody) due to the interaction between DesVII and DesVIII.

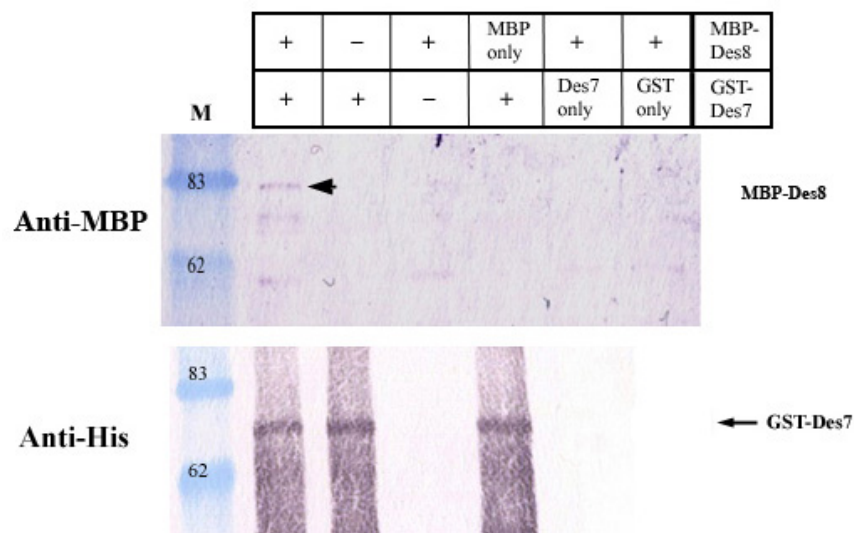


Figure 3-8 *In Vitro* S·tag Pull-down Assay. **Top**, Western-blot against α -MBP; **bottom**, Western-blot against α -His-tag; '+' represents the fusion protein was added; '**GST only**', '**Des7 only**', '**MBP only**' represented GST, DesVII, or MBP, respectively, instead of the fusion protein was added; '-' represents the fusion protein was not added.

Cloning, Expression and Purification of TylM2 and TylM3 Proteins. The

glycosylation activities of DesVII/DesVIII and AknS/AknT have been demonstrated *in vitro*. The trans-mycaminosyl activity of TylM2/TylM3 (Figure 3-1C) has been shown in the *S. venezuelae* heterologous expression system,¹⁵⁴ it is still worthwhile to test the glycosyltransferase activity *in vitro*. In addition, with the *in vitro* system, we can examine the substrate specificity of TylM2/TylM3 and attempt to gather structural evidence regarding the function of the GT and its helper protein.

We first tried to express TylM2 and TylM3 *in vitro* using the *E. coli* expression vector pET-28b(+) in the host BL21(DE3) strain. The expression of *N'*-His-TylM2 with plasmid TylM2-pET28 was performed in *E. coli* strain BL21(DE3). A low-temperature expression was tried with 0.5 mM IPTG induction at 16 °C for 3 days. However, the expression level of soluble *N'*-His-TylM2 was very low and the recombinant protein was degraded or precipitated during the purification procedure. An alternative strategy was the over-growth of *E. coli* culture at 37 °C for more than 24 h. More cell pellet was harvested and so was soluble *N'*-His-TylM2 protein. After purifying with Ni-NTA affinity chromatography and MonoQ anion-exchange chromatography, ~0.4 mg of *N'*-His-TylM2 was obtained from a 6-liter culture (Figure 3-9). Due to the presence of four rare arginine codon AGG in the TylM3 open reading frame, we chose the BL21-CodonPlus (DE3) as the *N'*-His-TylM3 expression host, which contains extra copies of tRNA that recognizes the rarely used codon in *E. coli*. The expression of *N'*-His-TylM3 was performed at 16 °C for 3 days, and 1 mg of recombinant protein was obtained from Ni-NTA purification of the lysate from a 6-liter culture (Figure 3-10). Although the expression quantities of *N'*-His-TylM2 and *N'*-His-TylM3 were low, we still

investigated the *in vitro* glycosylation assay with this GT/Helper protein pair. However, no glycosylation product was synthesized with ty lactone (**75**) and TDP-D-mycaminose (**74**) as the substrates.

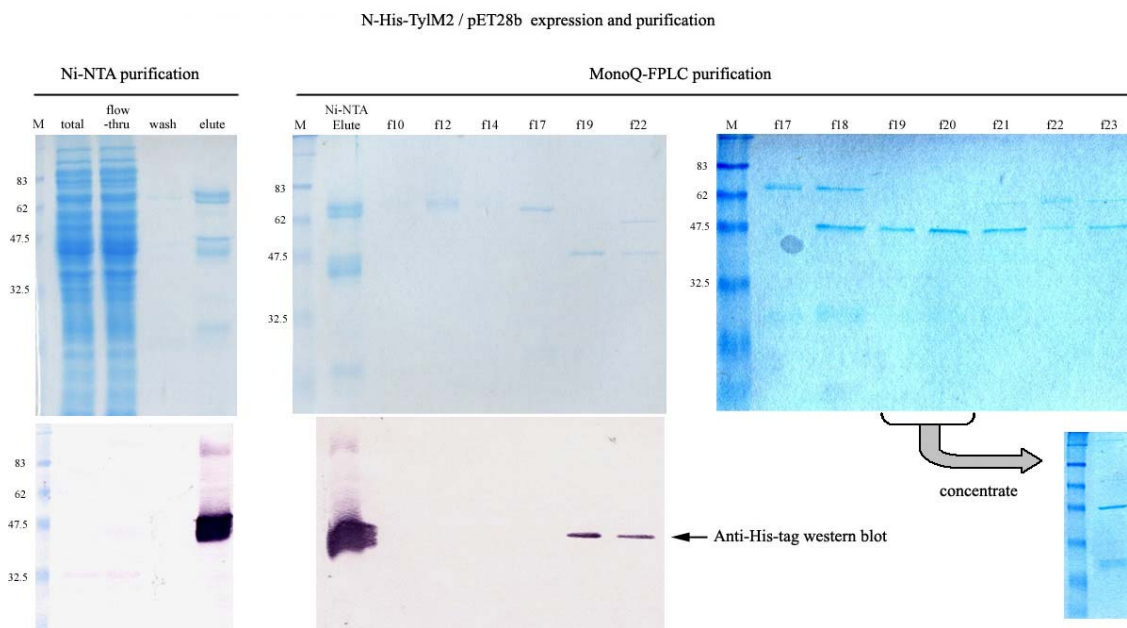


Figure 3-9 *Expression and Purification of N'-His-TylM2.* **Top**, SDS-PAGE with Coomassie blue staining; **bottom**, Western-blot against α -His-tag. Lane M is the molecular weight marker (kDa). Lane f# is the fraction number of the elute of MonoQ-FPLC purification.

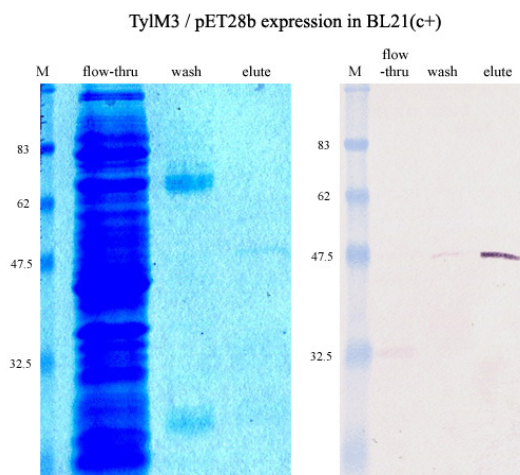
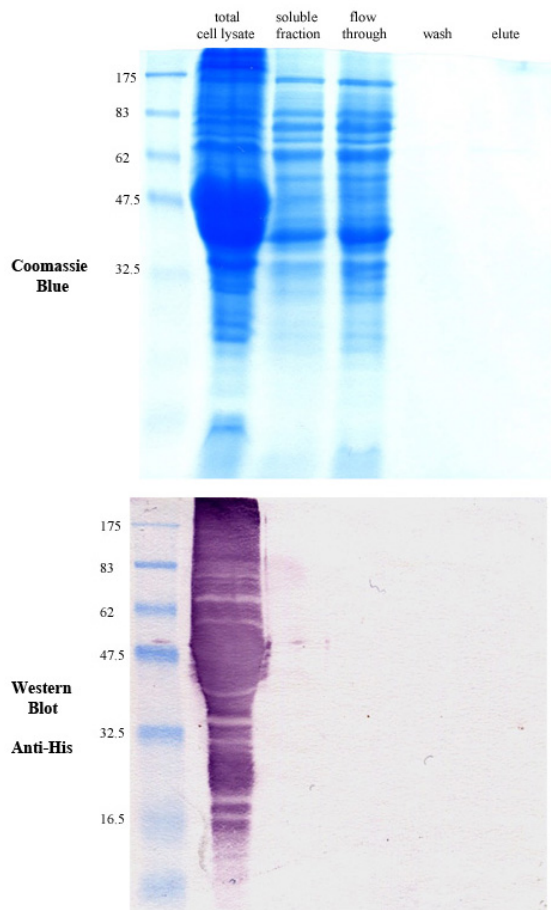


Figure 3-10 *Expression and Purification of N'-His-TylM3.* (left) SDS-PAGE with Coomassie blue staining; (right) western blot against α -His-tag

The low expressions of *N'*-His-TylM2 and *N'*-His-TylM3 were probably because of the rare *E. coli* codon usage which hampers the heterologous expression of the *Streptomyces* genes. For the next trial of the TylM2/TylM3 expression, we tried to exchange the rarely used *E. coli* arginine codons (AGG or AGA) to more frequently used codon (CGT) in these proteins. *TylM2* contains three rare arginine codons, R25^{AGA}, R422^{AGG}, and R432^{AGG}, and *TylM3* has four, R30^{AGG}, R143^{AGG}, R306^{AGG}, and R385^{AGG}. We changed the first two arginine codons of *TylM2* (R432 is the last residue.), and all four rare arginine codons of *TylM3*. The codon-exchanged *TylM2* and *TylM3* (*TylM2cx* and *TylM3cx*) were cloned into the pET-28b(+) vector and tested their expression in BL21(DE3) host. Unfortunately, the TylM2cx (calculated M.W. 48651 Da) was found to be completely in the insoluble fraction (Figure 3-11a), although the total expression quantity increased. The same negative results were observed in the codon-exchanged TylM3cx (calculated M.W. 46421 Da), either grown at 37 °C or 16 °C (Figure 3-11b).

To solve the insolubility problem, the *TylM3cx* was also cloned into MalE-pET vector to generate the maltose-binding-protein-fused TylM3cx. However, soluble MalE-TylM3cx was still absent after Ni-NTA affinity purification.

a) TylM2cx



b) TylM3cx

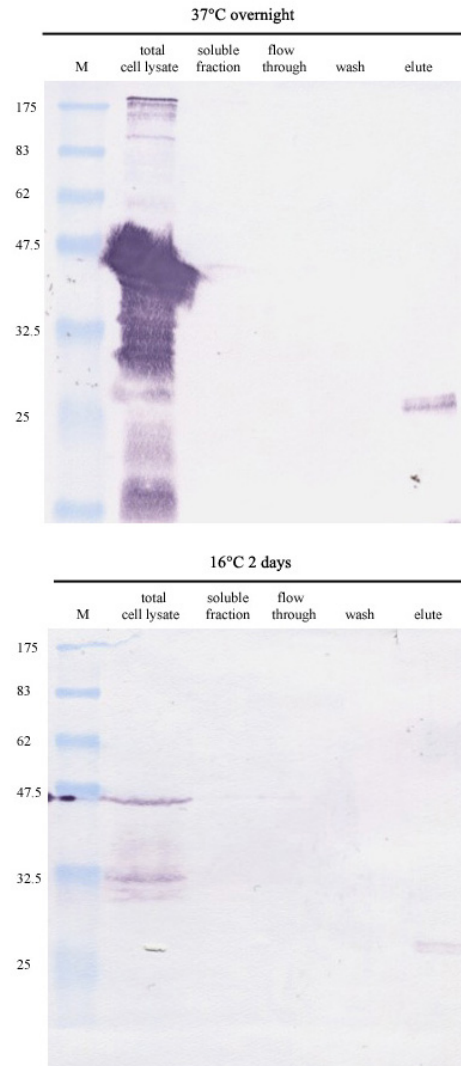


Figure 3-11 *Expression and Purification of Codon-Exchanged TylM2cx (a) and TylM3cx (b).* (a) **Top**, SDS-PAGE with Coomassie blue staining; **bottom**, Western-blot against α -His-tag; (b) both were Western-blot against α -His-tag; **top**, expression at 37 °C overnight; **bottom**, expression at 16 °C for two days.

Protein insolubility was an obvious hindrance in our attempts to overexpress TylM2 and TylM3. It has been reported that active glycosyltransferases can be obtained from refolding the denatured GT polypeptide chains. So, in the next trial, the denatured codon-exchanged TylM2cx and TylM3cx were purified from *E. coli* inclusion bodies and dissolved in the lysis buffer containing 8 M urea. During the serial dialysis-renaturing process, TylM2cx gradually aggregated and precipitated in low urea-concentration buffer. After renaturing, the total yield of TylM2cx was 20 mg from a 6 L culture (~148 μ M, cloudy solution) and that of TylM3cx was 18 mg from a 6 L culture (~6 μ M) (Figure 3-12). The renatured TylM2cx and TylM3cx were applied to the *in vitro* glycosylation assay using tylactone (**75**) and TDP-D-desosamine (**21**) as the substrates. However, on the TLC plate, we could not identify any glycosylation product based on the previous data from our group.¹⁶⁴ Surprisingly, the renatured TylM3cx protein also aggregated and precipitated 2 days after renaturation.

The glycosyltransferase EryCIII has been overexpressed and purified in its active form when the helper protein EryCII was co-expressed.¹⁵⁵ Similar result was independently observed in our succeeded in the coexpression of DesVII/DesVIII in separate plasmids.¹⁷⁴ In the last trial of TylM2/TylM3 overexpression, the same method was used to coexpress TylM2 and TylM3 using two plasmids in one cell. TylM2/pET-21 and TylM3/pET-29 were co-transformed into *E. coli* BL21(DE3) expression host. The strain carrying two different plasmids was grown for the overexpression of both TylM2 and TylM3. Unfortunately, neither TylM2 nor TylM3 was shown on the electrophoresis gel or western-blotting membrane (Figure 3-13).

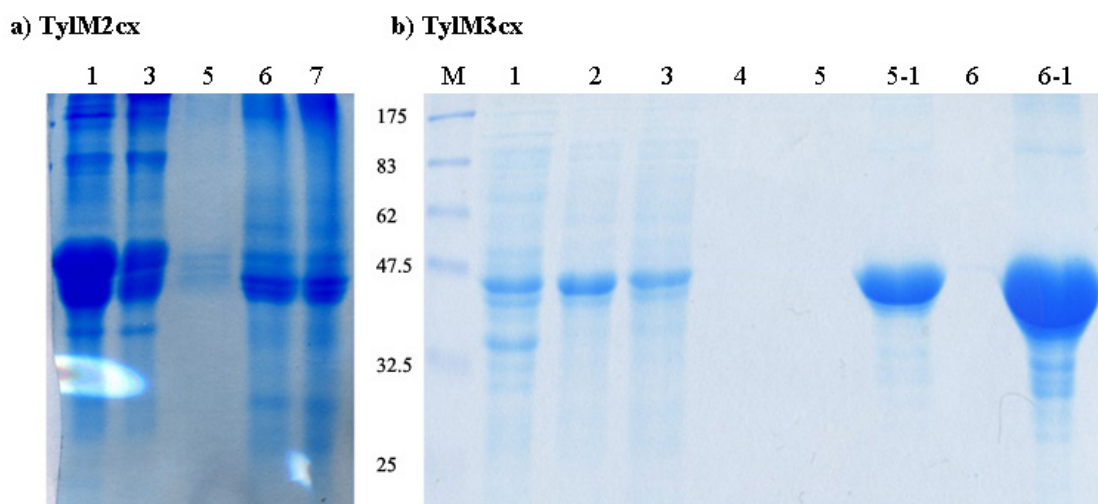


Figure 3-12 *Purification of denatured TylM2cx (a) and TylM3cx (b).* SDS-PAGE with Coomassie blue staining; Lane 1, total denatured lysate; lane 2, soluble fraction after centrifugation; lane 3, flow-through fraction of Ni-NTA chromatography; lane 4, wash fraction; lane 5, 5-1, eluate fraction; lane 6, 6-1, concentrated eluate fraction; lane 7, renatured TylM2cx eluate; **M**, molecular weight marker (kDa).

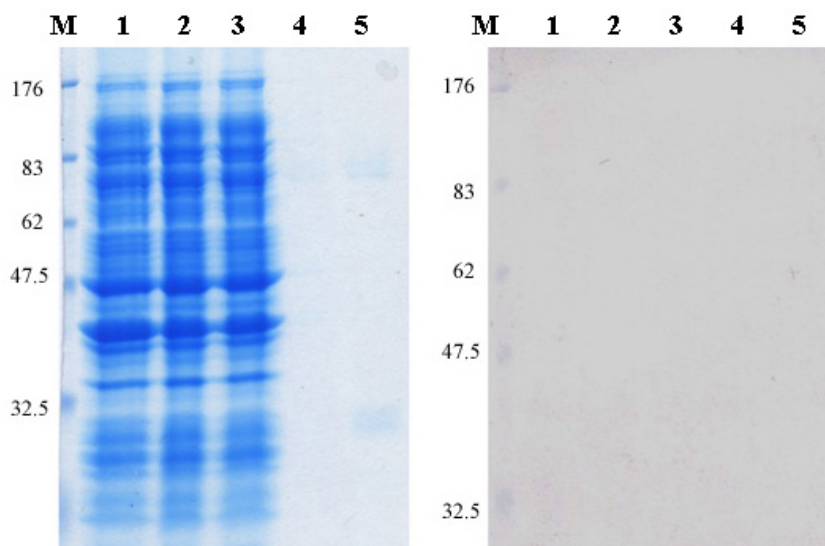
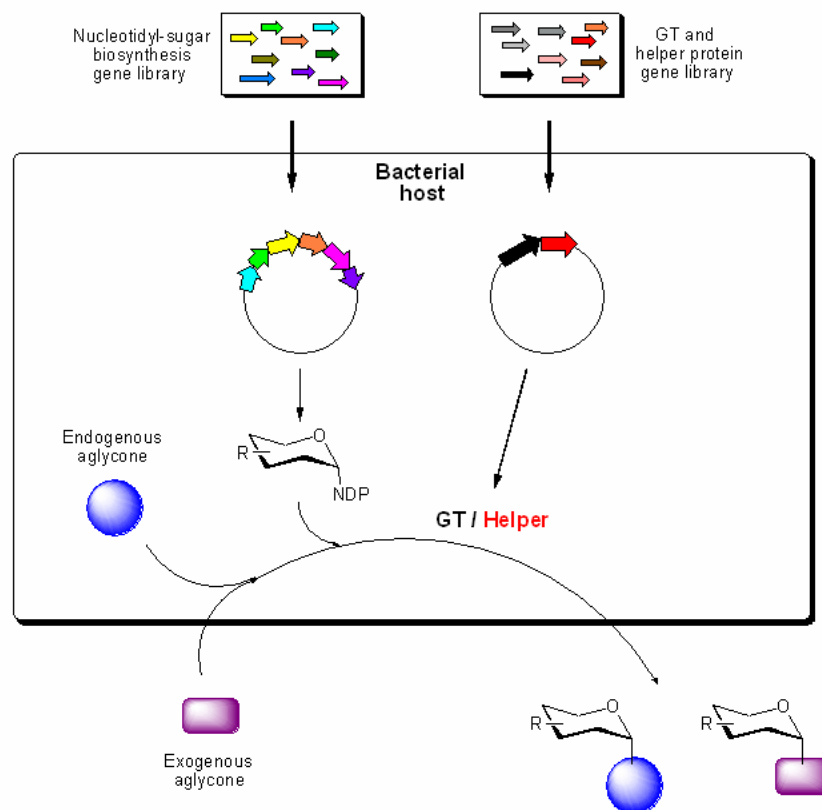


Figure 3-13 *Purification of coexpressed TylM2cx and TylM3cx.* (left) SDS-PAGE with Coomassie blue staining; (right) Western-blot against α -His-tag. Lane 1, total cell lysate; lane 2, soluble fraction after centrifugation; lane 3, flow-through fraction of Ni-NTA chromatography; lane 4, wash fraction; lane 5, eluate fraction; **M**, molecular weight marker (kDa).

In Vivo Test of Glycosyltransferase Tolerance of Different Helper Proteins Using a Two-Plasmid System. The discovery of the requirement of DesVIII for the DesVII activity and the presence of many DesVIII homologues in various natural product biosynthetic gene clusters raise an interesting question regarding the exchangeability of those GT/helper protein pairs. The more recent report of the activity of the erythromycin glycosyltransferase, EryCIII, can be activated by a noncognate auxiliary protein, AknT, prompted us to systematically test the tolerance of GTs to different helper proteins, especially those with distinct sugar or aglycone substrates (Figure 3-1).¹⁵⁵ It has been proposed that an *in vivo* two-plasmid combinatorial biosynthesis system, which contains a plasmid encoding all nucleotide sugar biosynthetic genes and a separate plasmid encoding a glycosyltransferase, can be used to generate novel glycosylated products derived from either aglycones produced by the host or exotic aglycones fed to the host.¹⁷⁵ We adapted this two-plasmid strategy to test the macrolide GT tolerance towards different helper proteins by comparing the quantities of the glycosylated compounds produced by the engineered hosts carrying different helper proteins with the same GT (Figure 3-14A).

A.



B.

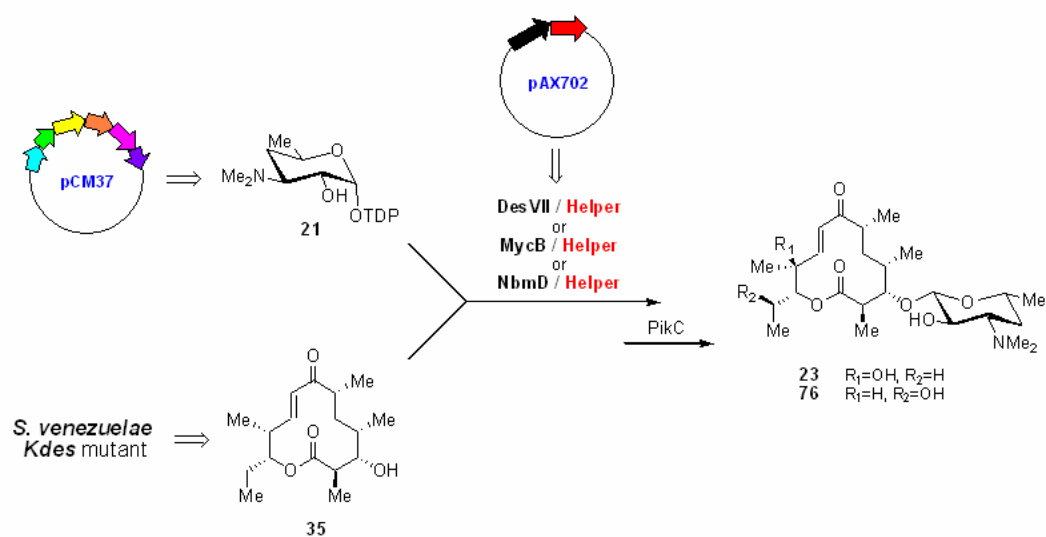


Figure 3-14 Two-plasmid system for *in vivo* biosynthesis of glycosylated products (A) and its adaption to test the GT tolerance to different helper proteins (B).

We chose the *Streptomyces venezuelae Kdes* mutant as the bacterial host for this two-plasmid glycosylation system. The wild type strain of *S. venezuelae* ATCC 15439 produces four macrolide antibiotics that include the 12-membered ring macrolides methymycin (**23**) and neomethymycin (**76**), and the 14-membered ring macrolides narbomycin (**77**) and pikromycin (**24**) (Figure 3-15). The *Kdes* mutant constructed by our group member contains a deletion of the entire TDP-D-desosamine (**21**) biosynthetic gene cluster including the desosaminyl transferase gene, *desVII*, and its helper protein gene, *desVIII*. The nucleotidyl-sugar biosynthetic plasmid, pCM37, which carries the six genes responsible for TDP-D-desosamine (**21**) biosynthesis, was constructed and transformed into the *Kdes* mutant. Although macrolide glycosyltransferases have relaxed substrate specificity, we selected three glycosyltransferases, DesVII, MycB and NbmD, that use TDP-D-desosamine (**21**) as their native sugar substrate to avoid complications in data analysis due to the low yield of the glycosylated products (Figure 3-16). Besides these three GTs, we selected their authentic helper proteins and six other helper proteins, which are responsible for different natural product glycosylation reactions (Figure 3-16). In total, 27 plasmids were constructed by combining each of the three GT genes and each of the nine helper protein genes. The three negative control plasmids which each contained only a single GT gene were also prepared to monitor the basal yields of the glycosylated product without the helper protein. After transformation of the GT/Helper protein plasmid into the *pCM37/Kdes* mutant, the doubly transformed *Kdes* mutant was cultured, and the culture medium was extracted to isolate the secreted

glycosylated products (Figure 3-14B). To simplify the analysis of the extracts, the two-plasmid-possessing *S. venezuelae* strains were grown under conditions favoring the formation of 12-membered ring macrolides, so that only **35**, **23** and **76** were analyzed in the crude extract (Figure 3-15).

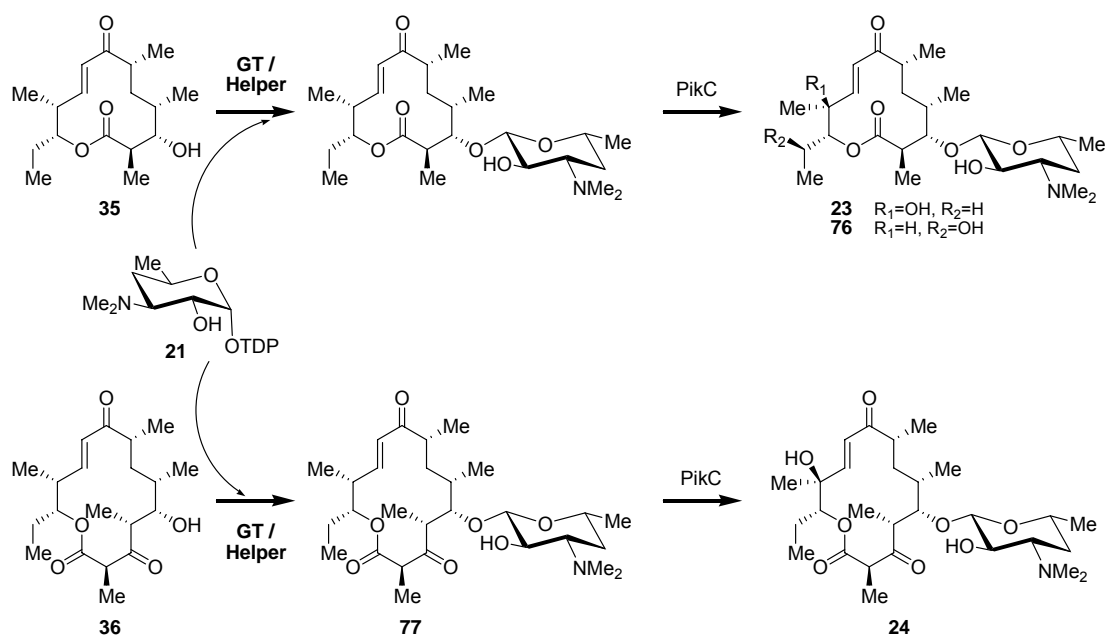


Figure 3-15 Final steps of the biosynthesis of macrolide antibiotics methymycin (**23**), neomethymycin (**76**), narbomycin (**77**), and pikromycin (**24**) in *Streptomyces venezuelae*. PikC=cytochrome P450 hydroxylase.

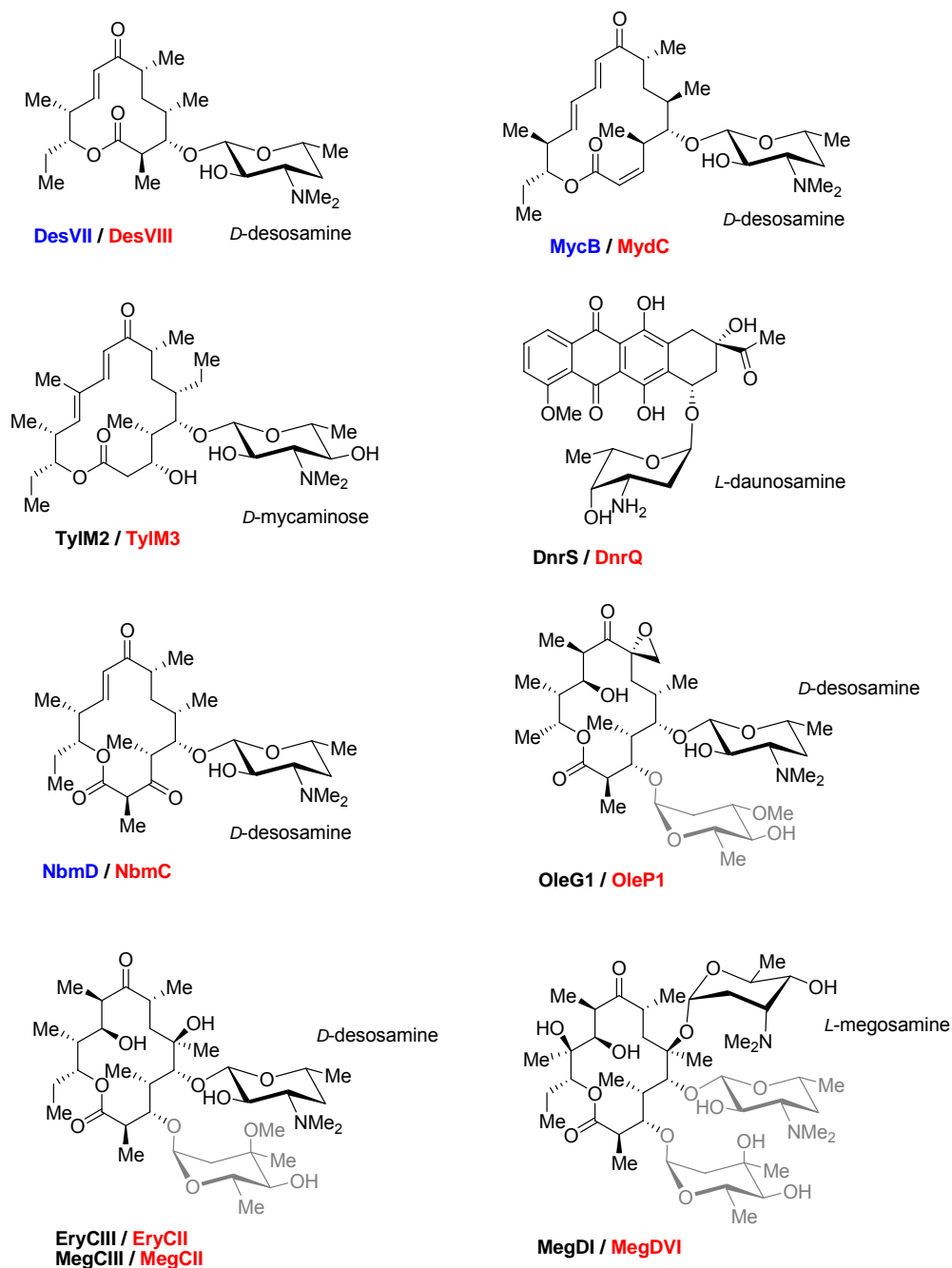


Figure 3-16 *The GTs (blue), helper proteins (red), and their natural glycosylated products.*

The three GTs and nine helper proteins are used to construct the 27 GT/Helper Protein plasmids. The sugar residues that are coupled by each enzyme pair are indicated.

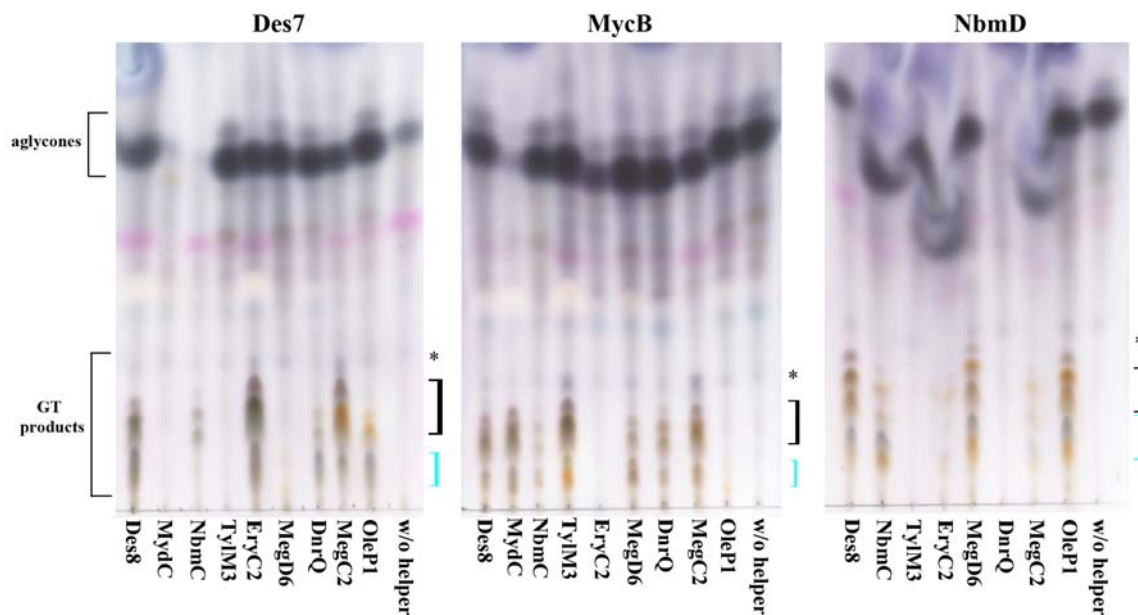


Figure 3-17 TLC analysis of the crude extracts from the two-plasmid-possessing *S. venezuelae* *Kdes* strains

The thin-layer chromatography results of the crude extracts obtained from the two-plasmid-possessing *S. venezuelae* *Kdes* strains are shown in Figure 3-17. As can be seen from Figure 3-17, many different helper protein homologues could compensate for the activity of the original helper protein. The extent of glycosylation by each GT/helper protein-carrying strain was estimated by measuring the integration of the intensity of the corresponding peaks of compounds **35**, **23**, and **76** from the LC-MS chromatogram. As listed in Table 3-8, the glycosylation ratios by DesVII and MycB depend on the specific helper protein used. The strains without any helper protein show only minimal glycosylation, which is consistent with the observation made by previous *in vitro* activity assay.¹⁵⁰ The results from the strains carrying glycosyltransferase NbmD

are not included in Table 3-8 because of the inconsistent results from separate experiments. To facilitate the data interpretation, we have normalized the extent of glycosylation by setting the baseline ratio (without the helper protein) to zero and that with the original helper protein to 100%.

Table 3-8 Glycosylation ratio by DesVII and MycB using different helper proteins (-, inconsistent results)

Helper protein	DesVII glycosylation ratio		MycB glycosylation ratio	
	Original ratio	Normalized ratio	Original ratio	Normalized ratio
DesVIII	68.1±1.0%	100.0%	79.4±2.7%	84.9%
MydC	56.6±5.7%	83.0%	93.2±1.6%	100.0%
NbmC	-	-	2.6±0.4%	1.0%
TylM3	0.4±0.2%	0.4%	26.7±6.8%	27.3%
MegDVI	61.6±0.8%	90.4%	1.6±0.5%	0.0%
EryCII	78.8±1.5%	115.8%	41.5±4.4%	43.5%
DnrQ	31.2±8.0%	45.8%	44.8±0.2%	47.1%
MegCII	46.0±2.0%	67.6%	69.4±12.9%	73.9%
OleP1	72.4±0.4%	106.3%	87.5±0.6%	93.8%
No helper	0.2±0.1%	0.0%	1.7±0.0%	0.0%

For the glycosylation by DesVII, the helper proteins, EryCII and OleP1, show higher activities than DesVIII, while MegCII, which catalyzes the same reaction as EryCII, exhibits only 67.6% activity of DesVIII (see Figure 3-16 for structures). MydC and MegDVI have almost full activity (> 80%), even though their original aglycone or NDP-sugar substrates are quite different. TylM3 does not show any helper protein activity toward DesVII in this *in vivo* assay. Surprisingly, DnrQ, which assists DnrS in

catalyzing the attachment of L-daunosamine to an aromatic aglycone, has about half (45.8%) the helping activity of DesVIII to DesVII.

For MycB-catalyzed glycosylation, TylM3 demonstrates 27.3% the activity of MydC, probably because both of their original aglycones are 16-member rings macrolides. DesVIII and OleP1 show fairly high activity (> 80%) as helper proteins to MycB, which is consistent with the high activities of MydC and OleP1 toward DesVII-catalyzed glycosylation. MegCII shows higher helper activity (73.9%) than EryCII (43.5%) in the MycB glycosylation assay, while the reverse is true for the DesVII glycosylation assay. Similar to the DesVII assay, DnrQ had about half the activity (47.1%) of MydC in the MycB glycosylation assay. MegDVI does not show any helper protein activity when paired with MycB. To our surprise, NbmD, which catalyzes the same reaction as DesVIII, demonstrates nearly zero activity as the helper protein toward MycB.

We also compared the relative extent of glycosylation by DesVII (Figure 3-18A) or MycB (Figure 3-18B) to the amino acid sequence identity of the homologous helper proteins to either DesVIII (Figure 3-18A) or MydC (Figure 3-18B). Unfortunately, no obvious correlation exists between the helper protein glycosylation efficiencies and their primary sequence identity to the authentic helper proteins.

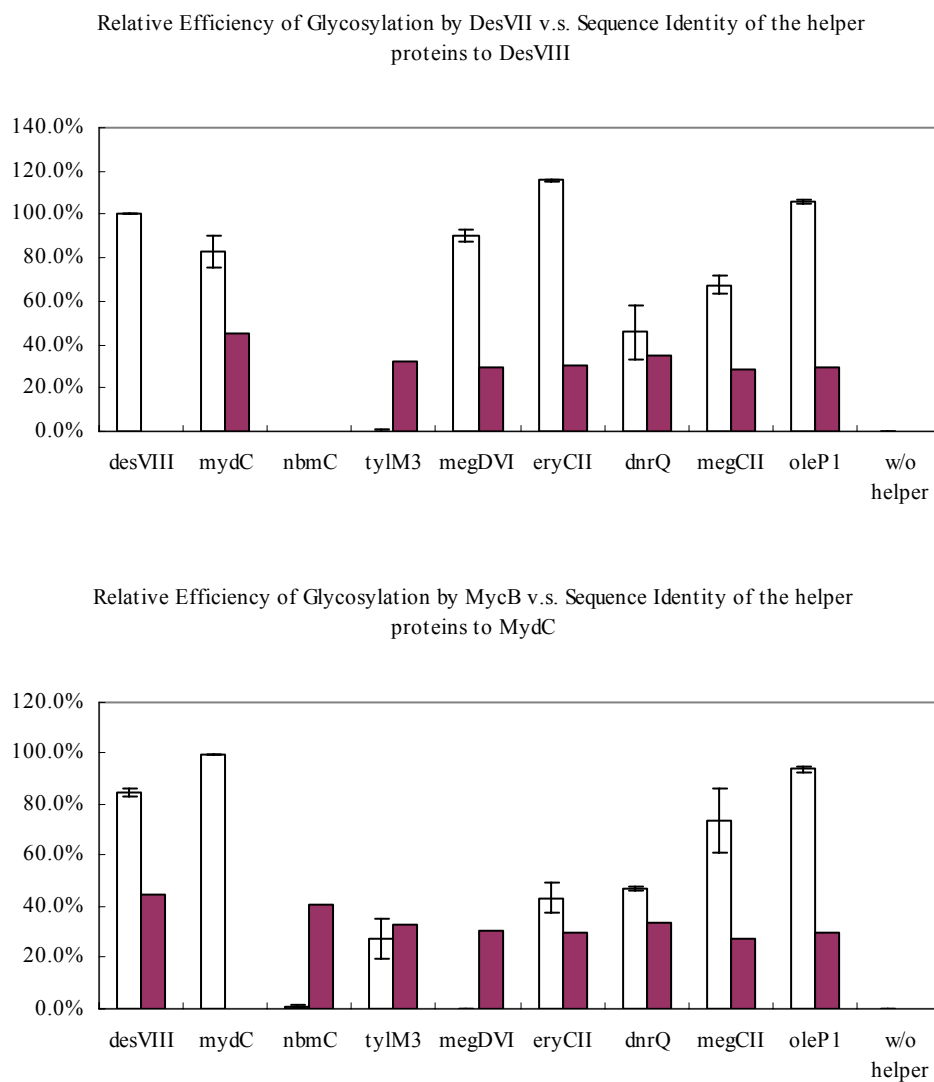


Figure 3-18 The alignment of DesVII (**A**) and MycB (**B**) glycosylation ratio (open bar) with amino acid sequence identities (solid bar) of helper proteins to DesVIII (**A**) and MydC (**B**)

4. CONCLUSION

The discovery that some glycosyltransferases need their specific auxiliary proteins for full activities refreshes the features of this important enzyme in glycochemistry and glycobiology. The helper protein studies in this chapter clearly reveal the weak protein-protein interaction between D-desosaminyl transferase DesVII and its helper protein DesVIII *in vivo* and *in vitro*. The lack of success in overexpressing and purifying the D-mycaminosyl transferase TylM2 and its helper protein TylM3 *in vitro* implicated the difficulty in folding and disordered structures of both GT and its auxiliary partner. Finally, using the *in vivo* two-plasmid system to test the tolerance of GT towards different helper proteins, our results demonstrated that the GT helper protein can be replaced by homologous proteins from other glycosylation pathways. Comparing the ratios of the glycosylated products generated with different helper proteins, we found several interesting traits between the efficiency of turnover and the similarity of the original substrate of the helper protein. However, no correlation between the catalytic efficiency of the helper proteins and the degree of homology of their primary sequences were identified. To unveil the mystery of the functions of the glycosyltransferase helper protein, more ingenious experiments need to be carried out in the future.

REFERENCES

1. Varki, A.; Cummings, R.; Esko, J.; Freeze, H.; Hart, G.; Marth, J., *Essentials of Glycobiology*. Cold Spring Harbor Laboratory Press: Cold Spring Harbor, New York, 1999.
2. Weymouth-Wilson, A. C., The role of carbohydrates in biologically active natural products. *Nat. Prod. Rep.* **1997**, 14, 99-110.
3. Thorson, J. S.; Hosted, T. J., Jr.; Jiang, J.; Biggins, J. B.; Ahlert, J., Nature's carbohydrate chemists: the enzymatic glycosylation of bioactive bacterial metabolites. *Curr. Org. Chem.* **2001**, 5, 139-167.
4. Salas, J. A.; Méndez, C., Biosynthesis pathways for deoxysugars in antibiotic-producing Actinomycetes: isolation, characterization and generation of novel glycosylated derivatives. *J. Mol. Microbiol. Biotechnol.* **2005**, 9, 77-85.
5. Salas, J. A.; Méndez, C., Engineering the glycosylation of natural products in actinomycetes. *Trends Microbiol.* **2007**, 15, (5), 219-232.
6. Walsh, C.; Meyers, C. L. F.; Losey, H. C., Antibiotic Glycosyltransferases: Antibiotic Maturation and Prospects for Reprogramming. *J. Med. Chem.* **2003**, 46, (16), 3425-3436.
7. Hutchinson, C. R., Combinatorial biosynthesis for new drug discovery. *Curr. Opin. Microbiol.* **1998**, 1, (3), 319-329.
8. Cane, D. E.; Walsh, C. T.; Khosla, C., Harnessing the Biosynthetic Code: Combinations, Permutations, and Mutations. *Science* **1998**, 282, (5386), 63-68.
9. Michels, P. C.; Khmelnsky, Y. L.; Dordick, J. S.; Clark, D. S., Combinatorial biocatalysis: a natural approach to drug discovery. *Trends Biotechnol.* **1998**, 16, (5), 210-215.
10. Walsh, C. T., Combinatorial Biosynthesis of Antibiotics: Challenges and Opportunities. *ChemBioChem* **2002**, 3, (2-3), 124-134.
11. Barton, W. A.; Lesniak, J.; Biggins, J. B.; Jeffrey, P. D.; Jiang, J.; Rajashankar, K. R.; Thorson, J. S.; Nikolov, D. B., Structure, mechanism and engineering of a nucleotidyltransferase as a first step toward glycorandomization. *Nat. Struct. Biol.* **2001**, 8, (6), 545-551.
12. Jiang, J.; Biggins, J. B.; Thorson, J. S., A General Enzymatic Method for the

- Synthesis of Natural and "Unnatural" UDP- and TDP-Nucleotide Sugars. *J. Am. Chem. Soc.* **2000**, 122, (28), 6803-6804.
13. Münster-Kühnel, A. K.; Tiralongo, J.; Krapp, S.; Weinhold, B.; Ritz-Sedlacek, V.; Jacob, U.; Gerardy-Schahn, R., Structure and function of vertebrate CMP-sialic acid synthetases. *Glycobiology* **2004**, 14, (10), 43R-51R.
 14. Hegeman, A. D.; Gross, J. W.; Frey, P. A., Concerted and Stepwise Dehydration Mechanisms Observed in Wild-Type and Mutated *Escherichia coli* dTDP-Glucose 4,6-Dehydratase. *Biochemistry* **2002**, 41, (8), 2797-2804.
 15. Mulichak, A. M.; Bonin, C. P.; Reiter, W.-D.; Garavito, R. M., Structure of the MUR1 GDP-Mannose 4,6-Dehydratase from *Arabidopsis thaliana*: Implications for Ligand Binding and Specificity. *Biochemistry* **2002**, 41, (52), 15578-15589.
 16. Vogan, E. M.; Bellamacina, C.; He, X.; Liu, H.-w.; Ringe, D.; Petsko, G. A., Crystal Structure at 1.8 Å Resolution of CDP-*D*-Glucose 4,6-Dehydratase from *Yersinia pseudotuberculosis*. *Biochemistry* **2004**, 43, (11), 3057-3067.
 17. Allard, S. T. M.; Beis, K.; Giraud, M.-F.; Hegeman, A. D.; Gross, J. W.; Wilmouth, R. C.; Whitfield, C.; Graninger, M.; Messner, P.; Allen, A. G.; Maskell, D. J.; Naismith, J. H., Toward a Structural Understanding of the Dehydratase Mechanism. *Structure* **2002**, 10, (1), 81-92.
 18. Field, R. A.; Naismith, J. H., Structural and Mechanistic Basis of Bacterial Sugar Nucleotide-Modifying Enzymes. *Biochemistry* **2003**, 42, (25), 7637-7647.
 19. Chen, H.; Agnihotri, G.; Guo, Z.; Que, N. L. S.; Chen, X. H.; Liu, H.-w., Biosynthesis of Mycarose: Isolation and Characterization of Enzymes Involved in the C-2 Deoxygenation. *J. Am. Chem. Soc.* **1999**, 121, (35), 8124-8125.
 20. Draeger, G.; Park, S.-H.; Floss, H. G., Mechanism of the 2-Deoxygenation Step in the Biosynthesis of the Deoxyhexose Moieties of the Antibiotics Granaticin and Oleandomycin. *J. Am. Chem. Soc.* **1999**, 121, (11), 2611-2612.
 21. Chen, H.; Thomas, M. G.; Hubbard, B. K.; Losey, H. C.; Walsh, C. T.; Burkart, M. D., Deoxysugars in glycopeptide antibiotics: Enzymatic synthesis of TDP-L-epivancosamine in chloroeremomycin biosynthesis. *Proc. Natl. Acad. Sci. USA* **2000**, 97, (22), 11942-11947.
 22. Raetz, C. R. H., Biochemistry of Endotoxins. *Annu. Rev. Biochem.* **1990**, 59, 129-170.
 23. Thorson, J. S.; Lo, S. F.; Liu, H.-w., Molecular Basis of 3,6-Dideoxyhexose Biosynthesis: Elucidation of CDP-Ascarbose Biosynthetic Genes and Their Relationship to Other 3,6-Dideoxyhexose Pathways. *J. Am. Chem. Soc.* **1993**, 115,

- (13), 5827-5828.
24. Thorson, J. S.; Lo, S. F.; Ploux, O.; He, X.; Liu, H.-W., Studies of the biosynthesis of 3,6-dideoxyhexoses: molecular cloning and characterization of the *asc* (ascarylose) region from *Yersinia pseudotuberculosis* serogroup VA. *J. Bacteriol.* **1994**, 176, (17), 5483-5493.
 25. Burns, K. D.; Pieper, P. A.; Liu, H.-w.; Stankovich, M. T., Studies of the Redox Properties of CDP-6-deoxy-L-threo-D-glycero-4-hexulose-3-dehydrase (E_1) and CDP-6-deoxy-L-threo-D-glycero-4-hexulose-3-dehydrase reductase (E_3): Two Important Enzymes Involved in the Biosynthesis of Ascarylose. *Biochemistry* **1996**, 35, (24), 7879-7889.
 26. Chang, C.-W. T.; Johnson, D. A.; Bandarian, V.; Zhou, H.; LoBrutto, R.; Reed, G. H.; Liu, H.-w., Characterization of a Unique Coenzyme B_6 Radical in the Ascarylose Biosynthetic Pathway. *J. Am. Chem. Soc.* **2000**, 122, (17), 4239-4240.
 27. Thorson, J. S.; Liu, H.-w., Characterization of the First PMP-Dependent Iron-Sulfur-Containing Enzyme Which Is Essential for the Biosynthesis of 3,6-Dideoxyhexoses. *J. Am. Chem. Soc.* **1993**, 115, (16), 7539-7540.
 28. Miller, V. P.; Thorson, J. S.; Ploux, O.; Lo, S. F.; Liu, H.-w., Cofactor Characterization and Mechanistic Studies of CDP-6-deoxy- $\Delta^{3,4}$ -glucoseen Reductase: Exploration into a Novel Enzymatic C-O Bond Cleavage Event. *Biochemistry* **1993**, 32, (44), 11934-11942.
 29. Lo, S. F.; Miller, V. P.; Lei, Y.; Thorson, J. S.; Liu, H.-w.; Schottel, J. L., CDP-6-Deoxy- $\Delta^{3,4}$ -Glucoseen Reductase from *Yersinia pseudotuberculosis*: Enzyme Purification and Characterization of the Cloned Gene. *J. Bacteriol.* **1994**, 176, (2), 460-468.
 30. Weigel, T. M.; Liu, L.-d.; Liu, H.-w., Mechanistic studies of the biosynthesis of 3,6-dideoxyhexoses in *Yersinia pseudotuberculosis*: purification and characterization of CDP-4-keto-6-deoxy-D-glucose-3-dehydrase. *Biochemistry* **1992**, 31, (7), 2129-2139.
 31. Weigel, T. M.; Miller, V. P.; Liu, H.-w., Mechanistic and stereochemical studies of a unique dehydration catalyzed by CDP-4-keto-6-deoxy-D-glucose-3-dehydrase: a pyridoxamine 5'-phosphate dependent enzyme isolated from *Yersinia pseudotuberculosis*. *Biochemistry* **1992**, 31, (7), 2140-2147.
 32. Pieper, P. A.; Guo, Z.; Liu, H.-w., Mechanistic Studies of the Biosynthesis of 3,6-Dideoxy Sugars: Stereochemical Analysis of C-3 Deoxygenation. *J. Am. Chem.*

- Soc.* **1995**, 117, (18), 5158-5159.
33. Gassner, G. T.; Johnson, D. A.; Liu, H.-w.; Ballou, D. P., Kinetics of the Reductive Half-Reaction of the Iron-Sulfur Flavoenzyme CDP-6-deoxy-L-threo-D-glycero-4-hexulose-3-dehydrase Reductase. *Biochemistry* **1996**, 35, (24), 7752-7761.
 34. Johnson, D. A.; Gassner, G. T.; Bandarian, V.; Ruzicka, F. J.; Ballou, D. P.; Reed, G. H.; Liu, H.-w., Kinetic Characterization of an Organic Radical in the Ascarrylose Biosynthetic Pathway. *Biochemistry* **1996**, 35, (49), 15846-15856.
 35. Thorson, J. S.; Liu, H.-w., Coenzyme B₆ as a Redox Cofactor: A New Role for an Old Coenzyme? *J. Am. Chem. Soc.* **1993**, 115, (25), 12177-12178.
 36. Agnihotri, G.; Liu, H.-w., PLP and PMP Radicals: A New Paradigm in Coenzyme B₆ Chemistry. *Bioorg. Chem.* **2001**, 29, (4), 234-257.
 37. Chen, X. M. H.; Ploux, O.; Liu, H.-w., Biosynthesis of 3,6-Dideoxyhexoses: *In Vivo* and *in Vitro* Evidence for Protein-Protein Interaction between CDP-6-deoxy-L-threo-D-glycero-4-hexulose-3-Dehydrase (E₁) and Its Reductase (E₃). *Biochemistry* **1996**, 35, (51), 16412-16420.
 38. Hong, L.; Zhao, Z.; Liu, H.-w., Characterization of SpnQ from the Spinosyn Biosynthetic Pathway of *Saccharopolyspora spinosa*: Mechanistic and Evolutionary Implications for C-3 Deoxygenation in Deoxysugar Biosynthesis. *J. Am. Chem. Soc.* **2006**, 128, (44), 14262 - 14263.
 39. Beyer, N.; Alam, J.; Hallis, T. M.; Guo, Z.; Liu, H.-w., The Biosynthesis of GDP-L-Colitose: C-3 Deoxygenation Is Catalyzed by a Unique Coenzyme B₆-Dependent Enzyme. *J. Am. Chem. Soc.* **2003**, 125, (19), 5584-5585.
 40. Alam, J.; Beyer, N.; Liu, H.-w., Biosynthesis of Colitose: Expression, Purification, and Mechanistic Characterization of GDP-4-keto-6-deoxy-D-mannose-3-Dehydrase (ColD) and GDP-L-colitose Synthase (ColC). *Biochemistry* **2004**, 43, (51), 16450-16460.
 41. Summers, R. G.; Donadio, S.; Staver, M. J.; Wendt-Pienkowski, E.; Hutchinson, C. R.; Katz, L., Sequencing and mutagenesis of genes from the erythromycin biosynthetic gene cluster of *Saccharopolyspora erythraea* that are involved in L-mycarose and D-desosamine production. *Microbiology* **1997**, 143, (10), 3251-3262.
 42. Xue, Y.; Zhao, L.; Liu, H.-w.; Sherman, D. H., A gene cluster for macrolide antibiotic biosynthesis in *Streptomyces venezuelae*: Architecture of metabolic diversity. *Proc. Natl. Acad. Sci. USA* **1998**, 95, (21), 12111-12116.

43. Borisova, S. A.; Zhao, L.; Sherman, D. H.; Liu, H.-w., Biosynthesis of Desosamine: Construction of a New Macrolide Carrying a Genetically Designed Sugar Moiety. *Org. Lett.* **1999**, 1, (1), 133-136.
44. Zhao, L.; Borisova, S. A.; Yeung, S.-M.; Liu, H.-w., Study of C-4 Deoxygenation in the Biosynthesis of Desosamine: Evidence Implicating a Novel Mechanism. *J. Am. Chem. Soc.* **2001**, 123, (32), 7909-7910.
45. Sofia, H. J.; Chen, G.; Hetzler, B. G.; Reyes-Spindola, J. F.; Miller, N. E., Radical SAM, a novel protein superfamily linking unresolved steps in familiar biosynthetic pathways with radical mechanisms: functional characterization using new analysis and information visualization methods. *Nucleic Acids Res.* **2001**, 29, (5), 1097-1106.
46. Szu, P.-h.; He, X.; Zhao, L.; Liu, H.-w., Biosynthesis of TDP-D-Desosamine: Identification of a Strategy for C4 Deoxygenation. *Angew. Chem. Int. Ed.* **2005**, 44, (41), 6742-6746.
47. Frey, P. A.; Reed, G. H., Radical Mechanisms in Adenosylmethionine- and Adenosylcobalamin-Dependent Enzymatic Reactions. *Arch. Biochem. Biophys.* **2000**, 382, (1), 6-14.
48. Frey, P. A., Radical Mechanisms of Enzymatic Catalysis. *Annu. Rev. Biochem.* **2001**, 70, 121-148.
49. Chen, D.; Walsby, C.; Hoffman, B. M.; Frey, P. A., Coordination and Mechanism of Reversible Cleavage of *S*-Adenosylmethionine by the [4Fe-4S] Center in Lysine 2,3-Aminomutase. *J. Am. Chem. Soc.* **2003**, 125, (39), 11788-11789.
50. Frey, P. A.; Magnusson, O. T., *S*-Adenosylmethionine: A Wolf in Sheep's Clothing, or a Rich Man's Adenosylcobalamin? *Chem. Rev.* **2003**, 103, (6), 2129-2148.
51. Sandala, G. M.; Smith, D. M.; Radom, L., Divergent Mechanisms of Suicide Inactivation for Ethanolamine Ammonia-Lyase. *J. Am. Chem. Soc.* **2005**, 127, (24), 8856-8864.
52. Kim, J.; Hetzel, M.; Boiangiu, C. D.; Buckel, W., Dehydration of (*R*)-2-hydroxyacyl-CoA to enoyl-CoA in the fermentation of α -amino acids by anaerobic bacteria. *FEMS Microbiol. Rev.* **2004**, 28, (4), 455-468.
53. Badet, B.; Vermoote, P.; Haumont, P.-Y.; Lederer, F.; Goffic, F. L., Glucosamine Synthetase from *Escherichia coli*: Purification, Properties, and Glutamine-Utilizing Site Location. *Biochemistry* **1987**, 26, (7), 1940-1948.
54. Teplyakov, A.; Obmolova, G.; Badet, B.; Badet-Denisot, M.-A., Channeling of Ammonia in Glucosamine-6-phosphate Synthase. *J. Mol. Biol.* **2001**, 313, (5),

1093-1102.

55. Mouilleron, S.; Badet-Denisot, M.-A.; Golinelli-Pimpaneau, B., Glutamine Binding Opens the Ammonia Channel and Activates Glucosamine-6P Synthase. *J. Biol. Chem.* **2006**, 281, (7), 4404-4412.
56. Bretona, C.; Muchab, J.; Jeanneau, C., Structural and functional features of glycosyltransferases. *Biochimie* **2001**, 83, (8), 713-718.
57. Ohtsubo, K.; Marth, J. D., Glycosylation in Cellular Mechanisms of Health and Disease. *Cell* **2006**, 126, (5), 855-867.
58. Dennis, J. W.; Granovsky, M.; Warren, C. E., Protein glycosylation in development and disease. *BioEssays* **1999**, 21, (5), 412-421.
59. Dennis, J. W.; Granovsky, M.; Warren, C. E., Glycoprotein glycosylation and cancer progression. *Biochim. Biophys. Acta* **1999**, 1473, (1), 21-34.
60. Enzyme Nomenclature. In (<http://www.chem.qmul.ac.uk/iubmb/enzyme/>): 1992-.
61. Coutinho, P. M.; Deleury, E.; Davies, G. J.; Henrissat, B., An Evolving Hierarchical Family Classification for Glycosyltransferases. *J. Mol. Biol.* **2003**, 328, (2), 307-317.
62. Campbell, J. A.; Davies, G. J.; Bulone, V.; Henrissat, B., A classification of nucleotide-diphospho-sugar glycosyltransferases based on amino acid sequence similarities. *Biochem J.* **1997**, 326, (3), 929-942.
63. Carbohydrate-Active enZYme (CAZ_Y). In (<http://www.cazy.org/>): 1998-.
64. Ünligil, U. M.; Rini, J. M., Glycosyltransferase structure and mechanism. *Curr. Opin. Struct. Biol.* **2000**, 10, (5), 510-517.
65. Zechel, D. L.; Withers, S. G., Glycosyl transferase mechanisms. *Comprehensive Natural Products Chemistry* **1999**, 5, 279-314.
66. Schuman, B.; Alfaro, J. A.; Evans, S. V., Glycosyltransferase Structure and Function. *Top. Curr. Chem.* **2007**, 272, 217-257.
67. Sinnott, M. L., Catalytic Mechanisms of Enzymic Glycosyl Transfer. *Chem. Rev.* **1990**, 90, (7), 1171-1202.
68. Ha, S.; Gross, B.; Walker, S., *E. Coli* MurG: A Paradigm for a Superfamily of Glycosyltransferases. *Curr. Drug Targets Infect. Disord.* **2001**, 1, (2), 201-213.
69. Berg, S.; Kaur, D.; Jackson, M.; Brennan, P. J., The glycosyltransferases of *Mycobacterium tuberculosis* - roles in the synthesis of arabinogalactan, lipoarabinomannan, and other glycoconjugates. *Glycobiology* **2007**, 17, (6), 35R-56R.
70. Tarbouriech, N.; Charnock, S. J.; Davies, G. J., Three-dimensional Structures of the Mn and Mg dTDP Complexes of the Family GT-2 Glycosyltransferase SpsA: A

- Comparison with Related NDP-sugar Glycosyltransferases. *J. Mol. Biol.* **2001**, 314, (4), 655-661.
71. Hu, Y.; Walker, S., Remarkable Structural Similarities between Diverse Glycosyltransferases. *Chem. Biol.* **2002**, 9, (12), 1257-1364.
 72. Mulichak, A. M.; Losey, H. C.; Lu, W.; Wawrzak, Z.; Walsh, C. T.; Garavito, R. M., Structure of the TDP-*epi*-vancosaminyltransferase GtfA from the chloroeremomycin biosynthetic pathway. *Proc. Natl. Acad. Sci. USA* **2003**, 100, (16), 9238-9243.
 73. Charnock, S. J.; Davies, G. J., Structure of the Nucleotide-Diphospho-Sugar Transferase, SpsA from *Bacillus subtilis*, in Native and Nucleotide-Complexed Forms. *Biochemistry* **1999**, 38, (20), 6380-6385.
 74. Liu, J.; Mushegian, A., Three monophyletic superfamilies account for the majority of the known glycosyltransferases. *Protein Sci.* **2003**, 12, (7), 1418-1431.
 75. Kikuchi, N.; Kwon, Y.-D.; Gotoh, M.; Narimatsua, H., Comparison of glycosyltransferase families using the profile hidden Markov model. *Biochem. Biophys. Res. Commun.* **2003**, 310, (2), 574-579.
 76. Lovering, A. L.; Castro, L. H. d.; Lim, D.; Strynadka, N. C. J., Structural Insight into the Transglycosylation Step of Bacterial Cell-Wall Biosynthesis. *Science* **2007**, 315, (5817), 1402-1405.
 77. Yuan, Y.; Barrett, D.; Zhang, Y.; Kahne, D.; Sliz, P.; Walker, S., Crystal structure of a peptidoglycan glycosyltransferase suggests a model for processive glycan chain synthesis. *Proc. Natl. Acad. Sci. USA* **2007**, 104, (13), 5348-5353.
 78. Méndez, C.; Salas, J. A., Altering the glycosylation pattern of bioactive compounds. *Trends Biotechnol.* **2001**, 19, (11), 449-456.
 79. Borisova, S. A.; Zhang, C.; Takahashi, H.; Zhang, H.; Wong, A. W.; Thorson, J. S.; Liu, H.-w., Substrate Specificity of the Macrolide-Glycosylating Enzyme Pair DesVII/DesVIII: Opportunities, Limitations, and Mechanistic Hypotheses. *Angew. Chem. Int. Ed.* **2006**, 45, (17), 2748-2753.
 80. Zhang, C.; Griffith, B. R.; Fu, Q.; Albermann, C.; Fu, X.; Lee, I.-K.; Li, L.; Thorson, J. S., Exploiting the Reversibility of Natural Product Glycosyltransferase-Catalyzed Reactions. *Science* **2006**, 313, (5791), 1291-1294.
 81. Minami, A.; Kakinuma, K.; Eguchi, T., Aglycon switch approach toward unnatural glycosides from natural glycoside with glycosyltransferase VinC. *Tetrahedr. Lett.* **2005**, 46, (37), 6187-6190.
 82. Melançon, C. E.; Thibodeaux, C. J.; Liu, H.-w., Glyco-Stripping and Glyco-Swapping.

- ACS Chem. Biol.* **2006**, 1, (8), 499-504.
83. Bode, H. B.; Müller, R., Reversible Sugar Transfer by Glycosyltransferases as a Tool for Natural Product (Bio)synthesis. *Angew. Chem. Int. Ed.* **2007**, 46, (13), 2147-2150.
84. Rupprath, C.; Schumacher, T.; Elling, L., Nucleotide Deoxysugars: Essential Tools for the Glycosylation Engineering of Novel Bioactive Compounds. *Curr. Med. Chem.* **2005**, 12, 1637-1675.
85. Griffith, B. R.; Langenhan, J. M.; Thorson, J. S., 'Sweetening' natural products via glycorandomization. *Curr. Opin. Biotechnol.* **2005**, 16, 622-630.
86. Thiericke, R.; Rohr, J., Biological Variation of Microbiol Metabolites by Precursor-directed Biosynthesis. *Nat. Prod. Rep.* **1993**, 10, (3), 265-289.
87. Zhao, L.; Sherman, D. H.; Liu, H.-w., Biosynthesis of Desosamine: Construction of a New Methymycin/Neomethymycin Analogue by Deletion of a Desosamine Biosynthetic Gene. *J. Am. Chem. Soc.* **1998**, 120, (39), 10256-10257.
88. Zhao, L.; Que, N. L. S.; Xue, Y.; Sherman, D. H.; Liu, H.-w., Mechanistic Studies of Desosamine Biosynthesis: C-4 Deoxygenation Precedes C-3 Transamination. *J. Am. Chem. Soc.* **1998**, 120, (46), 12159-12160.
89. Menzella, H. G.; Reeves, C. D., Combinatorial biosynthesis for drug development. *Curr. Opin. Microbiol.* **2007**, 10, (3), 238-245.
90. Yamase, H.; Zhao, L.; Liu, H.-w., Engineering a Hybrid Sugar Biosynthetic Pathway: Production of L-Rhamnose and Its Implication on Dihydrostreptose Biosynthesis. *J. Am. Chem. Soc.* **2001**, 122, (49), 12397-12398.
91. Melançon, C. E.; Yu, W.-l.; Liu, H.-w., TDP-Mycaminose Biosynthetic Pathway Revised and Conversion of Desosamine Pathway to Mycaminose Pathway with One Gene. *J. Am. Chem. Soc.* **2005**, 127, (35), 12240-12241.
92. Tang, L.; McDaniel, R., Construction of desosamine containing polyketide libraries using a glycosyltransferase with broad substrate specificity. *Chem. Biol.* **2001**, 8, (6), 547-555.
93. Lee, H. Y.; Khosla, C., Bioassay-Guided Evolution of Glycosylated Macrolide Antibiotics in *Escherichia coli*. *PLOS Biology* **2007**, 5, (2), 243-250.
94. Horan, A. C.; Brodsky, B. C., A Novel Antibiotic-Producing *Actinomadura*, *Actinomadura kijaniata* sp. nov. *Int. J. Syst. Bacteriol.* **1982**, 32, (2), 195-200.
95. Waitz, J. A.; Horan, A. C.; Kalyanpur, M.; Lee, B. K.; Loebenberg, D.; Marquez, J. A.; Miller, G.; Patel, M. G., Kijanimicin (Sch 25663), a Novel Antibiotic Produced by *Actinomadura kijaniata* SCC 1256. Fermentation, Isolation, Characterization and

- Biological Properties. *J. Antibiot.* **1981**, 34, (9), 1101-1106.
96. Bradner, W. T.; Claridge, C. A.; Huftalen, J. B., Antitumor Activity of Kijanimitin. *J. Antibiot.* **1983**, 36, (8), 1078-1079.
 97. Mallams, A. K.; Puar, M. S.; Rossman, R. R., Kijanimitin. 1. Structures of the Individual Sugar Components. *J. Am. Chem. Soc.* **1981**, 103, (13), 3938-3940.
 98. Mallams, A. K.; Puar, M. S.; Rossman, R. R., Kijanimitin. 2. Structure and Absolute Stereochemistry of Kijanimitin. *J. Am. Chem. Soc.* **1981**, 103, (13), 3940-3943.
 99. Mallams, A. K.; Puar, M. S.; Rossman, R. R.; McPhail, A. T.; Macfarlane, R. D.; Stephens, R. L., Kijanimitin. Part 3. Structure and Absolute Stereochemistry of Kijanimitin. *J. Chem. Soc., Perkin Trans. I* **1983**, 1497-1534.
 100. Tomita, F.; Tamaoki, T.; Shirahata, K.; Kasai, M.; Morimoto, M.; Ohkubo, S.; Mineura, K.; Ishii, S., Novel Antitumor Antibiotics, Tetrocarcins. *J. Antibiot.* **1980**, 33, (6), 668-670.
 101. Tomita, F.; Tamaoki, T., Tetrocarcins, Novel Antitumor Antibiotics. I. Producing Organism, Fermentation and Antimicrobial Activity. *J. Antibiot.* **1980**, 33, (9), 940-945.
 102. Tamaoki, T.; Kasai, M.; Shirahata, K.; Ohkubo, S.; Morimoto, M.; Mineura, K.; Ishii, S.; Tomita, F., Tetrocarcins, Novel Antitumor Antibiotics. II. Isolation, Characterization and Antitumor Activity. *J. Antibiot.* **1980**, 33, (9), 946-950.
 103. Kobinata, K.; Uramoto, M.; Mizuno, T.; Isono, K., A New Antibiotic, Antlermicin A. *J. Antibiot.* **1980**, 33, (2), 244-246.
 104. Morimoto, M.; Fukui, M.; Ohkubo, S.; Tamaoki, T.; Tomita, F., Tetrocarcins, New Antitumor Antibiotics. 3. Antitumor Activity of Tetrocarcin A. *J. Antibiot.* **1982**, 35, (8), 1033-1037.
 105. Shimotohno, K. W.; Endo, T.; Furihata, K., Antibiotic AC6H, A New Component of Tetrocarcin Group Antibiotics. *J. Antibiot.* **1993**, 46, (4), 682-684.
 106. Furumai, T.; Takagi, K.; Igarashi, Y.; Saito, N.; Oki, T., Arisostatins A and B, New Members of Tetrocarcin Class of Antibiotics from *Micromonospora* sp. TP-A0316. I. Taxonomy, Fermentation, Isolation and Biological Properties. *J. Antibiot.* **2000**, 53, (3), 227-232.
 107. Igarashi, Y.; Takagi, K.; Kan, Y.; Fujii, K.; Harada, K.-i.; Furumai, T.; Oki, T., Arisostatins A and B, New Members of Tetrocarcin Class of Antibiotics from *Micromonospora* sp. TP-A0316. II. Structure Determination. *J. Antibiot.* **2000**, 53, (3), 233-240.

108. Jiang, Z.-D.; Jensen, P. R.; Fenical, W., Lobophorins A and B, New Antiinflammatory Macrolides Produced by a Tropical Marine Bacterium. *Bioorg. Med. Chem. Lett.* **1999**, 9, (14), 2003-2006.
109. Nakashima, T.; Miura, M.; Hara, M., Tetrocarcin A Inhibits Mitochondrial Functions of Bcl-2 and Suppresses Its Anti-apoptotic Activity. *Cancer Res.* **2000**, 60, (5), 1229-1235.
110. Anether, G.; Tinhofer, I.; Senfter, M.; Greil, R., Tetrocarcin-A—induced ER stress mediates apoptosis in B-CLL cells via a Bcl-2—independent pathway. *Blood* **2003**, 101, (11), 4561-4568.
111. Kim, Y.-H.; Shin, H. C.; Song, D. W.; Lee, S.-H.; Furumai, T.; Park, J.-W.; Kwona, T. K., Arisostatins A induces apoptosis through the activation of caspase-3 and reactive oxygen species generation in AMC-HN-4 cells. *Biochem. Biophys. Res. Commun.* **2003**, 309, (2), 449-456.
112. Nakajima, H.; Sakaguchi, K.; Fujiwara, I.; Mizuta, M.; Tsuruga, M.; Magae, J.; Mizuta, N., Apoptosis and inactivation of the PI3-kinase pathway by tetrocarcin A in breast cancers. *Biochem. Biophys. Res. Commun.* **2007**, 356, (1), 260-265.
113. Winkler, R.; Hertweck, C., Sequential Enzymatic Oxidation of Aminoarenes to Nitroarenes via Hydroxylamines. *Angew. Chem. Int. Ed.* **2005**, 44, (26), 4083-4087.
114. Birkinshaw, J. H.; Dryland, A. M. L., Studies in the biochemistry of micro-organisms. 116. Biosynthesis of β -nitropropionic acid by the mould *Penicillium atrovenetum* G. Smith. *Biochem J.* **1964**, 93, (3), 478-487.
115. Brouillet, E.; Jacquard, C.; Bizat, N.; Blum, D., 3-Nitropropionic acid: a mitochondrial toxin to uncover physiopathological mechanisms underlying striatal degeneration in Huntington's disease. *J. Neurochem.* **2005**, 95, (6), 1521-1540.
116. He, J.; Magarvey, N.; Pirae, M.; Vining, L. C., The gene cluster for chloramphenicol biosynthesis in *Streptomyces venezuelae* ISP5230 includes novel shikimate pathway homologues and a monomodular non-ribosomal peptide synthetase gene. *Microbiology* **2001**, 147, (10), 2817-2829.
117. He, J.; Hertweck, C., Biosynthetic Origin of the Rare Nitroaryl Moiety of the Polyketide Antibiotic Aureothin: Involvement of an Unprecedented N-Oxygenase. *J. Am. Chem. Soc.* **2004**, 126, (12), 3694-3695.
118. Kirner, S.; Pée, K.-H. v., The Biosynthesis of Nitro Compounds: The Enzymatic Oxidation to Pyrrolnitrin of Its Amino-Substituted Precursor. *Angew. Chem. Int. Ed.* **1994**, 33, (3), 352.

119. Lee, J.; Simurdiak, M.; Zhao, H., Reconstitution and Characterization of Aminopyrrolnitrin Oxygenase, a Rieske *N*-Oxygenase That Catalyzes Unusual Arylamine Oxidation. *J. Biol. Chem.* **2005**, 280, (44), 36719-36727.
120. Kawai, H.; Hayakawa, Y.; Nakagawa, M.; Imamura, K.; Tanabe, K.; Shimazu, A.; Seto, H.; Otake, N., Arugomycin, a New Anthracycline Antibiotic. *J. Antibiot.* **1983**, 36, (11), 1569-1571.
121. Ishii, K.; Kondo, S.; Nishimura, Y.; Hamada, M.; Takeuchi, T.; Umezawa, H., Decilorubicin, a New Anthracycline Antibiotic. *J. Antibiot.* **1983**, 36, (4), 451-453.
122. Ishigami, K.; Hayakawa, Y.; Seto, H., Cororubicin, a New Anthracycline Antibiotic Generating Active Oxygen in Tumor Cells. *J. Antibiot.* **1994**, 47, (11), 1219-1225.
123. Hoeksema, H.; Mizesak, S. A.; Baczynskyj, L.; Pschigoda, L., Structure of Rubradirin. *J. Am. Chem. Soc.* **1982**, 104, (19), 5173-5181.
124. Mizesak, S. A.; Hoeksema, H.; Pschigoda, L. M., The Chemistry of Rubradirin. II. Rubranitrose. *J. Antibiot.* **1979**, 32, (7), 771-772.
125. Ganguly, A. K.; Sarre, O. Z.; Reimann, H., Chemistry of everninomicin antibiotics. III. Evernitrose, a Naturally Occurring Nitro Sugar from Everninomicins. *J. Am. Chem. Soc.* **1968**, 90, (25), 7129-7130.
126. Ganguly, A. K.; Sarre, O. Z.; Greeves, D.; Morton, J., Structure of everninomicin D. *J. Am. Chem. Soc.* **1975**, 97, (7), 1982-1985.
127. Ausubel, F. M.; Brent, R.; Kingston, R. E.; Moore, D. D.; Seidman, J. G.; Smith, J. A.; Struhl, K., *Current protocols in molecular biology*. Greene Publishing Associates, Inc., and John Wiley & Sons, Inc.: New York, 1987-1994.
128. Coligan, J. E.; Dunn, B. M.; Speicher, D. W.; Wingfield, P. T., *Current protocols in protein science*. John Wiley & Sons, Inc.: New York, 1995-2001.
129. Sambrook, J.; Russell, D. W., *Molecular Cloning: A Laboratory Manual*. 3rd ed.; Cold Spring Harbor Laboratory Press: Cold Spring Harbor, New York, 2001.
130. QIAGEN, *The QIAexpressionist: A handbook for high-level expression and purification of 6xHis-tagged proteins*. 5 ed.; QIAGEN GmbH, Germany: 2003.
131. Bradford, M. M., A rapid and sensitive method for the quantitation of microgram quantities of protein utilizing the principle of protein-dye binding. *Anal. Biochem.* **1976**, 72, (1-2), 248-254.
132. Oh, J.; Lee, S.-G.; Kim, B.-G.; Sohng, J. K.; Liou, K.; Lee, H. C., One-pot Enzymatic Production of dTDP-4-keto-6-deoxy-D-glucose from dTMP and Glucose-1-phosphate. *Biotechnol. Bioeng.* **2003**, 84, (4), 452-458.

133. Takahashi, H.; Liu, Y.-n.; Liu, H.-w., A Two-Stage One-Pot Enzymatic Synthesis of TDP-L-mycarose from Thymidine and Glucose-1-phosphate. *J. Am. Chem. Soc.* **2006**, 128, (5), 1432-1433.
134. He, X.; Liu, H.-w., Mechanisms of enzymatic C-O bond cleavages in deoxyhexose biosynthesis. *Curr. Opin. Chem. Biol.* **2002**, 6, (5), 590-597.
135. He, X.; Liu, H.-w., Formation of unusual sugars: mechanistic studies and biosynthetic applications. *Annu. Rev. Biochem.* **2002**, 71, 701-754.
136. Wong, A.; He, X.; Liu, H.-W., Novel enzymatic mechanisms in the biosynthesis of unusual sugars. In *Carbohydrate-Based Drug Discovery*, Wong, C.-H., Ed. Wiley-VCH Verlag GmbH & Co. KGaA: Weinheim, Germany, 2003; Vol. 2, pp 713-745.
137. Thibodeaux, C. J.; Melancon, C. E.; Liu, H.-w., Unusual sugar biosynthesis and natural product glycodiversification. *Nature* **2007**, 446, (7139), 1008-1016.
138. Merson-Davies, L. A.; Cundiiffe, E., Analysis of five tyiosin biosynthetic genes from the *tylBA* region of the *Streptomyces fradiae* genome. *Mol. Microbiol.* **1994**, 13, (2), 349-355.
139. Pissowotzki, K.; Mansouri, K.; Piepersberg, W., Genetics of streptomycin production in *Streptomyces griseus*: molecular structure and putative function of genes *strELMB2N*. *Mol. Gen. Genet.* **1991**, 231, (1), 113-123.
140. Gerratana, B.; Cleland, W. W.; Frey, P. A., Mechanistic roles of Thr134, Tyr160, and Lys 164 in the reaction catalyzed by dTDP-glucose 4,6-dehydratase. *Biochemistry* **2001**, 40, (31), 9187-9195.
141. Gross, J. W.; Hegeman, A. D.; Gerratana, B.; Frey, P. A., Dehydration is catalyzed by glutamate-136 and aspartic acid-135 active site residues in *Escherichia coli* dTDP-glucose 4,6-dehydratase. *Biochemistry* **2001**, 40, (42), 12497-12504.
142. Allard, S. T. M.; Cleland, W. W.; Holden, H. M., High Resolution X-ray Structure of dTDP-Glucose 4,6-Dehydratase from *Streptomyces venezuela*. *J. Biol. Chem.* **2004**, 279, (3), 2211-2220.
143. Gaisser, S.; Bohm, G. A.; Cortes, J.; Leadlay, P. F., Analysis of seven genes from the *eryAI-eryK* region of the erythromycin biosynthetic gene cluster in *Saccharopolyspora erythraea*. *Mol. Gen. Genet.* **1997**, 256, (3), 239-251.
144. Lamichhane, J.; Liou, K.; Lee, H. C.; Kim, C.-G.; Sohng, J. K., Functional characterization of ketoreductase (*rubN6*) and aminotransferase (*rubN4*) genes in the gene cluster of *Streptomyces achromogenes* var. *rubradiris*. *Biotech. Lett.* **2006**, 28,

- (8), 545-553.
145. Sohng, J.-K.; Oh, T.-J.; Lee, J.-J.; Kim, C.-G., Identification of a Gene Cluster of Biosynthetic Genes of Rubradirin Substructures in *S. achromogenes* var. *rubradiris* NRRL3061. *Mol. Cells* **1997**, 7, (5), 674-681.
 146. Hosted, T. J.; Wang, T. X.; Alexander, D. C.; Horan, A. C., Characterization of the biosynthetic gene cluster for the oligosaccharide antibiotic, Evernimicin, in *Micromonospora carbonacea* var. *africana* ATCC39149. *J. Ind. Microbiol. Biotechnol.* **2001**, 27, (6), 386-392.
 147. Zhao, Z.; Hong, L.; Liu, H.-w., Characterization of Protein Encoded by *spnR* from the Spinosyn Gene Cluster of *Saccharopolyspora spinosa*: Mechanistic Implications for Forosamine Biosynthesis. *J. Am. Chem. Soc.* **2005**, 127, (21), 7692-7693.
 148. Chen, H. Studies of the Biosynthesis of Bacterial Cell Wall and Antibiotic Ceoxysugar components: Yersiniose A, Mycarose, and Mycaminose. University of Minnesota, Minneapolis, 1999.
 149. Křen, V.; Martínková, L., Glycosides in Medicine: "The Role of Glycosidic Residue in Biological Activity". *Curr. Med. Chem.* **2001**, 8, (11), 1303-1328.
 150. Borisova, S. A.; Zhao, L.; Melançon, C. E., III; Kao, C.-L.; Liu, H.-w., Characterization of the Glycosyltransferase Activity of DesVII: Analysis of and Implications for the Biosynthesis of Macrolide Antibiotics. *J. Am. Chem. Soc.* **2004**, 126, (21), 6534-6535.
 151. Hong, J. S. J.; Park, S. H.; Choi, C. Y.; Sohng, J. K.; Yoon, Y. J., New olivosyl derivatives of methymycin/pikromycin from an engineered strain of *Streptomyces venezuelae*. *FEMS Microbiol. Lett.* **2004**, 238, 391-399.
 152. Hong, J. S. J.; Kim, W. S.; Lee, S. K.; Koh, H. S.; Park, H. S.; Park, S. J.; Kim, Y. S.; Yoon, Y. J., The Role of a Second Protein (DesVIII) in Glycosylation for the Biosynthesis of Hybrid Macrolide Antibiotics in *Streptomyces venezuelae*. *J. Microbiol. Biotechnol.* **2005**, 15, (3), 640-645.
 153. Lu, W.; Leimkuhler, C.; Gatto, G. J., Jr.; Kruger, R. G.; Oberthür, M.; Kahne, D.; Walsh, C. T., AknT Is an Activating Protein for the Glycosyltransferase AknS in L-Aminodeoxysugar Transfer to the Aglycone of Aclacinomycin A. *Chem. Biol.* **2005**, 12, (5), 527-534.
 154. Melançon, C. E., III; Takahashi, H.; Liu, H.-w., Characterization of *tylM3/tylM2* and *mydC/mycB* Pairs Required for Efficient Glycosyltransfer in Macrolide Antibiotic Biosynthesis. *J. Am. Chem. Soc.* **2004**, 126, (51), 12726-16727.

155. Yuan, Y.; Chung, H. S.; Leimkuhler, C.; Walsh, C. T.; Kahne, D.; Walker, S., In Vitro Reconstitution of EryCIII Activity for the Preparation of Unnatural Macrolides. *J. Am. Chem. Soc.* **2005**, 127, (41), 14128-14129.
156. Lee, H. Y.; Chung, H. S.; Hang, C.; Khosla, C.; Walsh, C. T.; Kahne, D.; Walker, S., Reconstitution and Characterization of a New Desosaminyl Transferase, EryCIII, from the Erythromycin Biosynthetic Pathway. *J. Am. Chem. Soc.* **2004**, 126, (32), 9924-9925.
157. Ju, T.; Cummings, R. D., A unique molecular chaperone Cosmc required for activity of the mammalian core 1 β 3-galactosyltransferase. *Proc. Natl. Acad. Sci. USA* **2002**, 99, (26), 16613-16618.
158. Ju, T.; Cummings, R. D., Chaperone mutation in Tn syndrome. *Nature* **2005**, 437, (7063), 1252.
159. Hendershot, L. M.; Bulleid, N. J., Protein-specific chaperones: The role of hsp47 begins to gel. *Curr. Biol.* **2000**, 10, (24), R912-R915.
160. Ellgaard, L.; Molinari, M.; Helenius, A., Setting the Standards: Quality Control in the Secretory Pathway. *Science* **1999**, 286, (5446), 1882-1888.
161. Buchner, J., Hsp90 & Co. - a holding for folding. *Trends Biochem. Sci.* **1999**, 24, (4), 127-162.
162. Invitrogen, *ProQuest™ Two-Hybrid System with Gateway® Technology*. Invitrogen Technologies: 2002.
163. Kieser, T.; Bibb, M. J.; Buttner, M. J.; Chater, K. F.; Hopwood, D. A., *Practical Streptomyces Genetics*. The John Innes Foundation: Norwich, England, 2000.
164. Melançon, C. E., III. Investigation and Engineering of Macrolide Antibiotic Sugar Biosynthesis and Glycosylation Pathways of Actinomycetes. The University of Texas at Austin, 2006.
165. Xue, Y.; Sherman, D. H., Biosynthesis and Combinatorial Biosynthesis of Pikromycin-Related Macrolides in *Streptomyces venezuelae*. *Metab. Eng.* **2001**, 3, (1), 15-26.
166. Borisova, S. A. Genetic and Biochemical Studies of the Biosynthesis and Attachment of D-Desosamine, the Deoxy Sugar Component of Macrolide Antibiotics Produced by *Streptomyces venezuelae*. The University of Texas at Austin, 2004.
167. Simon, R.; Priefer, U.; Pühler, A., A Broad Host Range Mobilization System for In Vivo Genetic Engineering: Transposon Mutagenesis in Gram Negative Bacteria. *Bio/Technology* **1983**, 1, (9), 784-791.

168. Baltz, R. H., Genetic recombination by protoplast fusion in *Streptomyces*. *Developments in Industrial Microbiology Series* **1980**, 21, 43-54.
169. Bierman, M.; Logan, R.; O'Brien, K.; Seno, E. T.; Rao, R. N.; Schoner, B. E., Plasmid cloning vectors for the conjugal transfer of DNA from *Escherichia coli* to *Streptomyces* spp. *Gene* **1992**, 116, (1), 43-49.
170. Zhao, L.; Beyer, N. J.; Borisova, S. A.; Liu, H.-w., β -Glucosylation as a Part of Self-Resistance Mechanism in Methymycin/Pikromycin Producing Strain *Streptomyces venezuelae*. *Biochemistry* **2003**, 42, (50), 14794 -14804.
171. Lambalot, R. H.; Cane, D. E., Isolation and characterization of 10-deoxymethynolide produced by *Streptomyces venezuelae*. *J. Antibiot.* **1992**, 45, (12), 1981-1982.
172. Fields, S.; Song, O.-k., A novel genetic system to detect protein-protein interactions. *Nature* **1989**, 340, (6230), 245-246.
173. Bartel, P.; Chien, C.-t.; Sternglanz, R.; Fields, S., Elimination of False Positives that Arise in Using Two-Hybrid System. *BioTechniques* **1993**, 14, (6), 920-924.
174. Yang, W.; Zhang, L.; Lu, Z.; Tao, W.; Zhai, Z., A New Method for Protein Coexpression in *Escherichia coli* Using Two Incompatible Plasmids. *Protein Expr. Purif.* **2001**, 22, 472-478.
175. Blanchard, S.; Thorson, J. S., Enzymatic tools for engineering natural product glycosylation. *Curr. Opin. Chem. Biol.* **2006**, 10, (3), 263-271.

Vita

Wei-luen (Allen) Yu was born in Tainan City, Taiwan on November 7th, 1972 to Chun-ming Yu and Ying-ying Fu. The Yu family lived in the neighborhood of National Cheng-Kung University in Tainan City. Allen finished his primary and secondary education in neighborhood schools. In 1991, Allen took the National College Entrance Examination and received admission to National Taiwan University (NTU), Department of Zoology. He attended NTU, in majoring Zoology from 1991 until 1995, during which time he accumulated more than 140 credit hours and engaged in various undergraduate research projects. He joined the research group of Dr. Chang-Po Chen of the Institute of Zoology, Academia Sinica as a research volunteer during the summer of 1993. In the summer of 1994, He joined the research group of Dr. Huai-Jen Tsai in the Institute of Fishery Science of NTU, and engaged in studies on the molecular physiology of marine fish. Allen completed his Bachelor of Science degree in Zoology, graduating in June 1995. He was subsequently admitted to the Institute of Molecular Medicine in NTU, and worked toward Master of Science degree from 1995 to 1997. During these two years, he joined Dr. Fang-Jen S. Lee's Research Group and dedicated to the studies of characterizing the ADP-ribosylation factors in *Saccharomyces cerevisiae* and *Homo sapiens*, and contributed to two research publications. Allen completed his Master of Science degree in June 1997 and then moved back to his hometown, Tainan, to begin his

career as a research assistant in the lab of Dr. Pao-Lin Kuo in the Department of Obstetrics & Gynecology, National Cheng-Kung University from 1998 to 2000. He joined a team working on the prenatal diagnosis of genetic diseases, including Thalassemia, Y-chromosome abnormalities involving male-infertility, Prader-Willi Syndrome, and Angelman Syndrome. In fall 2000, Allen was admitted to the Institute for Cellular and Molecular Biology at The University of Texas at Austin. He joined the research group of Dr. Hung-wen Liu in June 2001, in which he has contributed to two research articles and other research results currently prepared to be published.

Permanent address: 701 W. North Loop Blvd. Apt#101

Austin, TX 78751

This dissertation was typed by Wei-luen (Allen) Yu.